"STUDY OF FLATTENED AND FLATTENING FILTER FREE BEAM BASED ADVANCED TREATMENT TECHNIQUES IN RADIATION CANCER THERAPY"

A THESIS SUBMITTED TO

D.Y. PATIL EDUCATION SOCIETY (DEEMED TO BE UNIVERSITY), KOLHAPUR

(Declared u/s 3 of the UGC Act. 1956)

FOR THE DEGREE OF

DOCTOR OF PHILOSOPHY

IN MEDICAL PHYSICS

UNDER THE FACULTY OF

INTERDISCIPLINARY STUDIES

BY

Mr. Munirathinam.N

M. Sc. (Medical Physics)

UNDER THE GUIDANCE OF

ASST. PROF. (DR.) P.N. Pawaskar

M.Sc. Ph.D.

CENTRE FOR INTERDISCIPLINARY RESEARCH,

D. Y. PATIL EDUCATION SOCIETY (DEEMED TO BE UNIVERSITY), KOLHAPUR,

KOLHAPUR – 416 006 (M.S.) INDIA

YEAR - 2022

DECLARATION

I hereby declare that this thesis entitled, **"STUDY OF FLATTENED AND FLATTENING FILTER FREE BEAM BASED ADVANCED TREATMENT TECHNIQUES IN RADIATION CANCER THERAPY**" which is being submitted here with for the degree of Doctor of Philosophy in Medical Physics, under the faculty of Physics is an original report of my research, has been written by me and has not been submitted for any previous degree. The experimental work is almost entirely my own work; the collaborative contributions have been indicated clearly and acknowledged. Due references have been provided on all supporting literature and resources.

Place: Kolhapur

Date:

Research Student

Munirathinam.N

D. Y. Patil Education Society, Kolhapur

(Institution Deemed to be university, Declared u/s 3 of the UGC Act 1956)

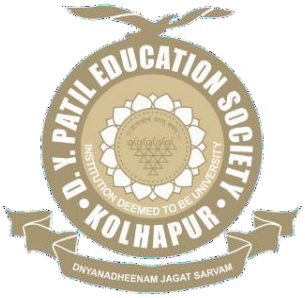

CERTIFICATE

This is to certify that the thesis entitled **"STUDY OF FLATTENED AND FLATTENING FILTER FREE BEAM BASED ADVANCED TREATMENT TECHNIQUES IN RADIATION CANCER THERAPY**" which is being submitted here with for the award of The Degree of Doctor of Philosophy in Medical Physics from D. Y. Patil Education Society, Kolhapur (Deemed to be University, Declared u/s 3 of the UGC Act 1956), under the Faculty of Physics, is the result of original Research work completed by **Mr. Munirathinam. N** under the supervision and guidance and to the best of our knowledge and belief the work bound in this thesis has not formed earlier the basis for the award of any Degree or similar title of this or any other University or examining body.

Date:

Place: Kolhapur

Research Guide,

Forwarded through,

ACKNOWLEDGEMENT

Foremost, I feel gratefully fortunate to have an opportunity to work with my supervisor, **Dr. P.N. Pawaskar**. I would like to gratefully acknowledge her continuous help, guidance and encouragement during my Ph.D.

I would like to acknowledge to Dr. Sanjay D. Patil, Chancellor, D. Y. Patil Education Society, (Deemed to be University), Kolhapur. My sincere thanks to Dr.Rakesh Kumar Mudgal,Vice Chancellor and Dr.Mrs Shimpa Sharma, Pro Vice Chancellor, for their valuable support.

My sincere gratitude is reserved for Dr. C. D. Lokhande, Research Director and Dean CIR, for his valuable insights and suggestions. My special thanks to Dr. V. V. Bhosale, Registrar, Dr. R.K. Sharma, Dean and Dr. Ashalata Patil, Vice Principal, D.Y. Patil Education Society, (Deemed to be University), Kolhapur

Also, I would like to thank the faculty members in Department of Medical Physics, D.Y. Patil Education Society, Dr. Mayakannan, Mrs.Pooja Patil and Mr. Shivakumar. I am also thankful to Mrs. Pooja. Jadhav, Mr. Ramadas and Mrs.Namratha for their best support throughout my Ph.D.

I sincerely thank Dr.S.H. Pawar, Ex-Vice Chancellor, D. Y. Patil Education Society, (Deemed to be University), Kolhapur. For facilitating and encouraging to carry out this research work

My special thanks to Aditya Birla Memorial Hospital, Pune for providing the necessary facilities and support. Special thanks to Miss.Rekha Dubey, Dr. Rajeev Shrivastav, Dr. Sayan Kondu, Dr.Birendra Kumar rout,Mr.Prabhu and Mr.Rambabu for the great support.

I express my gratitude to Dr. Arun, Mr. Bhargavan, Mr. Kanagavel, Mrs.Dipika, Dr. Govindaraj for timely suggestions and support.

Last but not least, I my deepest gratitude go to My Father Mr.G. Natraji and My Beloved Mother Mrs.Krishnamal and all of my family members. You have given a motivation and have provided me with steady guidance and encouragement.

Mr. Munirathinam.N,

Place: Kolhapur

Date:

CONTENTS

LIST OF TABLES

LIST OF FIGURES

ABBREVIATIONS

% DD	Percentage Depth Dose
2D	Two Dimensional
3D	Three Dimensional
3DCRT	Three Dimensional Conformal Radiation Therapy
AAA	Anisotropic Analytical Algorithm
AAPM	American Association Physicist In Medicine
AERB	Atomic Energy Regulatory Board
BEV	Beams Eye View
BJR	British Journal of Radiology
BOT	Beam on time
CAX	Central Axis
Cc	Cubic Centimeter
CI	Conformity Index
cm	Centimeter
CT	Computed Tomography
CTV	Clinical Target Volume
Dcalc	Calculated Dose
DHI	Dose Homogeneity Index
DIBH	Deep inspiration breath hold
Dmax	Dose Maximum
Dmeas	Measured Dose
Dmin	Dose Minimum
DMLC	Dynamlic Multi Leaf Collimator
DVH	Dose-Volume Histogram
Dw,Q0	Absorbed Dose to Water
Dx	Percentage dose at any selected depth

F	Field Size
FB	Flattened Beam
FC	Farmer Chamber
FDA	Food And Drug Administration
FF	Flattening Filter
FFB	Flattening Filter Beam
FFF	Flattening Filter Free
FFFB	Flattening Filter Free Beam
FS	Field Size
Gy	Gray
HD MLC	High Definition Multi Leaf Collimator
HVL	Half Value Layer
IAEA	International Atomic Energy Agency
ICRU	International Commission on Radiation Unites and Measurements
IEC	International Electro technical Commission
IGA	Increment gantry angle
IGRT	Image Guided Radiation Therapy
IMAT	Intensity Modulated Arc Therapy
IMRT	Intensity Modulated Radiation Therapy
IP	Inflection Point
ITV	Internal Target Volume
Kg	Kilo Gram
LINAC	Linear Accelerator
M	Meter
MCU	Main Control Unit
Mev	Mega Electron Volt
mGy	mille Gray
MLC	Multi Leaf Collimator
mm	Milli meter
MU	Monitor Unit

MV	Mega Voltage
NSCLC	Non-Small Cell Lung Carcinoma
OAR	Organ At Risk
PDD	Percentage Depth Dose
PET	Positron Emission Tomography
PMMA	Poly Methyl Metha Acrylate
QA	Quality Assurance
QI	Quality Index
RA	Rapid Arc
RFA	Radiation Field Analyzer
SAD	Source to Axis Distance
SBRT	Stereotactic Body Radiotherapy
Sc	Scatter Factor
Sc,p	Output Factor
SID	Source to Isocentre Distance
SRS	Stereotactic Radio Surgery
SSD	Source to Surface Distance
TG	Task Group
TPR	Tissue Phantom Ratio
TPS	Treatment Planning System
V30%	Volume encompassed by the 30% isodose curves
VMAT	Volumetric Modulated Arc Therapy
WHO	World Health Organization

INTRODUCTION

CHAPTER- I

CHAPTER-I

1. INTRODUCTION

1.1. CANCER:

Cancer is a disease in which cells divide or expand uncontrollably that move and infects other regions of the body. There are trillions of cells in an adult human body. Cell division is the process by which our body cells divide and multiply to make new cells as needed by the body. Cells die as they age or get damaged, and are replaced by new cells.

When this well-ordered mechanism fails, irregular or damaged cells grow and reproduce when they shouldn't. Tumors, which are tissue masses, can form from these cells. Tumors can be malignant or benign (benign).

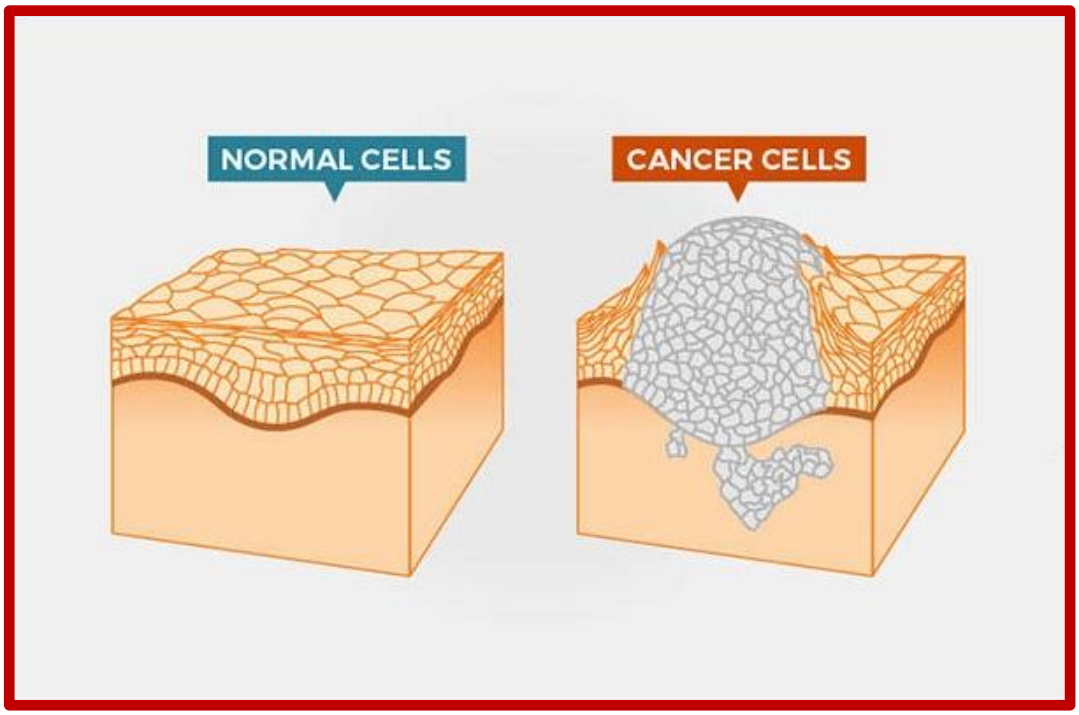

Figure1.1: Comparison of Cancerous cell and normal cells

The process through which cancer cells split off from the original (primary cancer cell) and migrate via the blood or lymph system, forming new tumours in other people.

Metastatic cancer refers to cancer that has spread to other regions of the body. Cancerous tumours are also known as malignant tumours. Many cancers, including leukemia's, produce solid tumours, whereas blood cancers do not.

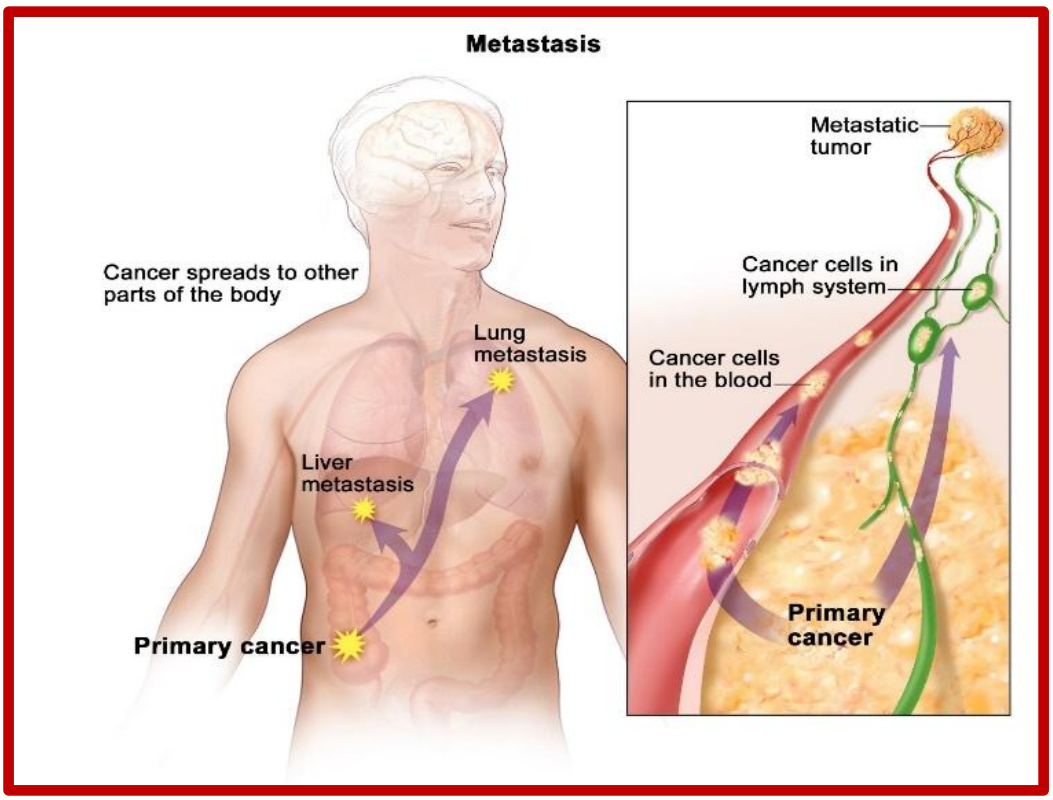

Figure1.2: Conversation of primary cancer into Metastatic cancer

When cells are divides more and more the normal organization of the tissues gradually disrupted. Rapid global population growth and age have contributed to the rise of cancer as a leading cause of death, which is partly due to large drops in stroke and coronary heart disease mortality a rate relative to cancer in many nations.

Cancer affects practically every region of the body, and all of them are potentially Life-threatening if not identified early. Carcinoma, sarcoma, lymphoma, and leukemia are the most common cancers. The most prevalent type of cancer is carcinoma, which develops in the head, neck, skin, breast, lung, esophagus, prostate, and cervix.

1.2. Cancer in India

No communicable diseases (NCDs) accounted for 72% of all fatalities worldwide. NCDs were projected to be responsible for 62.99 percent of all fatalities in India [1], with cancer being one of the primary causes (9 percent). According to the World Cancer Report, there are over 1.17 million new cancer cases each year, In 2018, India's population of 1.36 billion people saw 786,900 cancer deaths and 2.27 million 5-year prevalent cases. According to the journal, "one out of every ten Indians develops cancer during their lifetime," and "one out of every fifteen Indians dies of cancer [2]."

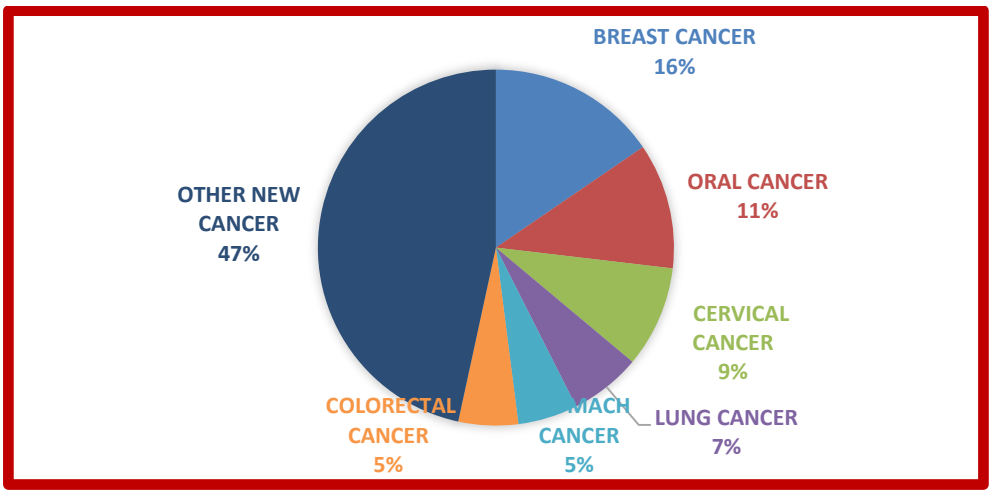

Figure1.3: India's cancer burden in 2018 was calculated by the World Cancer Report.

Lung cancer, mouth cancer, stomach cancer, and esophageal cancer were the most prevalent malignancies among men in India, the most frequent cancers in women were breast cancer and cervix uteri cancer. Lung cancer was identified at a stage where it had migrated to distant regions, while cancers of the brain, head and neck, breast, stomach, and cervix were detected after they had spread locally, malignancies of the brain, head and neck, breast, stomach, and cervix were identified after they had spread locally.

The most common causes and risk factors of cancer are:

1. Sun exposure
2. Alcohol
3. Smoking and tobacco use
4. Human papilloma virus
5. Immune deficiency
6. Oral contraceptives
7. Obesity / over weight
8. Age
9. Teenage pregnancy
10. Family history and genetics
11. Exposure to cancer-causing substances etc.

Above all risk factors presented by National Cancer Institute and American Cancer Society

1.3. History of radiotherapy

In 1895, Wilhelm Conrad Rontgen discovered x-rays, then in 1896, he found radioactivity, leading to the invention of radiotherapy. The research also centered on the development of ever more novel promising therapeutic devices. It can capable of treating tumours in the deep tissues throughout the next three decades (Megavoltage period). During this time, Cobalt teletherapy, which produces high-energy gamma rays [4], and later increasingly powerful electron linear accelerators, which can provide megavoltage X-rays [5], were introduced.

The devices could deliver a higher dose rate than previous models, allowing for more skin sparing treatment of deeper tumours. Because of the difficulty in regulating these sources and the possibility of causing excessive radiation in the

surrounding tissue, multi-field irradiation schemes have been developed [6]. However, a new period in RT's history was about to begin. The emergence of novel proton beam delivery devices marked the 1970s and 1980s. Even though computer-assisted protons accelerators were initially used in 1954 [7], it wasn't until the late 1970s that they were successfully used to treat a different type of tumour [8].

Another significant advancement in radiotherapy occurred at the end of the 1990s, when the creation of a 3D conformal RT (SRT) capable of treating patients with higher efficacy and safety was facilitated by the introduction of more advanced computers [9]. Standardized procedures in EBRT and Internal therapy have been established through scientific break trough's, trial and error, and technological advancements. Furthermore, advancements in the areas of radiobiology and radiation metrology were critical in making radiotherapy a successful cancer treatment option.

1.4. Role of radiation therapy

Surgery, chemotherapy and radiotherapy are the most common cancer treatment options. Given the resources available, they chose the best effective treatment currently available based on scientific data. They can be used separately or in combo. Only when the tumour is localized and modest in size is surgery likely to be highly for a limited group of malignancies, like as hematological neoplasms (lymphomas leukemia's) chemotherapy alone can be effective.). They are usually expected to be widespread immediately. Combined modality therapy necessitates tight communication amongst all members of the cancer treatment team. Despite the fact that cancer radiotherapy utilization rates vary greatly around the globe, Radiation is considered to be appropriate for roughly half of all cancer patients

[10].

1.5. Mechanisms and action of radiotherapy

Radiation therapy is divided into two types: EBRT and brachytherapy. Even if external and internal therapy are used, the interaction of radiation with tissue produces a wide range of results (Table 1). Radiotherapy acts primarily by killing tumour cells and stopping their reproduction [11]. These events can happen as a result of direct DNA or other important cellular molecules being damaged, or as a result of free radical production causing indirect cellular harm (e.g. X-rays or Gamma-rays).

S.No	EFFECT	RESULT
1.	Physics	Issue, transfer and absorption of energy
2.	Biophysics	Ionization and excitation phenomenon
3.	Physical-chemical	Direct alterations of atoms and molecules or indirect damage through the productions of free radical
4.	Chemical	The breaking of bonds, polymerization or de-polymerization phenomenon
5.	Biochemical	Molecular alterations
6.	Biochemical-biological	Damage to DNA, RNA, cytoplasm, enzymes
7.	Biological	Aberrations of various cellular components, morpho-functional and metabolic lesions, damage to the genetic material

Table 1: Radiation's effects on irradiated tissues

Unfortunately, radiation therapy can harm and kill normal cells, especially those that divide frequently. This can be reduced by focusing the radiation beam on the tumour and fractionating the overall dose, allowing normal tissue to heal and recover on its own [12].

1.6. Linear Accelerator

Modern linacs customize high-energy x-rays or electrons to the geometry of a tumour, destroying cancer cells while leaving healthy tissue unharmed. It comes with a number of built-in safety features to ensure that the dose is delivered exactly as intended It is also checked by a medical physicist on a regular basis to ensure that it is in good functioning order.

A common medical linear accelerator's general operating principle can be stated as as shown in Picture 1.4: The electron gun and the magnetron or klystron, which produce microwaves, receive these pulses at the same time. An electron from an electron gun is pulsed into the accelerator structure at the appropriate time.

Magnetron is a high-power oscillator that generates 3GHz microwave pulses with adoration times of a few microseconds and a repetition rate of several hundred per second. A microwave amplifier, on the other hand, is a klystron.

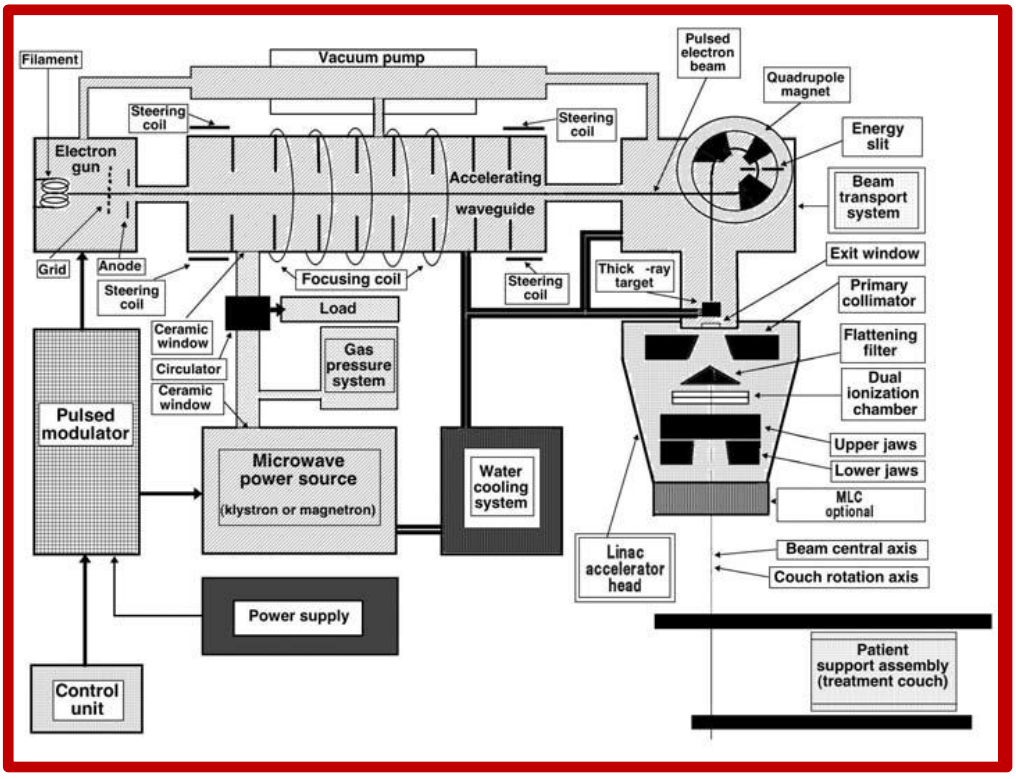

Figure 1.4: Schematic Diagram of a Medical linear accelerator with its components.

It will be powered by a low-power microwave generator. Because klystrons have longer time duration and can generate higher power levels than magnetrons, they are recommended for beam energies larger than 20 MeV [13]. The accelerator tubes in Linacs with energy up to 6 MeV are very short, A longer accelerator tube is often placed perpendicular to the treatment head axis in higher energy Linacs, and Bending magnets are used to deflect electrons by 90 (or 270) degrees. The treatment head is the final component of Linacs. It consists of various components like target, collimator, scatter foil, monitor ionization chambers, flattening filters and, in some circumstances, additional beam altering devices are all included. Both x-ray and electron treatment techniques are available on modern linear accelerators. When accelerated electrons collide with a high-atomic-number object, Bremsstrahlung photon beams are created.

Photons have an average energy of around one-third of their maximum energy. Accelerated electrons hit with a thin scattering foil in the electron therapy procedure. Because the scattering foil stops most of electrons from undergoing bremsstrahlung production, the original pencil beam is turned into a uniformly fluence broad electron beam. A shielding material with a high density, such as a lead-tungsten alloy, is used to enclose the therapeutic beam in the primary collimator. It is the therapeutic beam collimator's initial define layer, and it provides adequate leakage radiation protection.

Megavoltage bremsstrahlung has a significantly forward peaked intensity distribution, meaning that the majority of photons follow the same path as the electrons impinging on the target. The generated bremsstrahlung beam is sent through a flattening filter to make the beam. The filter has a conical form and is made up of a variety of proton-numbering materials. A linac uses a specialized

flattening filter for each photon energy.

The flattened x-ray beam is then sent into monitor ionization chambers, which are either transmission chambers or plan-parallel chambers with a diameter larger than the beam's cross-sectional area. The major function of the monitor chambers is to control the immediate dosage rate, cumulative dose, symmetry foil, and beam flatness. The secondary collimation system consists of two pairs of adjustable lead or tungsten jaws that collimate the beam into rectangular fields varying in size from 0 x 0 cm2 to 40 x 40 cm2.

Figure 1.5: **Elekta Versa HD Medical linear accelerator installed in Aditya Birla Memorial Hospital**

1.7. Multileaf collimators

MLCs with 40 to 80 sets of narrow, tightly neighboring tungsten leaves, each with a typical width of 10 mm or less at the linac isocenter, can be found in modern linacs. MLCs with leaf widths of less than 5 mm at the isocenter are known as micro MLCs. They're used to shape irregular fields with a maximum field dimension of less than 10 cm, like head and neck fields, or irregular fields with a

maximum field dimension of less than 3 cm, like radiosurgery fields.

The MLCs can either be built into the linac head and used instead of the upper or lower secondary collimator jaws, or they can be installed on the linac head and used in conjunction with both. A typical MLC coupled to a linac head is used in conjunction with the upper and lower collimator jaws.

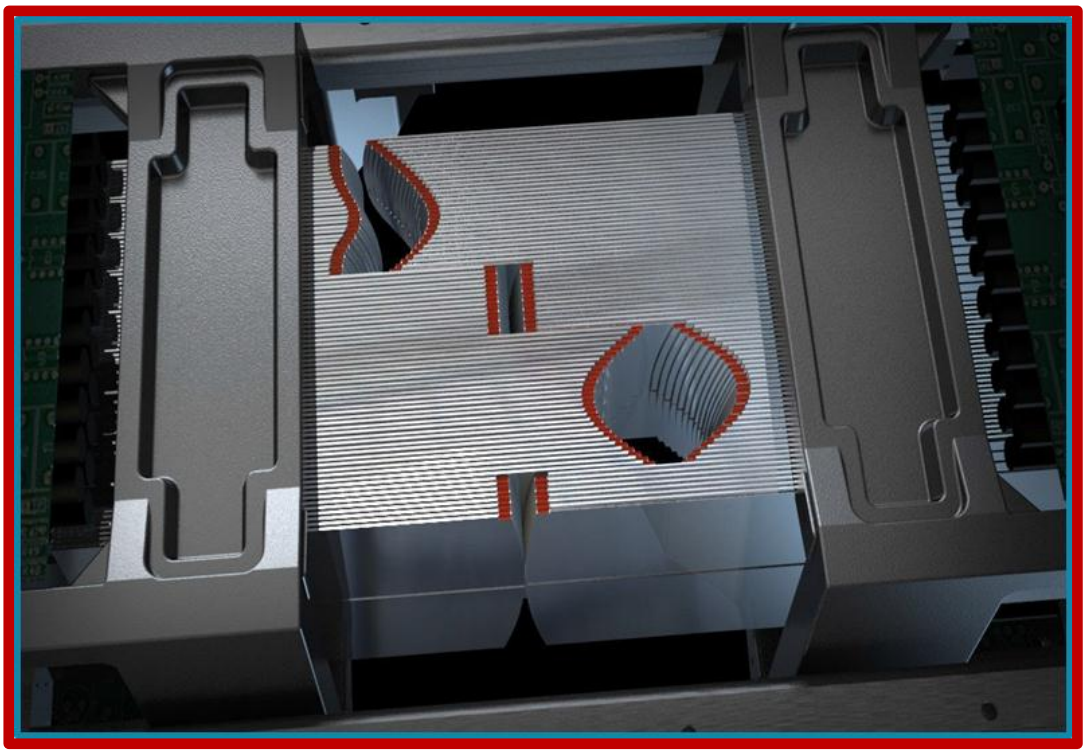

Figure 1.6: MLC with 80 pairs of leaves abutting (Agility MLC).

Each leaf is individually motorized and computer controlled, allowing for better than 1 mm placement precision and the generation of irregular radiation fields that conform to the target cross section in the beam's eye view (BEV). Each leaf is driven independently by a small DC motor, as seen in Fig. 1. A complex servo mechanism senses the position of the leaves and controls and verifies it using electronic or optical/video techniques.

1.1.8 Flattening filter

Since its first application in 1953 [11, 12], the FF has been an integral part of a accelerator, and It was used to compensate for differences in photon fluence across

the field. Simplifying dose calculations It's important to note that the first computer-based TPS that allowed for 3D dose distribution calculations didn't appear until decades later.

The usage of the flattening filter, on the other hand, comes with trade-offs. The reduction in dosage rate caused by beam attenuation in a flattening filter's material is arguably the most critical [13].

The implementation was restricted to circular fields with a diameter of up to 3 cm and no significant intensity difference as compared to an unflattened beam. The scientists were inspired to do this research because they wanted to shorten the time it took to provide radiosurgery treatments. Tomotherapy, a specialized equipment that gives Therapy in slices, was introduced in 1993. A dedicated Multileaf collimator is employed to further modulate the beam in this machine, which also uses an unflattened beam [14].

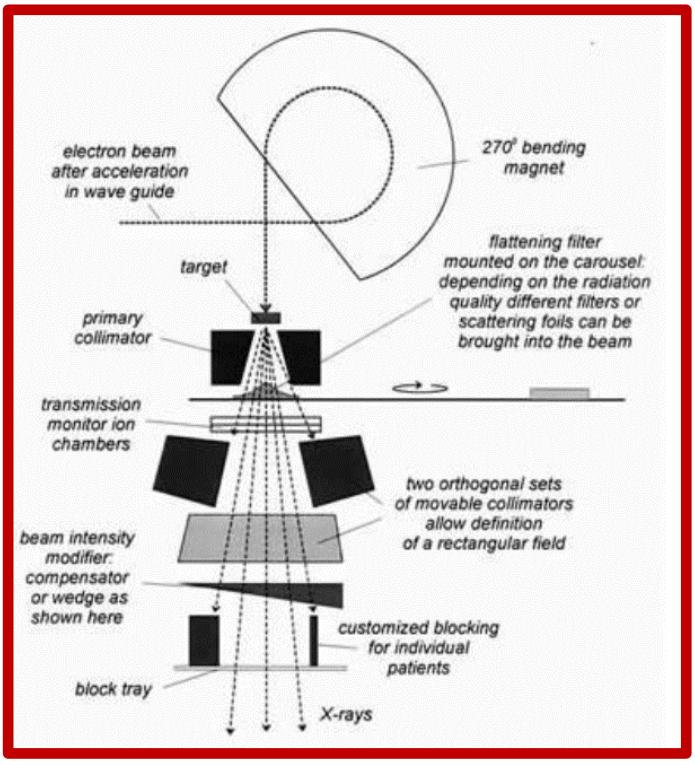

Figure 1.7: Beam transporting system of Linacs head showing Flattening filter location

The majority of scattering in the treatment head is caused by the FF [15, 16]. According to Monte Carlo simulations, this produces fluctuations in quality of the beam out from the central axis [17] and is the principal reason of electrons contamination [18–19]. Other Monte Carlo investigations use commercially available Linacs to study various aspects of flattening filter free (FFF) beams [20–21], where a FF was removed for modelling purposes. There were also some preliminary treatment planning experiments and analogical dosimetric measurements made with dedicated new Elekta versa HD linear accelerators without a flattening filter.

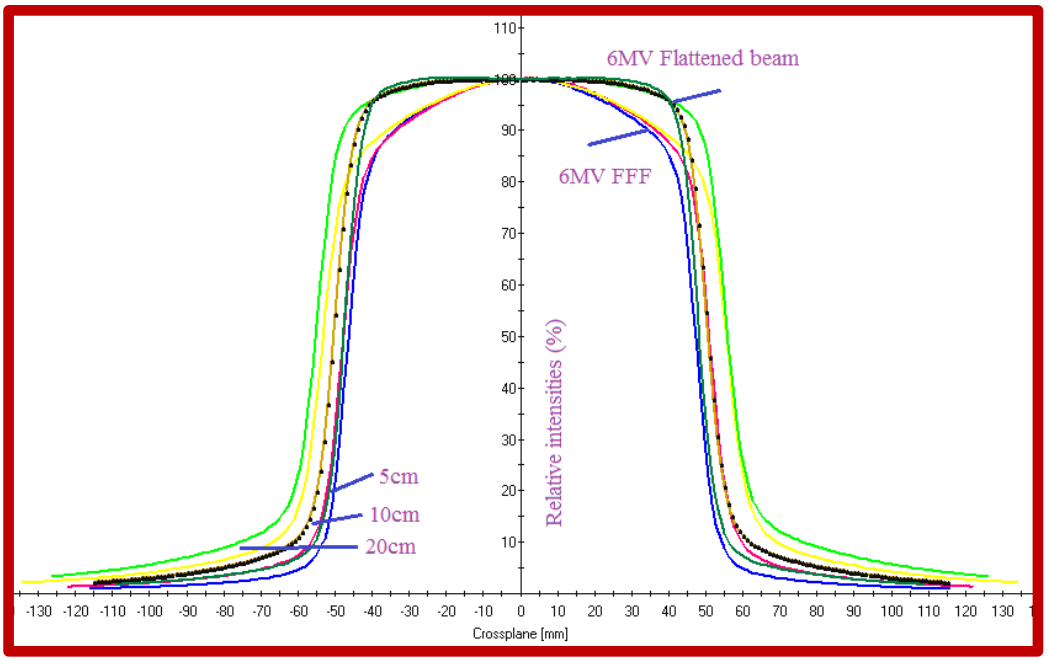

Figure 1.8: A graphic illustration of the 6MV photon crossbeam profile in a 10x10 cm field size for both FFFB and Flattened beams at depths of 5, 10.0, and 20.0 cm for both FFFB and Flattened beams.

1.8 References

1. Prashant Mathur and Krishnan Sathishkumar "Cancer Statistics, 2020: Report from National Cancer Registry Programme, India"JCO Global Oncology no.6(2020) 1063-1075,July 16,2020

2. "WHO Regional Office for India: Indian Health for All database [online database]."

3. Rontgen WC Uber eine neue Art von Strahlen. Vorl¨aufige Mitteilung. Vol. 30. Sitzung: Sitzungsberichte¨der physikalisch-medicinischen Gesellschaft zu W¨urzburg; 1985. pp. 132–141.

4. Boone MLM, Lawrence JH, Connor WG, et al. Introduction to the use of protons and heavy ions in radiation therapy: historical perspective. Int. *J. Radiat. Oncol. Biol. Phys.* 1977;3:65–69. https://doi.org/10.1016/0360-3016(77)90229-2. [PubMed] [Google Scholar]

5. Fry D W, Harvie RB, Mullett L, et al. A travelling-wave linear accelerator for 4-MeVelectrons. *Nature.* 1948;162:859861. https://doi.org/10.1038/162859a0 PMid:18103121. [PubMed] [Google Scholar]

6. Suit H, Goitein M, Munzenrider J. Evaluation of the clinical applicability of proton beams in definitive fractionated radiation therapy. *Int. J. Radiat. Oncol. Biol. Phys.* 1982;8:2199–2205. https://doi.org/10.1016/0360-3016(82)90570-3. [PubMed] [Google Scholar]

7. Hall EJ The Physics and Chemistry of Radiation Absorption. *Radiobiology for the radiologists.* 4th edition. Philadelphia: JB Lippincott; 1994. pp. 8–10. [Google Scholar]

8. Ying CH. Update of Radiotherapy for Skin Cancer. *Hong Kong Dermatology & Venereology Bulletin.* 2001;9(2):52–59. [Google Scholar]

9. Mohan R. Field shaping for three-dimensional conformal radiation therapy and Multileaf collimation. *Semin. Radiat. Oncol.* 1995; 5:86–99. https://doi.org/10.1016/S1053-4296(95)80003-4.[PubMed] [Google Scholar]

10. G.Delaney, S. Jacob, C. Featherstone, and M. Barton "The role of Radiotherapy in cancer Trement " Cancer, vol. 104, no. 6, pp. 1129–1137, 2005.

11. C. W. Miller, "An 8-MeV linear accelerator for X-ray therapy," Proceedings of the IEE -Part I: General, vol. 101, no. 130, pp. 207–221, 1954.

12. G. R. Newbery and D. K. Bewley, "The performance of the medical research council 8mev linear accelerator" Br J Radiol, vol. 28, pp. 241–51, May 1955.

13. P. F. O'Brien, B. A. Gillies, M. Schwartz, C. Young, and P. Davey, "Radiosurgery with unflattened 6-mv photon beams," Med Phys, vol. 18, no. 3, pp. 519–21, 1991.

14. T. R. Mackie, T. Holmes, S. Swerdloff, P. Reckwerdt, J. O. Deasy, J. Yang, B. Paliwal and T. Kinsella," Tomotherapy: a new concept for for the delivery dynamic conformal radiotherapy," Medical physics, vol. 20, p. 1709, 1993.

15. P. L. Petti, M. S. Goodman, T. A. Gabriel, and R. Mohan, "Investigation of buildup dose from electron contamination of clinical photon beams," Med Phys, vol. 10, no. 1, pp. 18–24, 1983.

16. T. C. Zhu and B. E. Bj¨arngard, "The fraction of photons undergoing head scatter in x-ray beams," Phys Med Biol, vol. 40, pp. 1127–34, Jun 1995.

17. P. C. Lee, "Monte carlo simulations of the differential beam hardening effect of a flattening filter on a therapeutic x-ray beam," Med Phys, vol. 24, pp. 1485–9, Sep 1997.
18. B. Nilsson, "Electron contamination from different materials in high energy photon beams," Phys Med Biol, vol. 30, pp.139-51, Feb 1985.
19. E. E. Klein, J. Esthappan, and Z. Li, "Surface and buildup dose characteristics for 6, 10, and 18 mv photons from an elekta precise linear Accelerator" j Appl clin Med Phys,vol.4.1pp.1-7,2003
20. R. Jeraj, T. R. Mackie, J. Balog, G. Olivera, D. Pearson, J. Kapatoes, K. Ruchala and P. Reckwerdt, "Radiation characteristics of helical tomotherapy," Med Phys, vol. 31, pp. 396–404, Feb 2004.
21. E. Ishmael Parsai, D. Pearson, and T. Kvale, "Consequences of removing the flattening filter from linear accelerators in generating high dose rate photons are Suitable for medical use: Measurement-based MC simulation," Nuclear Instruments and Methods in Physics Research Section B: Beam Interactions with Materials and Atoms, vol. 261, no. 1, pp. 755–759, 2007

EBRT

CHAPTER- II

CHAPTER-II

2.0 EXTERNAL BEAM RADIOTHERAPY

Basically the radiation therapy is classified into two different categories known as External beam radiotherapy or Teletherapy and internal radiation therapy or brachytherapy.

EBRT is the most often used radiation therapy. It uses a machine outside the body to emit radiation. It can treat large parts of the body if necessary. A beam of X rays or electrons, or a combination of beams, is aimed at the tumour and/or surrounding tissues. Each fraction treatment takes 2 to 10 minutes and is given once in a day or twice in a day (administered around 6 hours apart). The majority of treatment fraction last between 4 and 7 weeks.

In the last few decades, several key improved approaches in radiotherapy treatment have arisen, transforming the face of cancer treatment.

EBRT can be classified into the following categories:

1. Three-dimensional conformal radiation therapy
2. Intensity modulated radiation therapy
3. Rapid Arc or Volumetric Modulated Arc Therapy
4. Stereotactic Body Radiation Therapy
5. Stereotactic radio Surgery

The above radiation therapy techniques are prescribed depending on the patient's individual circumstances.

2.1 Three-dimensional conformal radiation therapy

3DCRT is a therapeutic method in which the radiation beams are shaped to fit the tumour. Previously, in conventional radiotherapy, the radiation treatment was tailored to the tumor's height and width, exposing healthy tissue to the beams.

When compared to 2DCRT, 3DCRT was certified in the 1990s [1] because it reduced damage to normal tissue and improved dosage conformity. The tumour can now be properly located due to better in imaging technology. The targeting information can be utilized in conformal radiation therapy to precisely focus [2] on the tumour while avoiding neighboring surrounding cells.. Because of the precision of the targeting, larger doses of radiation can be used in treatment, which is more successful in reducing and destroying cancers.

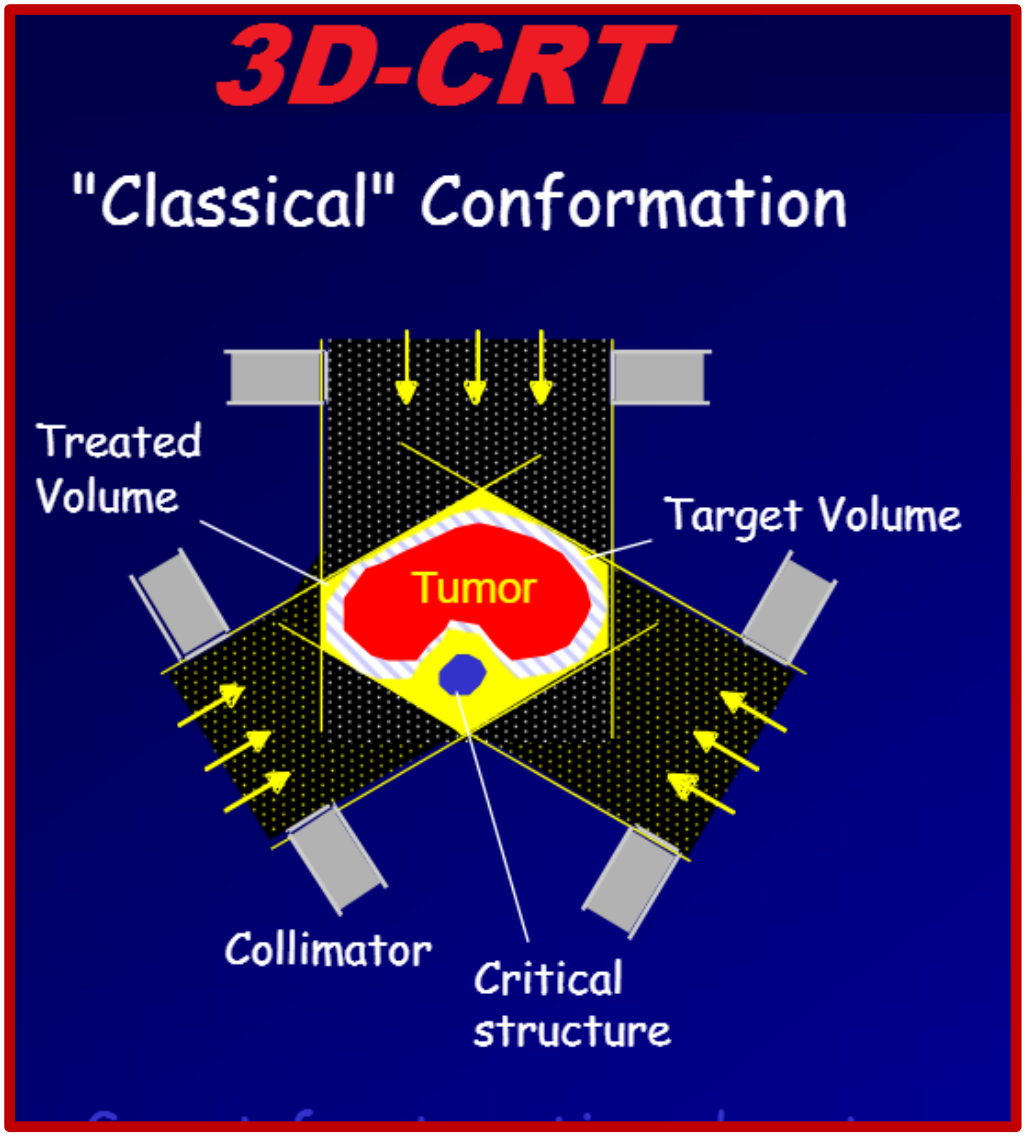

Figure 2.1: The Image Representing 3DCRT Planning Approach

The goal of 3DCRT treatment planning is to provide a target-conforming dose distribution while minimizing dosage exposure to healthy tissues [3]. Anatomical

data is collected using two-dimensional (2D) image slices, which are then integrated to form the 3D portrayal. After that, the structures and targets are demarcate using the segmentation technique. The required fields 2–4 and treatment beams are built, and MLC confirms the tumour has appropriate margins. The optimization problem in this case requires modifying constantly several parameters such as number of fields, their aperture, beam weights, their directions and other beam modifiers.

2.2 Intensity modulated radiotherapy

In IMRT, we can achieve a greater dose gradients and a higher level of dosage uniformity within the target (Webb et al., 2001), which is considered advanced than 3DCRT [4]. To allow for greater dose shaping flexibility, IMRT uses non-uniform beam intensities rather than uniform beam intensities. Within the target volume, IMRT can also be used for dose painting, IMRT is a conformal therapeutic technique that not only conforms dose to target volumes, but also to sensitive structures. Conformal therapy is defined as the geometric structuring of a beam so that its contour matches to the target's BEV.

When the target is not appropriately geometrically separated from the organs in risk or When the target wraps itself around organs in danger, or when no combination of uniform intensity beams can reliably separate the target from the organ in danger., then adding modulation to a geometrical beam, it’s possible that using a beam is the only way to properly treat the tumour while reducing the exposure to the nearby OARs. Another potential benefit of IMRT is the ability to simultaneously provide several dosage levels to target volumes. This opens up the possibility of delivering a simultaneous in-field boost to well-located primary tumour locations [5, 6].

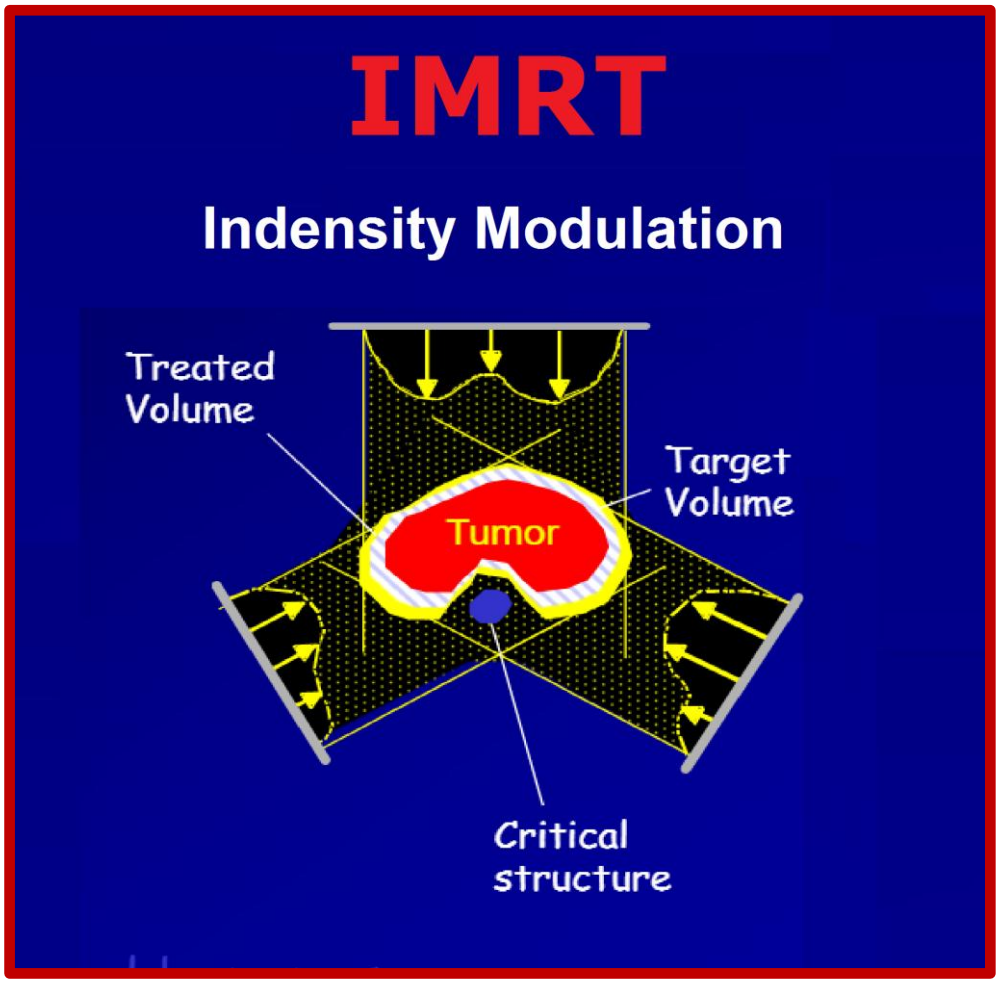

Figure 2.2: The Image Representing IMRT Planning Approach

Inverse treatment planning

One of the key advantages of IMRT over the traditional technique is inverse planning. The person who chooses the beam directions, target dosage goals, and dose restrictions for the OARs structures surrounding the tumor volume is the central concept of it. The user can set the minimum and maximum doses to PTV and OARs, for example [5,6]. TPS automates the optimization process by dividing the beam into smaller beams, known as beam lets, based on the stated requirements. Each beam's intensity is then adjusted to obtain a dosage distribution that is as close to the required as achievable. If the actual dose distribution fails to fulfil the requirements, the optimization procedure can be repeated by changing the treatment plan's goals and limitations.

The disadvantage of IMRT is that it produces a higher number of MU, resulting in a higher integral body dosage and a higher risk of secondary cancers [7].

2.3 Volumetric Modulated Arc Therapy

When VMAT was first presented in 2007, it was described as a new radiation technology that allowed simultaneous change of three parameters during treatment delivery: gantry rotation speed, treatment aperture shape by MLC leaf movement, and dose rate [8]. Yu originally introduced the previous model of arc therapy, known as IMAT, in 1995 [9], and it needed the use of several overlapped arcs to produce a suitable dose coverage [10].

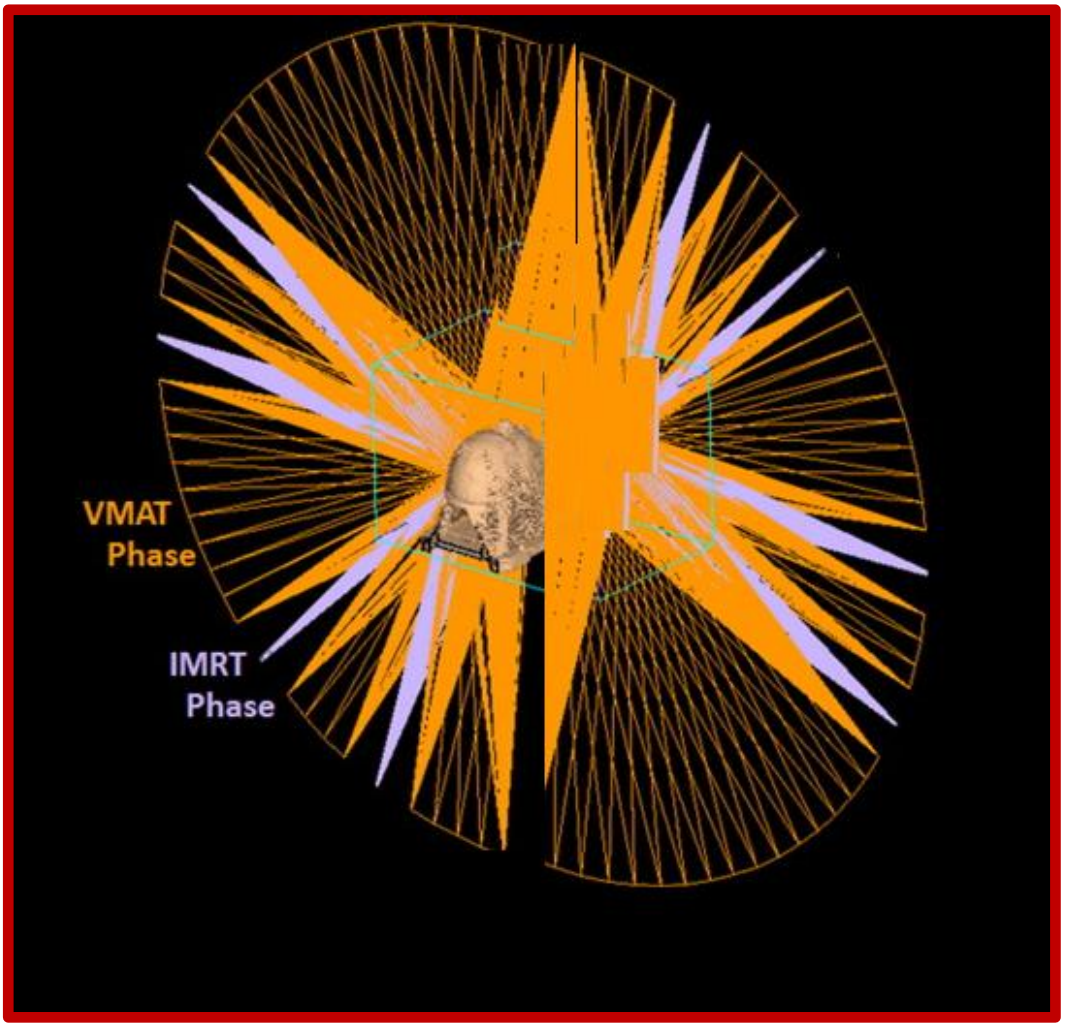

.

Figure 2.3: The Single Image Representing comparison of IMRT and VMAT planning and delivery.

The target is constantly irradiated with VMAT technology, while the source of the beam rotates in single or multiple arcs around the patient (11). A high degree of conformal dose coverage is achieved in substantially less time than with current techniques by simultaneously regulating gantry speed, gantry position, collimator angle, leaves of the MLC and dose rate. VMAT therapy sessions are often completed in 5 minutes or less [12], and include real patient 3D imaging to ensure the target's position.

Several VMAT systems are currently marketed under various names (Rapid Arc, Varian; Smart Arc, Phillips; and Elekta VMAT, Elekta)

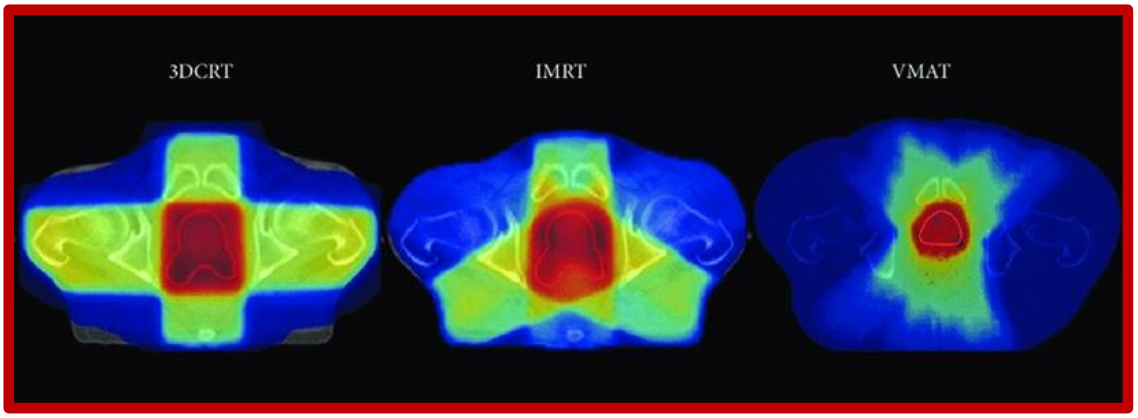

Figure 2.4: The isodose distribution generated from 3DCRT, IMRT AND VMAT Planning with 6 MV Photon energy

2.4 Stereotactic Body Radiation Therapy

This is a type of EBRT that allows massive doses of radiation to be delivered precisely to tiny tumours. SRS techniques and procedures were used to develop stereotactic body radiation treatment (SBRT), which began in the early 1990s at the Karolinska Institute (Stockholm, Sweden). In the late 1990s, Robert Timmerman, Lech Papiez, and colleagues from Indiana University have started a phase 1 trial of SBRT for medically hopeless lung cancer. [13]

Patient positioning devices, tumor identification and tracking software, reducing high-dose radiation exposure to normal tissue, preventing or controlling for organ movements (e.g., respiratory motion), SBRT is characterized by stereotaxic usage and sub-centimeter accuracy of the supplied dosage. [14,15] The shape and stage of the tumour, its volume (1–35 cm3), pathology, invasiveness, and the patient's performance level are all used to determine whether SBRT is an appropriate treatment. Detailed simulation study, Target contouring, better planning, and radiation treatment delivery are all important parts of an SBRT operation.

SBRT has been utilised to treat many small cancers (up to 6-7 cm) as well as a few larger tumours (up to 3-5 cm) across the body. The number of malignancies that have been effectively treated with SBRT in India and around the world continues to rise. The most prevalent cancers include primary lung, pancreas, and bile duct tumours, primary and metastatic liver tumours, kidney, prostate cancer, and other cancers. pelvic tumours, sarcomas, and metastatic cancers throughout the body are among them.

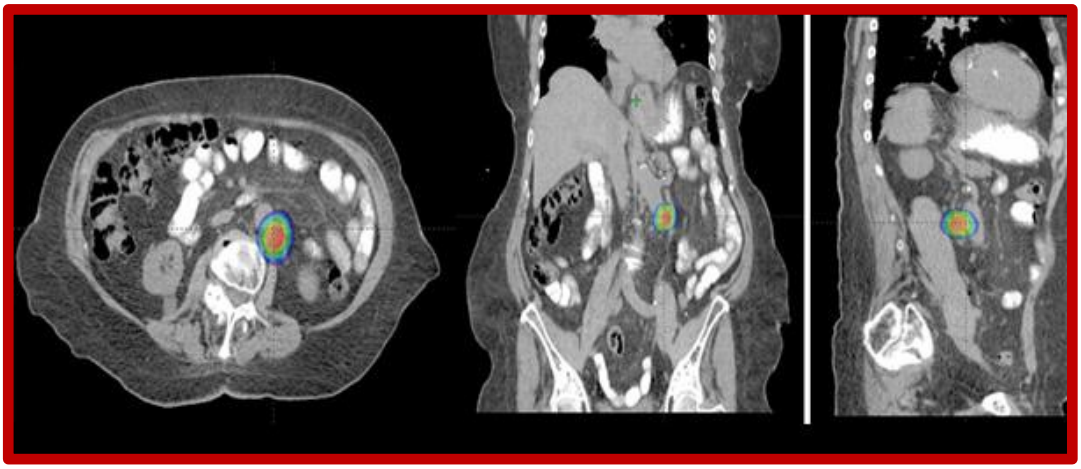

Figure 2.5: The amount of SBRT radiation provided to this site and the isodose distribution obtained by VMAT Planning (axial, coronal, and sagittal) with a 6 MV FFF photon beam as can be seen, the radiation dose is distributed very accurately to avoid as much normal tissue as possible.

This process usually takes 3-5 treatments spread out over a period of 1-2 weeks to complete. This differs from the normal daily EBRT, this is often delivered over a period of many weeks

We may be able to offer SBRT is the recommended treatment option for patients who have previously received a complete dose of external beam radiation therapy and now have recurring but localized cancers in certain highly selected scenarios. SBRT is a still-evolving therapy that necessitates specialist clinical and technical Expertise.

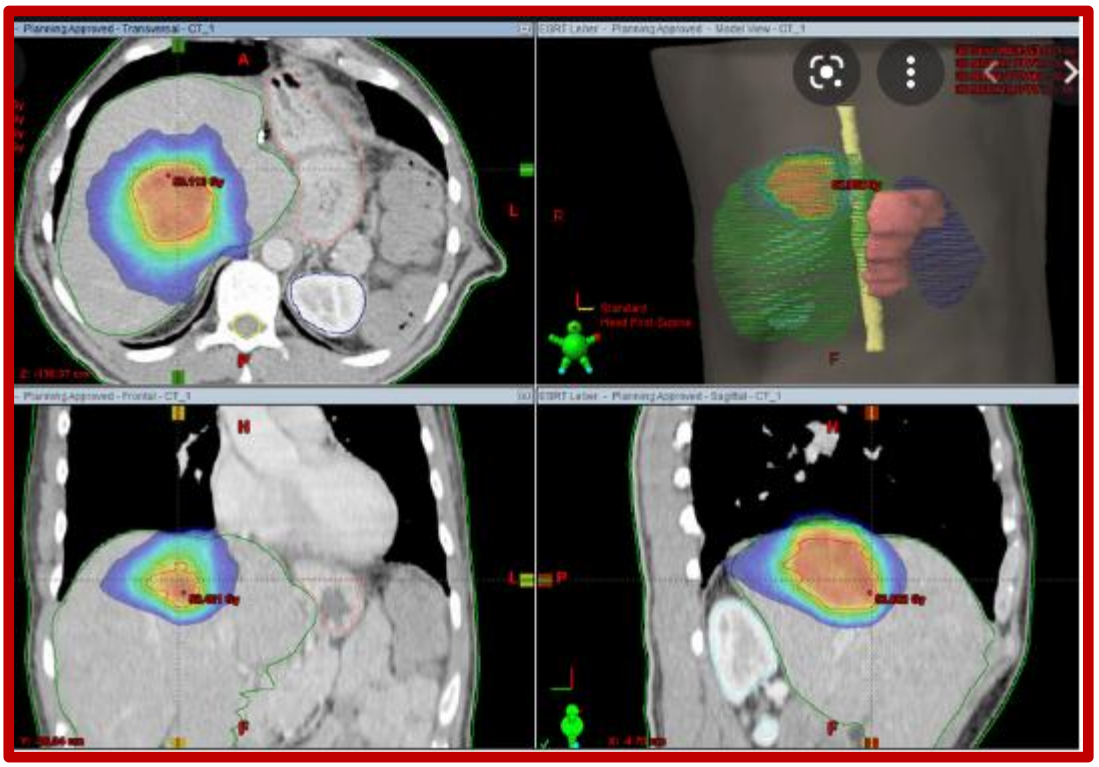

Figure 2.6: SBRT treatment plan of liver metastasis (total dose of 50 Gy with 5x10Gy, 65%-isodose)

2.5 Stereotactic Radio Surgery (SRS)

In 1951, Dr. Lars Leskell and Borje Larsson invented the idea of radiosurgery for the treatment of intractable intracranial disorders. SRS has been used to treat trigeminal neuralgia, arteriovenous malformations, vascular malformations, and benign and malignant malignancies of the intracranial and spinal cavities.

It isn't surgery in the traditional sense because there is no scar. Stereotactic radiosurgery, on the other hand, using 3D imaging, significant doses of radiation can be precisely focused on the afflicted area while healthy tissue in the surrounding area is spared.

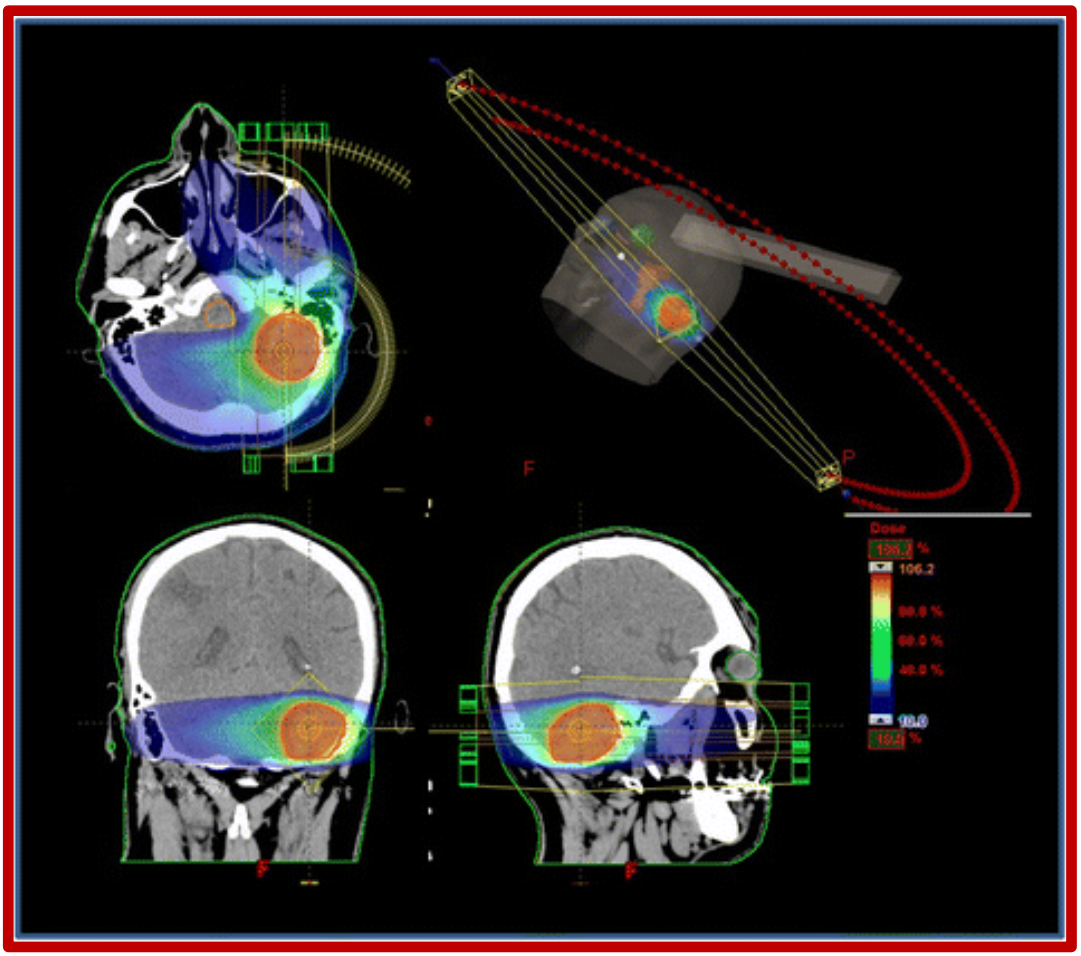

Figure 2.7: Two partial co-planar arcs and volumetric modulated arc treatment are used in SRS treatment for a patient with left cerebellar metastases (VMAT).

In most cases, SRS of the brain and spine may be accomplished in just one session. Lung, liver, adrenal, and other soft tissue malignancies are treated with body radiosurgery, which usually requires many (three to five) sessions.

2.6 Active Breathing Coordinator (ABC)

In radiotherapy, motion is a significant obstacle. It's a problem that has effects across the entire workflow, including treatment planning, imaging, and delivery, and it has

to be addressed immediately. As a result, using Active Breathing Coordinator to manage and coordinate breathing may improve target localization and Allow clinicians to increase the dosage to the tumour by reducing the PTV margin [16].

By extending the distance between the tumour and the crucial tissue by holding deep inspiration breaths, breath-hold therapies with Active Breathing Coordinator can minimize dosage to essential structures like the spinal cord. It enables clinicians and patients to determine an appropriate breath-hold intensity and duration. This allows for potential margin reduction, dosage escalation, and hypo fractionation by immobilizing internal anatomy directly linked to breathing volume.

Figure 2.8: The Single Image Representing ABC breath hold and CT simulation

It can reduce not just the volume of irradiated lung cells, but also the dose to normal tissue in thoracic treatments. One of the problems of radiation therapy for the left breast is preventing dosage to the heart. Using Active Breathing Coordinator with moderate deep inspiration breath-hold (mDIBH) increases lung volume, reducing the dose by increasing the distance between the chest wall and the heart [17-18].

2.7 Treatment Planning System (TPS)

TPS calculates the treatment dose based on the radiation machine's output solely. TPSs are used to create radiation treatment plans based on a CT dataset generated

from a patient's CT simulation. Individual plans are to be optimized using the optimization algorithm, which is commonly used by the TPS for both forward and inverse planning approaches.

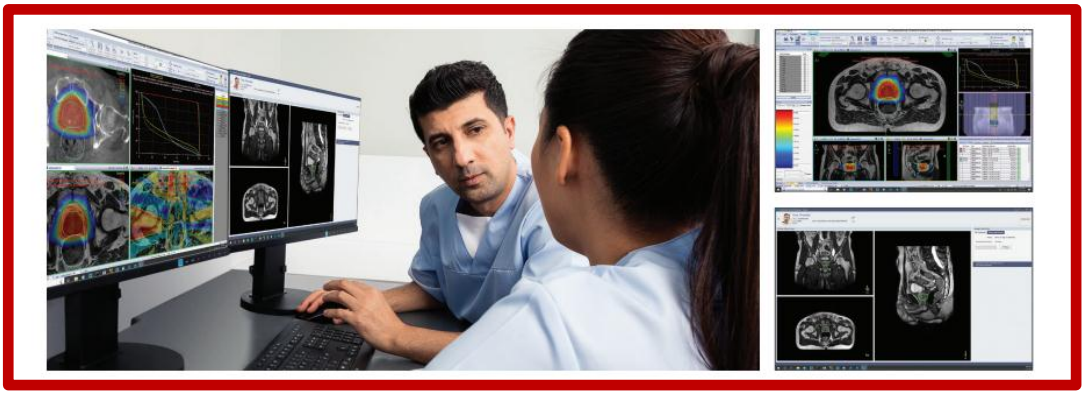

Figure 2.9: The Monaco TPS has been used for radiotherapy treatment plans in this illustration.

The absorb dose is defined as the quantity of ionising radiation/energy absorbed per unit of mass by the tissue/medium. As a result, dose calculation entails computing the energy absorbed by the medium at all points where it may or may not pass through it. Due to interaction between particles and medium, a variety of physical processes occur. At any location of interest, the dose is contributed in three ways. When beam particles interact with the media, energy is released.

Secondary photons and electrons may result from the released energy depositing or scattering away from the initial contact location. For correct dose computation, an appropriate dose calculation algorithm will include both physical processes involved in the beam particle media interaction, and it should be rapid enough for clinic use.

2.8 References

1.Xingsheng Hu, Wenwu He, Shimin Wen, Xuqin Feng,Xi Fu, Yusong Liu, "Is IMRT Superior or Inferior to 3DCRT in Radiotherapy for NSCLC? A Meta-Analysis" PLoS One. 2016 Apr 21.

2. Jemal A, Siegel R, Ward E, Murray T, Xu J, Thun MJ. Cancer statistics, 2007. *CA Cancer J Clin* 2007; 57: 43–66. [PubMed] [Google Scholar]

3. Wagner H. Image-guided conformal radiation therapy planning and delivery for non-small-cell lung cancer. *Cancer Control* 2003; 10: 277–288. [PubMed] [Google Scholar]

4. Hsieh CH, Chung SD, Chan PH, et al: Intensity modulated radiotherapy for elderly bladder cancer patients. Radiat Oncol 2011, 6:75.

5.Cilla S, Caravatta L, Picardi V: et al. Clin Oncol (R Coll Radiol): Volumetric Modulated Arc Therapy with Simultaneous Integrated Boost for Locally Advanced Rectal Cancer; 2011.

6. Lee TF, Ting HM, Chao PJ, Fang FM: Dual Arc Volumetric-modulated Arc Radiotherapy (VMAT) of Nasopharyngeal Carcinomas: A Simultaneous Integrated Boost Treatment Plan Comparison with Intensity-modulated Radiotherapies and Single Arc VMAT. Clin Oncol (R Coll Radiol) 2011, 24:196–207.

7.Hall EJ, Wuu CS: Radiation-induced second cancers: the impact of 3D-CRT and IMRT. Int J Radiat Oncol Biol Phys 2003, 56:83–88.

8.Otto K. Volumetric modulated arc therapy: IMRT in a single gantry arc. *Med Phys* 2008;35:310–7 [PubMed] [Google Scholar]

9. Yu CX, Li XA, Ma L, Chen D, Naqvi S, Shepard D, et al. Clinical implementation of intensity-modulated arc therapy. *Int J Radiat Oncol Biol Phys* 2002;53:453–63 [PubMed] [Google Scholar]

10. Yu CX. Intensity-modulated arc therapy with dynamic multileaf collimation: an alternative to tomotherapy. *Phys Med Biol* 1995;40:1435–49 [PubMed] [Google Scholar]

11.Guckenberger M, Richter A, Krieger T, Wilbert J, Baier K, Flentje M: Is a single arc sufficient in volumetric-modulated arc therapy (VMAT) for complex-shaped target volumes? Radiother Oncol 2009, 93:259–265.

12. Kavanagh BD, Kelly K, Kane M. The promise of stereotactic body radiation therapy in a new era of oncology. Front Radiat Ther Oncol. 2007;40:340–51. [PubMed] [Reference list]

13. Smink KA, Schneider SM. Overview of stereotactic body radiotherapy and the nursing role. Clin J Oncol Nurs. 2008 Dec;12(6):889–93. [PubMed] [Reference list]

14. Read PW. Stereotactic body radiation therapy: 2007 Update. Community Oncol. 2007 Oct;4(10):616–20. [Reference list]

15.Committee on Radiation Source Use and Replacement, National Research Council. Radiation source use and replacement: abbreviated version. Washington DC: National Academies Press Radiotherapy; 2008. pp. 117–33. Also available at http://www.nap.edu/catalog.php?record_id=11976. [Reference list]

16. Partridge, M., et al., Improvement in tumour control probability with active breathing control and dose escalation: a modelling study. Radiother Oncol, 2009. 91(3): p. 325-9.

17. Kashani, R., et al., Short-term and long-term reproducibility of lung tumor position using active breathing control (ABC). Int J Radiat Oncol Biol Phys, 2006. 65(5): p. 1553-9.

18. Hanley, J., et al., Deep inspiration breath-hold technique for lung tumors:

the potential value of target immobilization and reduced lung density in dose escalation. Int J Radiat Oncol Biol Phys, 1999. 45(3): p. 603-11.

CHAPTER -III

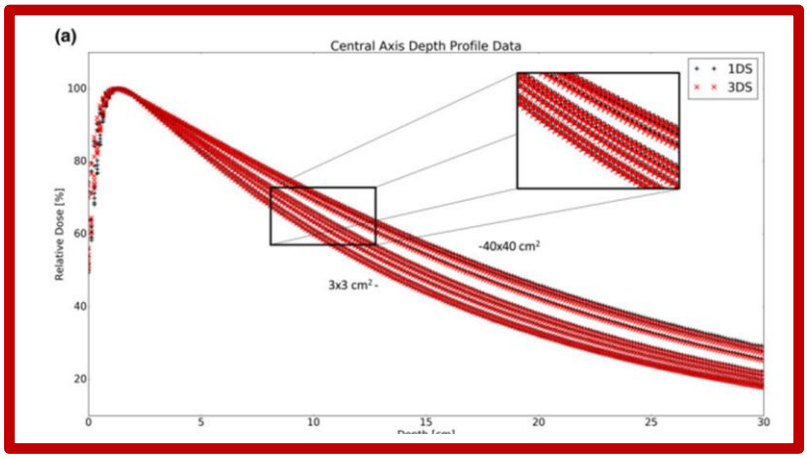

MATERIALS AND METHODS

CHAPTER-III

3.0 MATERIALS AND METHODS:

This study used several dosimetry equipment to commission the FF and FFF based medical linear accelerators.

1. FF & FFF Based Medical linear accelerator
2. Radiation Filed Analyzer
3. Electrometer with ion chambers
4. 2D Array detection

A brief description of the above equipment's is given below

3.1. Versa HD Linear Accelerator

Versa HD is a new medical linear accelerator that was introduced on April 15, 2013. Versa HD has FF and FFF Photon Beams with energies of (6,10,15MV) as well as electron energies. A novel, cutting-edge Multileaf collimator family, developed exclusively for Elekta versa HD, enables for extremely precise dose distribution while considerably lowering dosage supplied to healthy tissues. Versa HD sets the standard for cancer therapy with high-precision beam shaping and tumour targeting, as well as the ability to deliver radiation dosages three times faster than earlier Elekta linear accelerators. Versa HD allows high-definition, high-speed beam shaping over a customizable 40 cm x 40 cm field when fully integrated with the Agility 160-leaf Multileaf collimator (MLC).

Dynamic arc therapy and Step-and-shoot therapy are two working modes for 3DCRT, IMRT, and VMAT techniques that allow for successful treatment. With this unique combination of rapid MLC leaf speed and the new High Dose Rate mode, clinicians can fully leverage high dose rate delivery and push advanced therapies like SRT and SRS to new heights – all while preserving treatment time.

Only the measurement and modification of photon beam data for FF and FFF will be investigated in this study.

Figure 3.1. Versa HD machine Capable of deliver the FF and FFF Beam

3.2. Radiation Filed Analyzer (PTW Freiburg)

Radiation field analyzer (MP3-PTW Freiburg) used to measure FF & FFF beam parameters contain water phantom, lifting table, Main Control Unit (MCU) with integrated dual channel electrometer, water reservoir and TMR set. The positional reproducibility is ± 0.1 mm and the positional accuracy is ± 0.5 mm. The approximate volume of the water phantom is 206 litres. The water phantom has the Mylar foil window of thickness 0.1 mm for lateral beam scanning. The detector holder material is made up of Poly vinylidene fluoride (PVDF) which is near to air density. Water phantom is placed on motorized double telescope lift table mechanism. The maximum table load capacity is 250 kg. The vertical travel range is 740-1240 mm from the finished floor level. The leveling table plate thickness is 19 mm. The vertical range for leveling frame adjustment is 20 mm and horizontal

adjustment is 15 mm. The MCU has the dimension of 390 x 75 x 360 mm3. The operating polarizing voltage is between -400 V to +400 V. The time constant is 40 ms and it contains 14-bit Analog to Digital Converter (ADC) for optimized gain control. The maximum resolution is 0.1 pC with low range and 30 pC with high range. The leakage current is <0.5 pA with low range and < 2 pA with high range. The MCU can communicate to computer through RS232 connectivity.

Figure 3.2. MP3 Water phantom system (RFA) –PTW Freiburg GmbH

The Semiflex chamber used for measurement has a measuring volume of 0.125 cm^3 with outer diameter of 7 mm with an air cavity length of 10 mm and central electrode diameter of 1 mm. The outer wall is made up of Poly Methyl Methacrylate (PMMA) with thickness of 0.12 g / cm2 and inner wall is graphite / epoxy with the thickness of 0.07 g / cm2. The Semiflex ion chamber detector used for measurements is shown in Figure 3.16. High-energy photon and electron radiation are measured in waterproof thimble chambers.

3.3 Ion Chambers (PTW Freiburg)

3.3.1. Model 31010 0.125 cm^3 Semiflex ion chamber

The Semiflex chambers are used for therapeutic dosimetry, primarily in motorized water phantoms, to measure dose distribution. They have a flexible connection cord and a short stem for mounting. The nominal practical energy range for photons is 30 kV to 50 MV, and for electrons it is 6 MeV to 50 MeV. The wall is made of graphite and is protected by an acrylic coating. The guard rings are made to fit the volume of the measurement device. Each chamber includes an acrylic build-up cover for in-air 60Co beam measurements and also a calibration certificate for absorbed dose to water or in-air kerma calibration. Each measurement must be corrected for air density. Both chambers have a cylindrical shape and a 5.5 mm inner diameter; the only difference is the length of the measuring volume. We used two Semiflex chamber for beam data measurement .Semiflex chamber we used to take measurement for following filed sizes **5x5,10x10 ,15x15, 20x20, 30x30, 40x40 cm2** and For small filed we used SRS Diode chamber

• Water phantoms with ventilated responsive volumes of 0.125 cm3 and 0.3 cm3 are suitable for application.

• Over a wide energy range, there is an uniform energy response.

Figure 3.3: 0.125 cm^3 Semiflex ion chamber (PTW Model 31010)

3.3.2 Dosimetry Diode SRS Type 60018

Dosimetry with a waterproof silicon detector in 6 MV photon beams up to field size. **2x2, 3x3 , 5x5 , 10x10 cm^2**

The Diode SRS is intended for dose measurements in photon fields of up to 10 10 cm2 with a maximum energy of 6 MV. It is feasible to measure beam profiles with high resolution and a low dwell time thanks to this detector's great responsiveness. A common use is the measurement of small filed beam profiles for stereotactic radio surgery (SRS).

- A detector with a maximum photon Energy of 6 MV was designed for measurements in small photon fields.
- Outstanding spatial resolution
- A high level of response
- Extremely low noise
- A thin entrance window can be used to take measurements near surfaces and interfaces

Figure 3.4: Diode SRS (PTW Model 60018)

3.3.3 N 34045 Advanced Markus®

In this investigation, we employed an advanced markus chamber and a Model N34045 Advanced Markus® Plane Parallel Ion Chamber to evaluate surface dosage. The Advanced Markus® chamber, Model N34045, is the most recent advancement in electron chamber technology, with better performance over the well-known Markus® chamber. Within the nominal useable range of 2 to 45 MeV, the chamber has a flat energy response. The Markus® chamber's design is comparable to the Model N34045's, with the same external dimensions. It fits into the Markus® chamber's existing solid phantom cavities as a result. Internal dimensions are comparable to the Markus®, with the addition of an enhanced guard ring design and 1 mm electrode spacing. The impact of scattered radiation beam from the housings is greatly decreased as a result of the high level of shielding, allowing for absolute electron dosimetry without perturbation effects. The chamber's modest sensitivity capacity makes it ideal for assessing dose distribution with high spatial resolution in water phantoms. The entry window is made of 0.03 mm thick polyethylene. The Model N34045 comes with a 0.87 mm thick protective acrylic cover for use in water. Because the chamber is evacuated to the atmosphere, each measurement must be corrected for density. It comes with a 1-meter cable, a variety of connections, and a foam-padded carrying box.

In this study Markus chamber used for Surface dose measurement for 6FFF and 10FFF beams.

Figure 3.5: Advanced Markus® Chamber (PTW Model N 34045)

3.4. Electrometer with ion chambers (Unidos, PTW)

The UNIDOS is high-precision reference class electrometer that significantly fulfills the recommendations of International Electro technical Commission (IEC 60731). The UNIDOS E electrometer used in our study is shown Figure 2.5.

Figure 3.6: UNIDOS E electrometer (PTW Model T10010)

The electrometer's primary screen has a large, high-contrast graphic electro luminescent display with a wide viewing angle that shows all measured values, selected chambers, and correction factors in detail. It is capable of concurrently

measuring and showing the measured dosage, dose rate, current, charge, average rate, and dose per monitor unit. The maximum operating bias voltage is ± 400 V, programmable in steps of ±50 V. The mains operating power supply is 90 – 240 V, 50 / 60 Hz, the battery operational is optional. UNIDOS E can

be connected to personal computer through bidirectional Recommended Standard 232 (RS-232) port. The leakage through electrometer is < ±1 fA. The electrometer has a linearity of < ±0.5% in the whole range. The FC65-G Farmer chamber is a water proof vented ion chamber suitable for electron and photon beam dosimetry. It‟s sensitive volume is 0.6 cc. The outer electrode wall material is graphite and the inner electrode is made up of aluminum. The recommended polarizing voltage is +400 volt and the leakage < 4 x 10 - 15 A. Former chamber used in this study for absolute dose measurement

Figure 3.7: 0.6cc Farmer chamber (PTW Model 30013)

3.5. 2D Array detector (PTW 4D Octavius system)

The 2D-Array is made up of 729 vented plane-parallel ionization chambers with a 0.6 g/cm2 graphite wall that are organized in a 27 x 27 matrix and cover a 27 x 27 cm2 area. The 2D array detector used in our study is shown in figure 3.17.

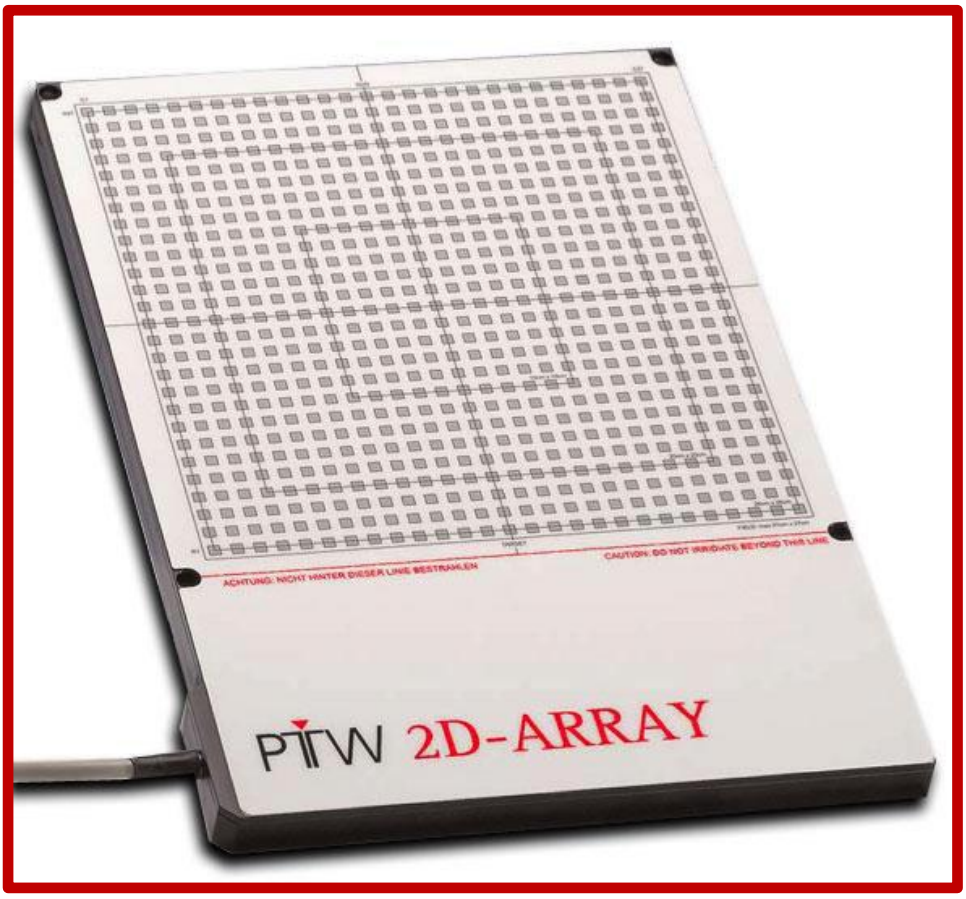

Figure 3.8: Schematic view of PTW Seven29 2D array

Each chamber has a cross section of 5 mm x 5 mm and a height of 5 mm and is air-filled. The chambers are separated by 5 millimeters. The distance between adjacent chambers' centres is 10 mm. Poly methyl methacrylate makes up the 2D array that surrounds the substance (PMMA).

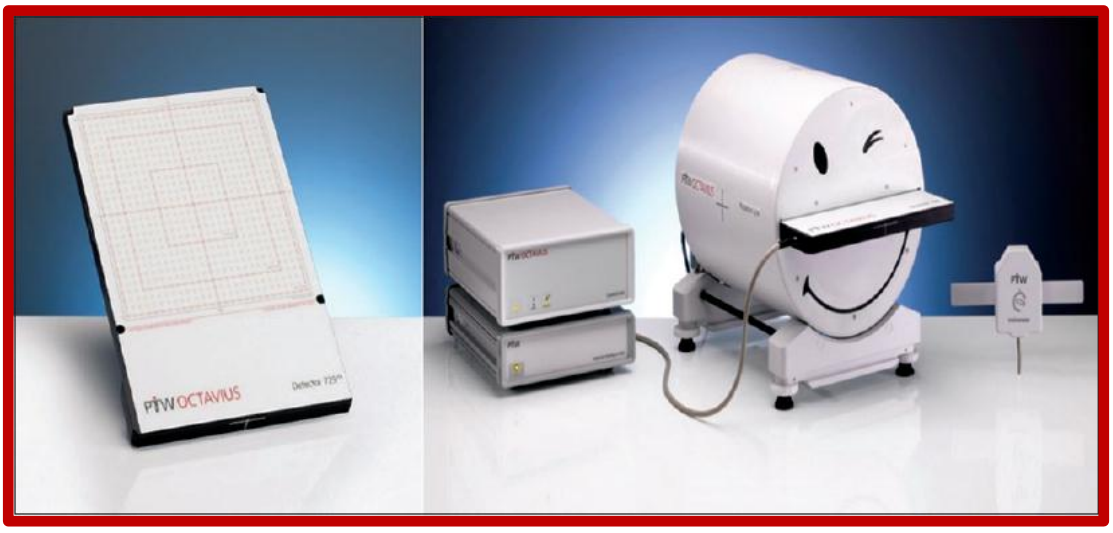

Figure 3.9: 2D- ARRAY inserted in a 4D Octavius phantom.

3.6. Measurements of beam data

The algorithm was commissioned for clinical use of 6,10,15 MV photon beams and for 6FFF and 10FFF beams. Commissioning was done by measuring beam data as required by Monaco treatment planning system for Monte carlo dose calculation algorithm. Machine specific beam data at reference condition were acquired using RFA and other dosimetric detectors as recommended. Beam data requirements includes PDD, open beam profiles along cross plane for different field sizes. Smallest field size used for measurement is 3x3 cm2 and the largest being 40x40cm2. Moreover, output factors were also measured by placing the detector at central axis at reference depth. Additionally, Diagonal profile for the maximum field size 40x40cm2 were also acquired.

PDD are measured along central axis up to the depth of 30 cm in water. Open beam profiles are acquired at five different depths (Dmax, 5,10,20 and 30cm) and the scan limit is 35mm beyond 50% dose laterally. Output factors are measured in SSD 95cm with detector placed at 5cm depth in water deeper than the electron contamination range. Reference dose in Gy for reference MU at the calibration depth at 10x10 cm2 were measured. Measurements of profile & PDD for Add-on materials includes MLC transmission factor for each photon energy, dosimetric leaf gap for modeling of the rounded leaf edge transmission were also performed.

3.7. Patients specific QA

After patient's plan is approved, the plan needs to be verified. This is normally accomplished via a composite plan or a field-based technique. The patients plan was transferred to PTW Versoft. The PTW 4D octavius phantom with seven29 array dector setup as per PTW manual procedure. The senven29 ionization chambers can sometimes require a warm-up time and/or dose before irradiation.

VeriSoft is a software package used for reconstructing the dose fluence maps to these measuring points. The software package also evaluates the resemblance of dose fluence maps with gamma analysis. Dose distributions and comparisons are evaluated numerically and graphically in three-dimension. Radiation dose to the phantom from the specific plans were calculated in TPS. plans were delivered to phantom and measured using 729 detector arrays. Using VeriSoft software the calculated and measured dose fluence maps were compared. Doses were compared in coronal, sagittal and transversal directions.

8. Gamma analysis 2D

Under normal clinical conditions, patients were utilized to assess the delivery of treatment regimens. With a single Arc, VMAT plans with 6 FFF were constructed. Each design was recalculated using an initial grid spacing of 2.5 mm and then 5 mm on a CT dataset of the 4D Octavius phantom. Inhomogeneity corrections were deleted during import into the planning system to guarantee that variations in Hounsfield units of a static detector/phantom did not introduce mistakes. A 2D standard global gamma threshold of 3% /3 mm with a 10% minimum threshold was used to compare each plan to the computed plans after delivery.

CHAPTER -IV

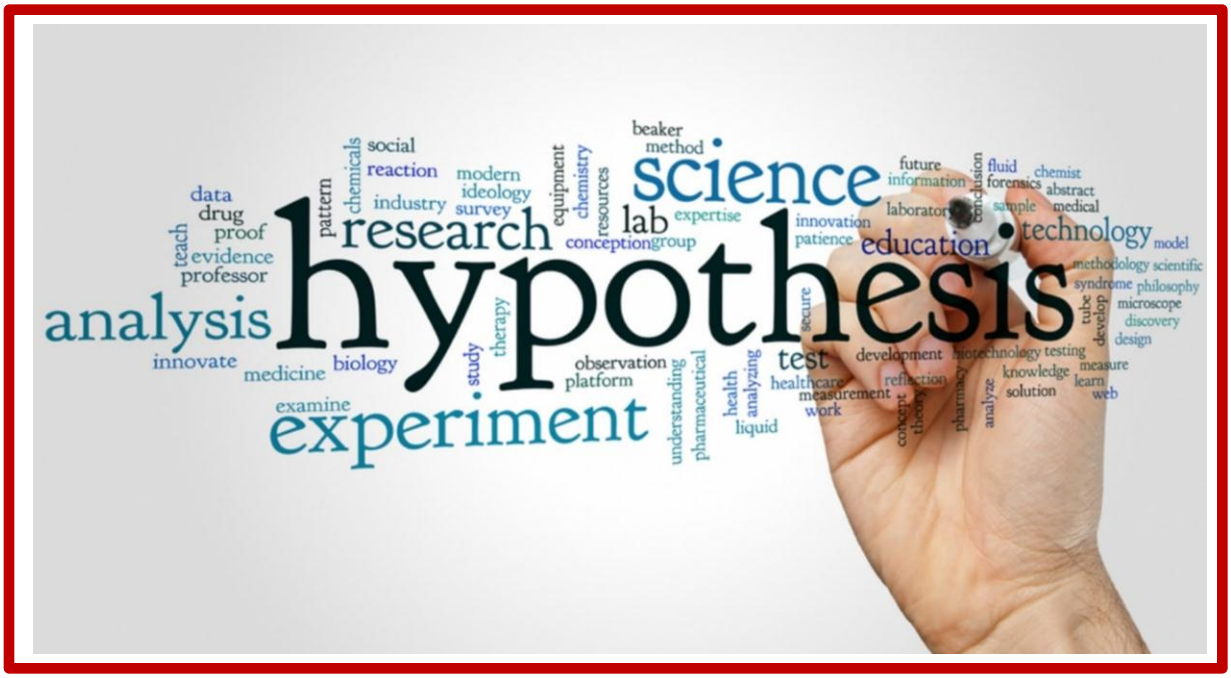
hypothesis
science
research
analysis
experiment
technology
education
lab
test
data
drug
proof
evidence
professor
teach
pattern
chemicals
social
reaction
industry
modern
ideology
survey
equipment
chemistry
resources
beaker
method
conception
group
expertise
innovation
patience
laboratory
future
information
fluid
forensics
chemist
abstract
sample
medical
methodology
scientific
syndrome
philosophy
microscope
discovery
design
measure
learn
web
knowledge
solution
analyze
pharmacy
reflection
development
biotechnology
testing
healthcare
measurement
work
health
analyzing
liquid
pharmaceutical
understanding
observation
platform
study
therapy
secure
innovate
medicine
biology
examine

CHAPTER-IV

4. Aims of the work

The goal of the study presented in this thesis was to investigate the dosimetric effect of removing a flattening filter from a medical linear accelerator.

1. The first goal was to commission and analyze basic dosimetric parameters of FFF photon beams, as well as to compare them to flattened photon beams produced at 6 MV and 10 MV using a Versa HD advanced linear accelerator.

*** The objective of this project was to correctly commission the new VERSA-HD (Elekta®) FFF beams in Monaco TPS and determine the variations in BEAM characteristics between FF and FFF beams.**

2. The second goal was to assess the Implementation of a FFFB in various cancer types and determine the dosimetric difference in plan quality between flattened and non-flattened beams.

* **Dosimetric comparison of flattened and flattening filter-free beams for liver stereotactic body irradiation in deep inspiration breath hold, and free breathing conditions- (small tumour)**

*** Study of Treatment Techniques for Ca Cervix Using Flattened and non-flattened beams.**

3.The third aim was to evaluate the important role of Angular space/increment size parameters in advance treatment techniques and find the suitable Angular space/increment size for VMAT.

* **Dosimetric characteristics of VMAT plans with respect to a different increment of gantry angle size for Ca cervix**

CHAPTER -V

Flattening Filter-Free Beam-Based Medical Linear Accelerator Commissioning and Dosimetric Characteristics

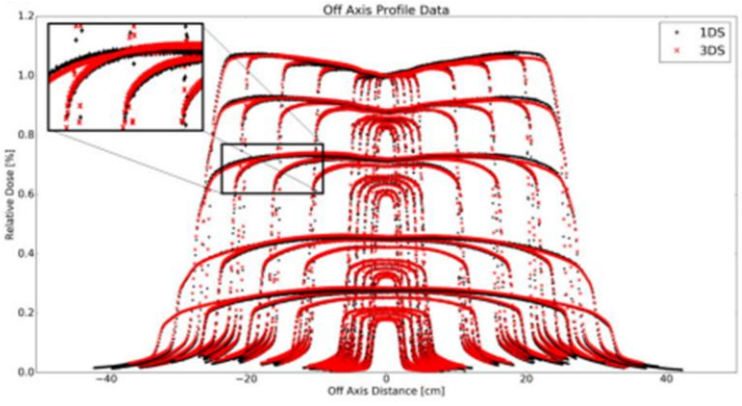

CHAPTER-V

Flattening filter-free beam-based Medical linear accelerator commissioning and dosimetric characteristics

5.1 Introduction

Elekta Versa HD is a modern linear accelerator that was released in 2013. (Elekta medical Systems, Crawley, UK). It can produce photon beams that are flattened and flattening filter free, as well as electron beams. It is a new Elekta Versa HD accelerator platform with numerous critical aspects that differ from the Clinic series. The versa HD machine offers a high dose rate, for 6 MV FFF beams, dose rates can reach 1400 MU/min and for 10 MV FFF beams dose rates can reach up to 2400 MU/min.

Versa HD with Agility 160-leaf Multileaf Collimator (MLC) also delivers highly conformal beam shaping, which is crucial for maximizing dosage to the target while conserving healthy tissues in the surrounding area. Importantly, this great targeting accuracy is available over a wide field-of-view, allowing high-definition (HD) beams to be delivered to a wide range of complex targets.

Due to the removal of the flattening filter, a new type of FFF technology aims to provide faster treatment by increasing dose rate and reducing head scatter and leakage radiation with lower out-of-field dose. FFF is expected to be used largely in SRT or hypo fractionated treatment with dosage per fraction escalation. When delivery time is limited, for respiratory gated or breath-hold treatments, a high dosage rate may be beneficial.

The parameters of FFF beams from various linear accelerators have been summarized in a number of publications based on Monte Carlo based dose calculations or dosimetric measurements. FFF beams have already been employed in medical practice in tomotherapy machine [1,2. MD Anderson Cancer Center

published a MC analysis of Clinac 2100 6 & 8 MV FFF [3,4]. Later, with a Varian Clinac 21EX FFF prototype, the same group of writers measured 6 MV and 18 MV FFF beams [5]. Dosimetric characteristics of 6 and 10 MV FFF photons from 2 machine (Elekta Precise) FFF prototypes are also available [6, 7]. For the Elekta SL25 model, Parsai et al. published an MC simulation of photon FFF beams (6 and 10 MV). Versa HD is the first C-arm linear accelerator to use FFF bundles in clinical practice, allowing for the creation of FFF beams of variable field size, limited only by the physical restrictions of the accelerator's collimator.

Despite the fact that Versa HD has been installed in a large number of hospitals around the globe, there is a lack of understanding about how to commission and carry out the various measurements as per guidelines, as well as validate the dosimetric data for modern linear accelerators, which adds to physicists' workload. We present a framework based on our commissioning and data validation experience with the Versa HD linear accelerator, which is the second installation in India, that describes the current accelerator's dosimetric features and compares our findings to previous evidence on FFF technology, emphasizing the importance of accurately measuring and modelling the dose distribution they deliver.

This chapter contains a report on the precise commissioning and investigation of the dosimetric properties of flattening (FF) and flattening filter free (FFF) photon beams generated by an Elekta versa HD medical accelerator at 6 MV and 10 MV. These properties include the accuracy of commissioning/Modeling Elekta versa HD photon beam energies in the Monaco TPS using a Monte Carlo dose calculation algorithm, as well as the percentage depth dose, dose rate, beam profile, out-of-field, energy spectra, scatter factor, surface dose, and the accuracy of commissioning/Modeling Elekta versa HD photon beams in the Monaco TPS

5.2 Materials and methods

5.2.1 Advanced Medical Linear accelerator

The new Versa HD machine can deliver flattened and unflattened photon beams (6 MV &10 MV) and electron beams (4, 6, 8, 9, 12, and 15 MeV). The flattening filter was installed in the treatment head of a medical accelerator to produce a nearly equal dose at a particular depth and to flatten the conical-shaped photon beams created by the bremsstrahlung phenomena. The FF is usually bell-shaped and made of high-Z material. Elekta versa HD, on the other hand, has the option of removing the flattening filter, resulting in high dosage rates along the Center axis, with dose rates for 6 MV FFF beams is 1400 MU/min and 10 MV FFF is 2400 MU/min.

The four photon beams are also known as 6FB, 10FB, 6FFFB, and 10FFFB. The following dose rates are available for these bundles:

- 6FB &10FB: 100 to 600 MU/min,
- 6FFFB: 400 to 1400 MU/min,
- 10FFFB: 400 to 2400 MU/min.

Versa HD is in charge of beam creation, guiding, and dose calibration for each bundle individually. When the flattening filter was removed, the machine output remained unchanged, and absolute measurement was performed for a flattened beam. The AAPM TG-51 formalism [8] was used to calibrate the photon beams, with 100 MU equaling 100cGy at Dmax at SSD 100 cm and a field size of 10x10 cm^2.

5.2.2 Multi-leaf collimator

A pair of sculpted diaphragms attached orthogonally to the Multileaf collimator establishes the maximum field size of the Elekta Versa HD, which is 40 x 40 cm^2

(MLC). The MLCs replace the jaws in an orthogonal orientation, therefore there are no backup jaws or diaphragms. The 80-pair interdigitating MLCs have an estimated leaf width of 5 mm at the isocenter throughout all leaves. The Agility collimator uses 9 cm thick tungsten MLCs with a 3.5 cm/s leaf speed. The carriage can go up to 3 cm/s, resulting in an MLC speed of 6.5 cm/s. Leaf location is exact with the Rubicon optical tracking system (Elekta). [9].

MLCs have a tongue-and-groove interleaf gap of less than 0.1 mm and are defocused from the source to reduce interleaf leakage. The primary collimator speed of the Agility collimator is 9 cm/s, and the isocenter clearance is 45 cm. [10] Unless otherwise noted, all measurements were collected using the International Electro Technical Commission (IEC) 1217 requirements with a gantry and collimator angle of 0°.

5.2.3 Beam data acquisition:

After thoroughly testing all of the mechanical characteristics of the Elekta Versa HD, the beam data was obtained according to the guidelines of the AAPM TG-106 methodology. A PTW MP3-M water tank (PTW, Freiburg, Germany) with a scanning range of 50 X 50 X 40 cm3 was used for the measurements. The chamber was mounted at the vertical level of the linac isocenter using PTW's TRUFIX technology after accounting for the shift for the chamber effective point of measurement (EPOM). Prior to acquisition, a radiation beam center check was done to ensure that the chamber was aligned with the horizontal plane's center axis (CAX). Photon PDD measurements were conducted along the CAX for both the ionization field and the reference using a PTW Semiflex 31010 chamber with a 0.125 cc active volume. A PTW 60018 Diode SRS (active volume = 0.03 mm^3) was used to acquire PDD data once more. In-plane and cross-plane photon profile

scans were performed using a PTW Semiflex 31010 chamber and a PTW 60018 Diode SRS. The acquisition sampling time for PTW Semiflex was set to 0.3 s, while it was set to 0.6 s for PTW 60018 Diode SRS.

PTW's MEPHYSTO mc^2 navigation software was used to process all of the scanned PDD and profile scans. A least-squares approach was used to smooth the PDD data, which was then interpolated to 0.2 mm spacing and normalized to 100% at the depth of maximum dose (dmax). By correcting for CAX's positional deviation, the smoothened profile scans were rendered symmetric. The CAX data were normalized to 100 percent of the beam profiles. The raw and processed PDD and profile data were compared to ensure that the shapes were identical.

5.2.4 PDD & Profiles

All beam data was obtained in a large water phantom (50 X 50 X 40 cm^3) with a 90 cm gap between the source and the surface. For 11 distinct field sizes, percentage depth dose curves (PDDs) were obtained:

MEASURED FIELD SIZES										
1x1 cm^2	2x2 cm^2	3x3 cm^2	4x4 cm^2	5x5 cm^2	7x7 cm^2	10x10 cm^2	15x15 cm^2	20x20 cm^2	30x30 cm^2	40x40 cm^2

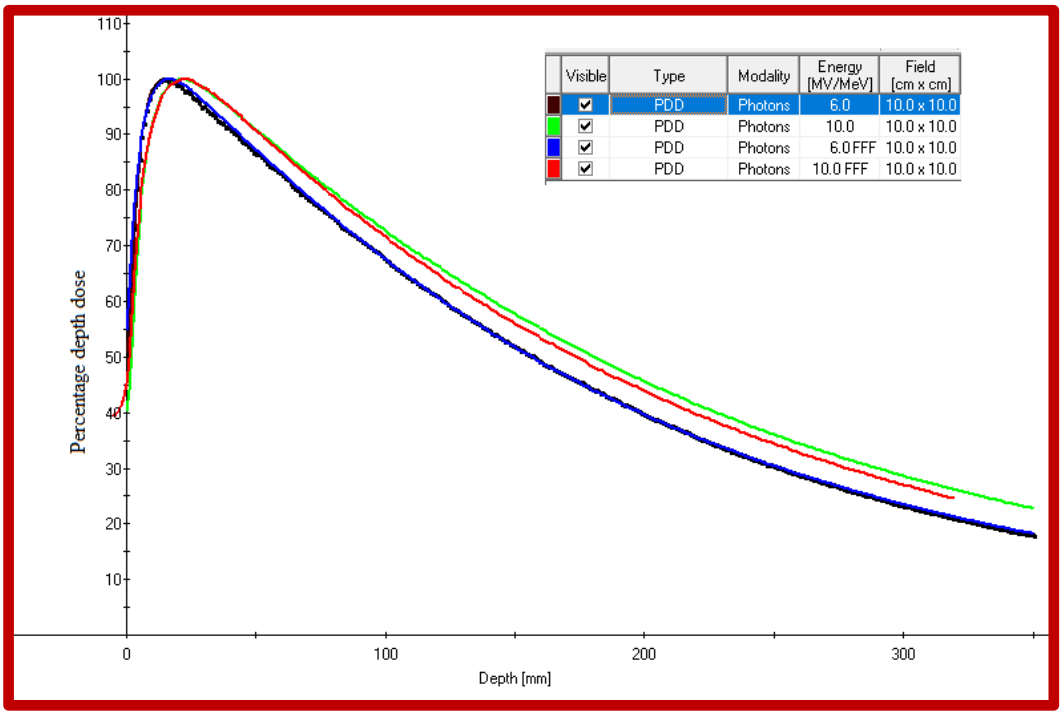

Figure 5.1: PDD Comparison of measured 6FB,6FFFB and 10FB,10FFFB at for reference Field size

In-plane and cross-plane profile scans were obtained at various depths (dmax, 5 cm, 10 cm, and 20 cm) for different field sizes indicated below.

MEASURED FIELD SIZES							
2x2 cm^2	3x3 cm^2	5x5 cm^2	10x10 cm^2	15x15 cm^2	20x20 cm^2	30x30 cm^2	40x40 cm^2

For field sizes more than 3x3 cm^2, PDD and profile were measured with cylindrical chamber volume of 0.125 cm^3. whereas for smaller field width, diode SRS (PTW 60018) was used to prevent the partial volume irradiation effect seen in the larger chamber. Using the MEPHYSTO mc^2 software, the raw profile scans were treated with a smoothing filter and interpolated in 0.2 mm steps (PTW). Flatness, symmetry, horn, and penumbra were characterized inside the centre 80% of the processed profile's full width at half maximum (FWHM). (10) Flatness is defined as the maximum ratio between any two data points inside the specified

region (100 Dmax / Dmin), whereas symmetry is defined as the maximum ratio between two symmetric data points. (100 D(x) / D(-x)).

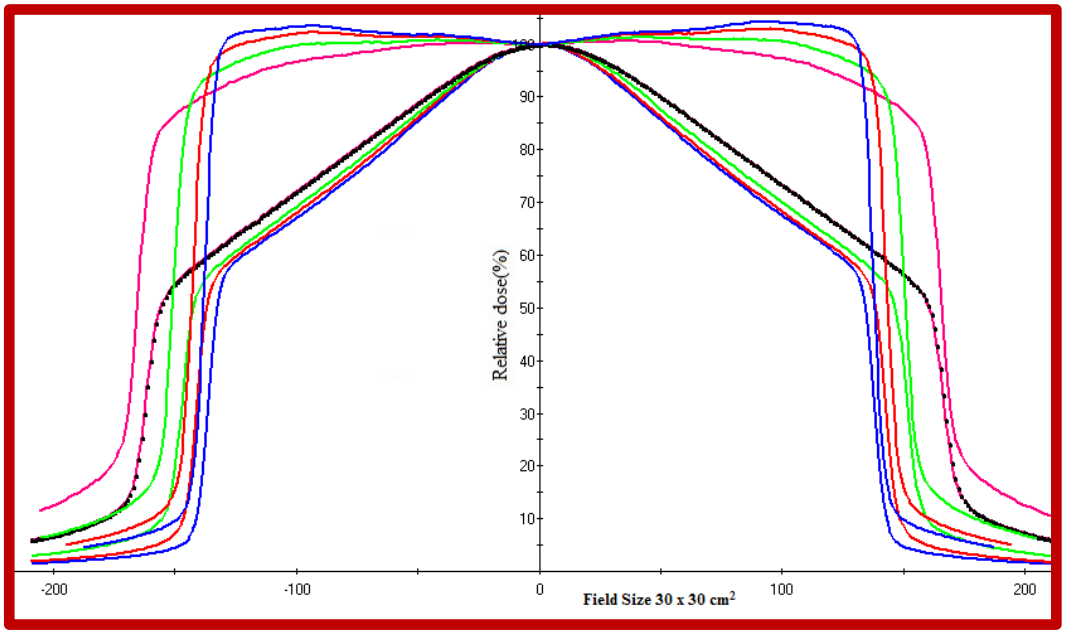

Figure 5.2: Profile Comparison of measured 6FB,6FFFB at all measured depths Dmax,5,10,20cm for field size of 30 x 30 cm^2

5.2.5 Surface dose

The surface dose was calculated using an advanced Markus chamber (PTW34045-0.02cc Parallel Plate Chamber) in a solid water phantom. We compared the chamber's reaction to measurements of no build-up and 1 mm solid water build-up at the depth of maximal dose

.5.2.6 Penumbra evaluation

Penumbra is defined as the spatial distance between the 80% and 20% of the CAX value in the profile scan of a flattened beam.

In FFF a difference in position between 80% and 20% relative dose point of a profile - cannot be applied to FFF beams normalized to the central axis, as dose inside a field can be as low as 30 % depending on the beam's energy and field size **figure 5.4 &5.5.** To overcome this limitation, P¨onisch et al [11] proposed for FFF

beams normalization to the inflection point of a profile's penumbra. The same normalization is used in our study.

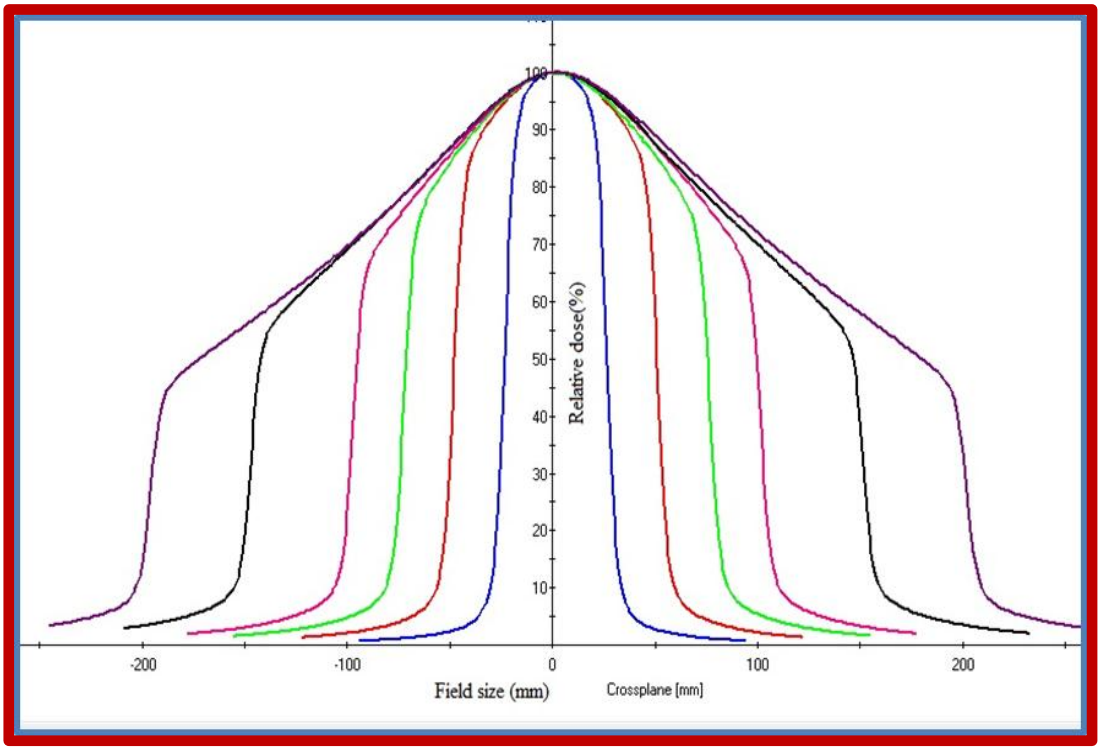

Figure 5.3: 6 FFF Profile at for the 30 x 30 cm^2 field at depths of Dmax,5,10,20cm

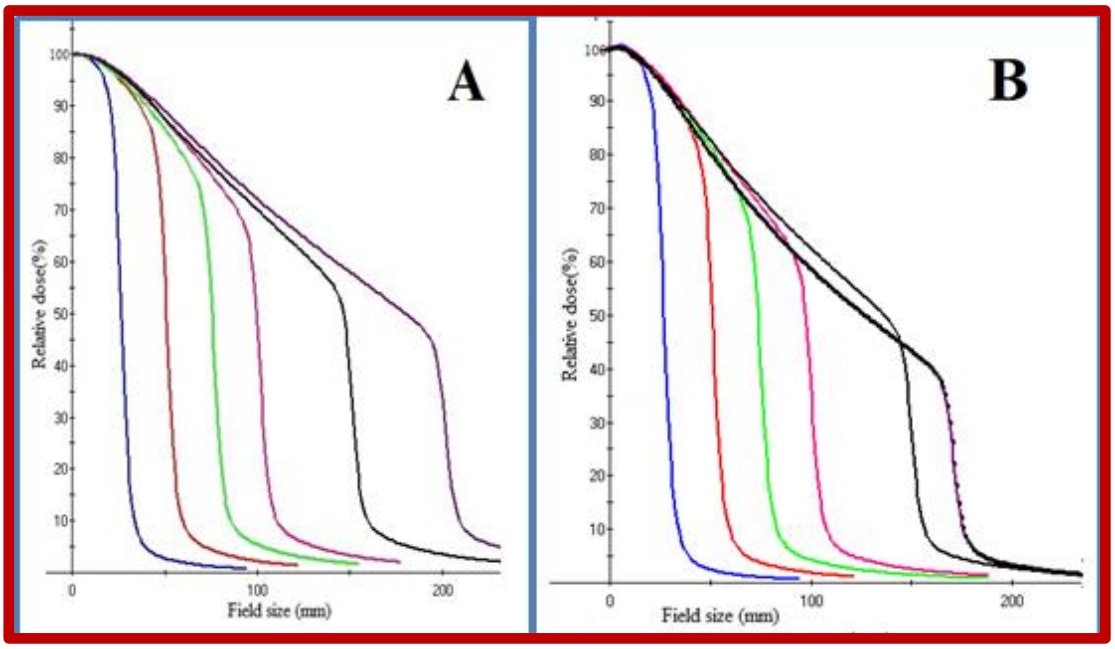

Figure 5.4: Measured profiles for all field sizes at 10 cm depth for X6FFF (A) And X10FFF (B)

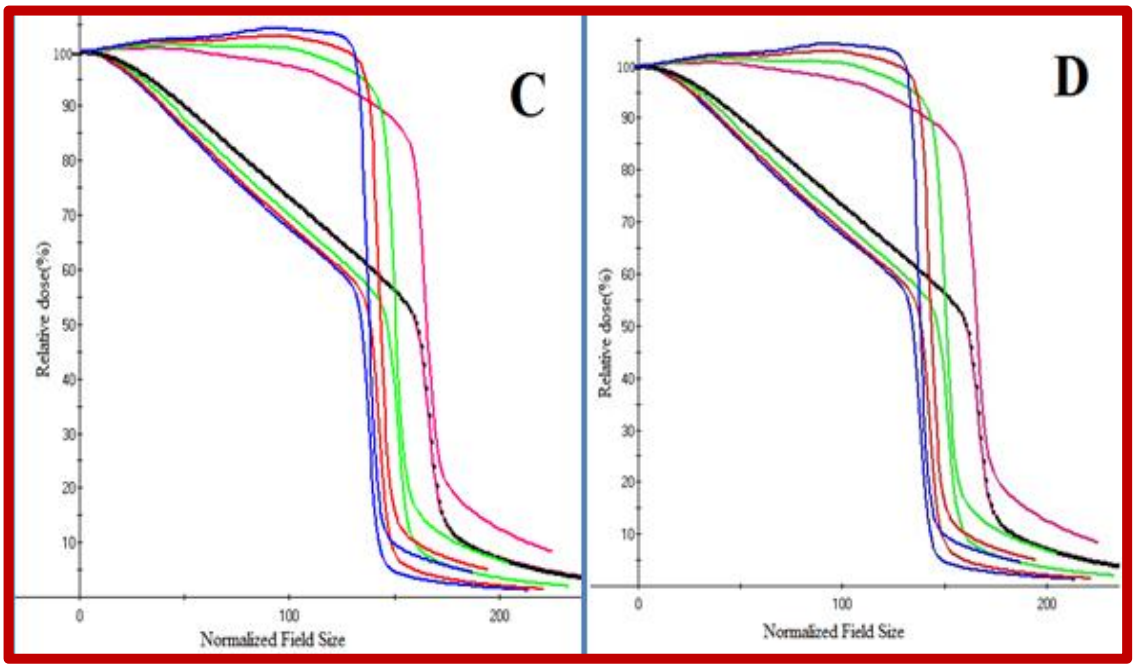

Figure 5.5: For the 30 x 30 cm^2 field at all measured depths Dmax, 5, 10, 20 cm for 6 FB and 6FFFB(C) and 10FB and X10FFFB (D).

5.2.7 Out of field dose

A half-profile of a dose up to 40 cm off the central axis was measured for X6, X6FFF, X10, X10FFF for the following depths and field sizes to determine out-of-field dosage:

• field size: 5x5 cm^2, 10x10 cm^2

• depth: 5 cm, 10 cm, 20 cm

5.2.8 MLC Transmission

The assessment of MLC transmission can be done in two ways, although we used point dose measurement. Under the various points of the patient plane with SSD 100 cm, point dose measurements were taken using a PTW 0.6cc farmer chamber and a UNIDOSE electrometer.

The ratio of the greatest closed-field reading to the open-field reading at the CAX was used to calculate the leaf transmission factor for each of the energies. The maximum transmission suggested by the IEC for MLCs is 1%. [14]

5.2.9 Beam modeling and evaluation of the model

Modeling in Monaco® TPS

In Monaco® 5.0 treatment planning systems, measured 6FFF and 10 FFF beam data were used to generate linac, Monaco TPS can simulate photon sources, electron contaminate, off-axis softening, profile correction, collimator, and multi-leaf collimator (MLC) parameters (transmission, tongue and groove, leaf width etc). While the Elekta expert ®'s team built the Monaco® model externally, the Monaco TPS includes the positions, sizes, and weights of primary and secondary Gaussian X-photon sources.

The secondary photon source is usually located near the bottom of the primary collimator; however, this can be altered. The sizes and spectra of primary and secondary photon sources are unique to Monaco®. These spectra are also affected by the angle of the beam with respect to the main axis, allowing for off-axis softening modelling [15].

Models were generated externally in Monaco®. The virtual source modelling (VSM) of the linac is used to avoid full simulation of the treatment unit source and head., while patient dose distribution is determined using MC. The model parameters are initially established using reference values that are representative of a specific linac type (Versa-HD in this case). Several parameters are changed to account for linac-to-linac differences and to reduce discrepancies between measurements and estimated dosage distributions.

The spectra of primary photons, secondary photons, and electron sources are described by equations (1), (2), and (3), respectively.

- First, the energy spectra of primary photon and secondary photon sources are optimized by adjusting bpri and bsec. This enables for the comparison of measured and predicted PDD curves with depths greater than zmax.

$$P_{pri}(E) = \left(\frac{E}{E_{max}}\right)^{-b_{pri}} - 1 \quad (1)$$

$$P_{sec}(E) = e^{-b_{sec}E} - e^{-b_{sec}E_{max}} \quad (2)$$

$$P_{el}(E) = e^{-E/\langle E_e \rangle} \quad (3)$$

- Because the parameterized Padé function used for flattened beams is not suitable to FFF peaked profiles, off-axis fluence adjustment is done with a table of multipliers. After this stage, the size of the primary photon source can be changed to match the estimated penumbra to the measured dose profiles. Modifying the b parameters with the angle from the central axis accounts for off-axis softening.
- The next stage is to optimise output factors by adjusting the weight and dimension of the secondary photon source. This may have an impact on depth-dose distribution, necessitating a re-optimization of photon energy spectrum. The size of the secondary source is determined by its angle with the central axis. The size of the primary photon source has an effect on the outputs for different field sizes. 22 centimeters
- To improve build-up dose modelling and match surface lateral dose profiles, surface dose distribution is used to optimize electron source characteristics (size, Ee, and weight).
- To improve model matching, additional procedures such as MLC, jaw transmission, and tip leakage are included at the end.

5.3 Results

5.3.1 Depth dose curve and Surface dace

Beyond zmax, PDD values of FFF and flattened beams correspond within 1%, although at reference field size, surface dosage is 0 to 3% lower for FFF beams (Table:5.1).

Field size	Energy		Deviation
	6 FB	6 FFFB	
10 x 10	21.182	21.062	0.12
20 x 20	31.456	28.497	2.959
Field size	10 FB	10 FFFB	Deviation
10 x 10	17.533	20.485	2.952
20 x 20	29.636	26.954	2.682

Phantom: Solid water Phantom with SAD Setup, Chamber :0.02cc Advanced Markus Chamber (Parallel Plate)

Table:5.1 Surface Dose Measurement

Several articles show that FFF beams have a larger surface dose when TPR20/10 is different [16], but others agree with current results when FFF and flattened beams have the same TPR20/10 (16,17).

The maximal dose depths for 6FB, 6FFFB, and 10FB,10FFFB beams are 1.5, 1.7, and 2.16,2.3 cm, respectively (table 5.2). Higher low-energy components in FFF photon beam spectra tend to raise surface dosage, but higher maximum photon energy and reduced electron contamination offset this and push the dose maximum deeper. Huang et al. discovered around 3 mm shifts in z max [18] with FFF beams and found the same impact.

Energy	SSD (cm)	D_{max} (mm)	PDD (1 mm)	PDD (50 mm)	PDD (100 mm)	PDD (200 mm)	TPR20/10
X6	100	15.0	55.2	86.2	67.5	39.7	0.6865
X6 FFF	100	17.0	62.5	87.3	67.6	39.6	0.6825
X10	100	21.6	44.0	91.0	72.6	45.6	0.7354
X10 FFF	100	23	49.7	90.7	71.61	43.89	0.7166

PDD = percentage depth dose, TPR20/10 = tissue-phantom ratio at the depths of 20 and 10 cm

Table 5.2: Depth dose curve parameters

The spectrum is softened by removing the flattening filter, and the nominal energies of FFF beams are increased to match the TPR20/10 of flattened beams. The low-energy components of FFF photon spectra should be greater, and the maximal energy components should be higher. FFF beams, on the other hand, have a greater low-energy photon component than flattened beams, although having the same mean energy. In the case of FFF beams, the electron source weight is smaller, the flattening filter is responsible for a considerable fraction of the contaminated electrons, which is consistent. The electron mean energies for 6FFFB and X10FFFB beams in Monaco® are 1.24 and 2.07 MeV, respectively.

PDDs that have been modelled closely match measured data, with 100% test passing rates across all field sizes. On TPS-calculated PDDs for fields 5 x 5 cm2 and beam quality 6FFFB and 10FFFB, there is a minor overestimation of the dosage around the depth of dose maximum. This effect is less than 0.7 percent. In every example, the model and measurements in the build-up region are within 0.8 mm. As a result, the improvement in low-energy photon components and decrease in electron contamination appears to be beneficial. as it accurately mimics the

surface dosage at all field sizes. [19] simply changed high-energy photon spectra bins and discovered larger differences in the buildup area.

5.3.2 Profiles

The largest dose is on the central axis of FFF profiles, and it gradually decreases towards the field boundary. With increased field size and beam energy, this non-flattened shape becomes more prominent (figure:5.4, and 5.5, table 5.3). The in-field part of a profile for X6 and X6FFF beams, as well as X10 and X10FFF beams, is nearly identical up to a field size of 3x3 cm^2. For FFF beams, profile differences with depth are smaller (figure 5.5).

Field size	2x2	5x5	10x10	20x20	30x30	40x40
6 FB	1.261	1.0695	1.048	1.050	1.041	1.044
6 FFFB	1.064	1.042	1.158	1.357	1.591	1.846
10 FB	1.088	1.276	1.048	1.033	1.025	1.0376
10 FFFB	1.062	1.072	1.242	1.514	1.829	2.177

Table 5.3: Maximum and minimum dosage ratios inside the field (within 80% of the field size) for various field sizes recorded at a depth of 10 cm (SSD 90 cm)

5.3.3 Penumbras

At dmax, the penumbra of 6FFFB is roughly 0.3 mm sharper than the penumbra of 6 FB. The difference between 6 FB and 6FFFB penumbras rapidly fades as depth increases, and at a depth of 12 cm, the penumbras of 6 FB and 6 FFFB are nearly similar. The flattened beam provides sharper penumbra beyond this range. For all examined depths, 10BFFFB has a sharper penumbra than 10 FB; the difference between penumbras reaches up to 0.6 mm at the dmax and gradually diminishes with depth (Figure 5.6). For all beams, a small broadening of penumbra was seen

as field size increased. In the transverse and radial directions, this widening happens at a significantly quicker pace for FFF beams.

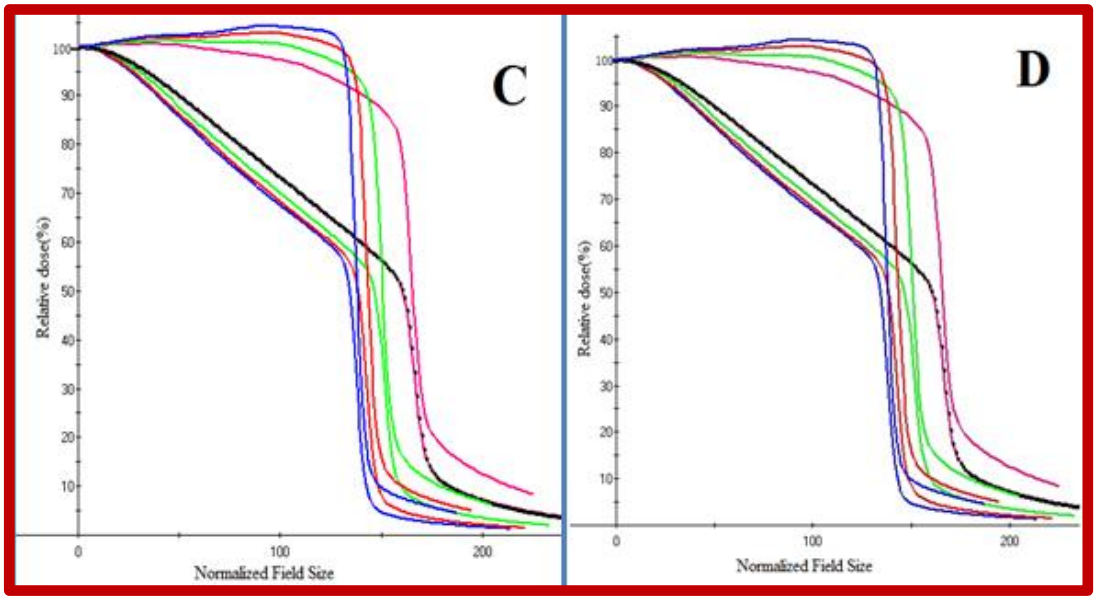

Figure 5.6: For the 30 x 30 cm^2 field at all measured depths Dmax,5,10,20cm for 6 FB and 6 FFFB(C) and 10 FB and 10 FFFB (D).

5.3.4 Out of field dose

Low-energy photons are less likely to pass through the MLC leaves or the jaws. Outside of the field, removing the flattening filter reduces the dose by 20 to 50 percent near the field border. This effect increases with distance from the central axis at all depths, with dosage decrease being greatest at shallow depths in the toe region. The FFF out-of-field dosage reduction is particularly obvious at small field sizes. Inline and crossline dose patterns are similar in the out-of-field.

Figures 5.7 and 5.8 demonstrate the ratio of (half) dose profiles of an FFF and a flattened beam for various field widths and depths. In most cases, the out-of-field dose deposited by FFF beams is smaller than that produced by flattened beams. There is a significant dosage reduction effect at the edge of a field and at longer distances from the edge. In the intermediate zone, the FFF/flattened dosage ratio reaches its maximum, and in some cases, an FFF beam can deposit more dose than

a flattened beam. At a distance of around 20 cm from the centre axis, the dosage ratio curve begins to grow. As field size and depth rise, the dose reduction effect of an FFF beam rapidly reduces.

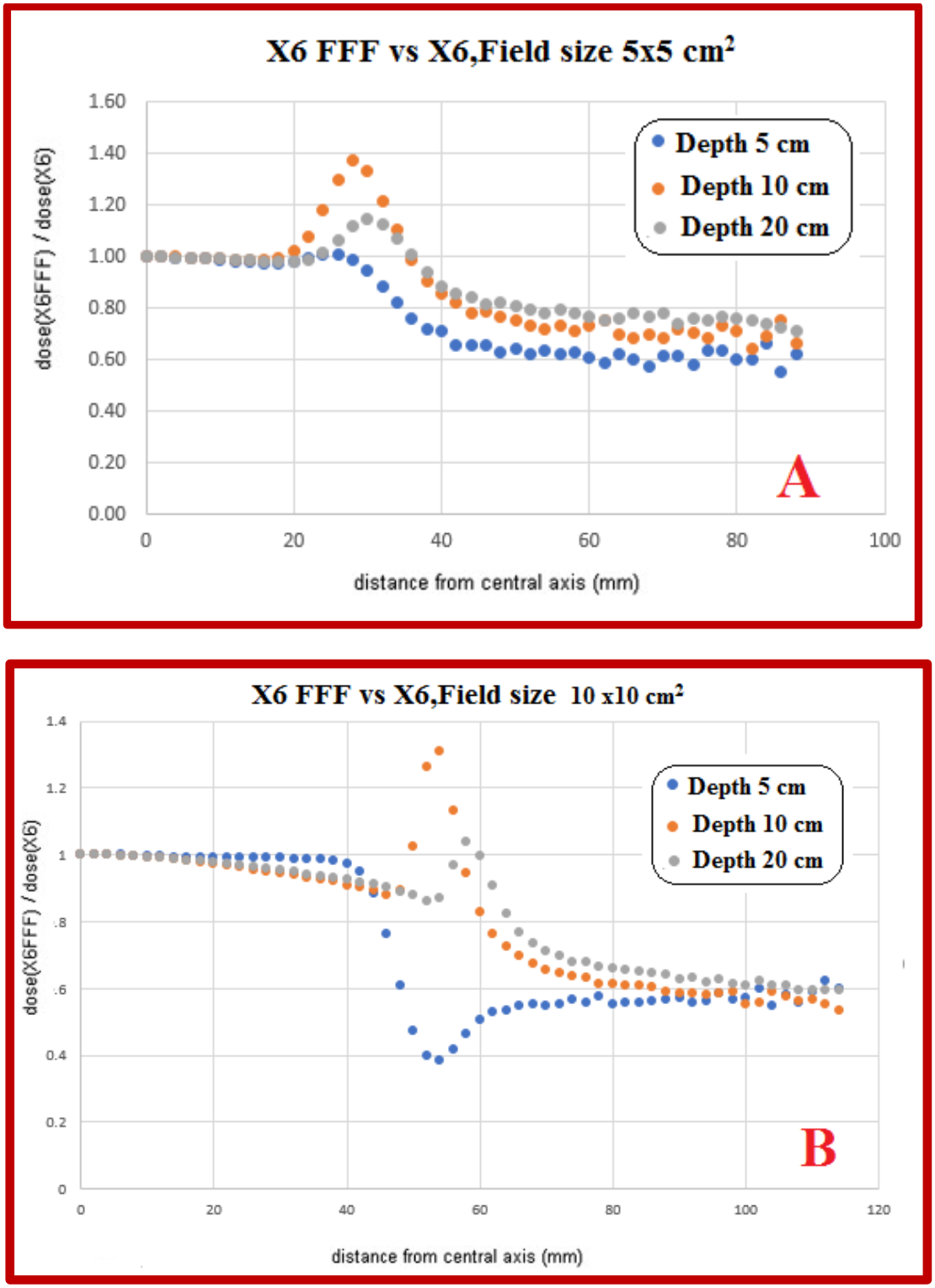

Figure 5.7: Out-of-field dose ratios for X6FFF/X6 (A, B) are shown for two selected field sizes.

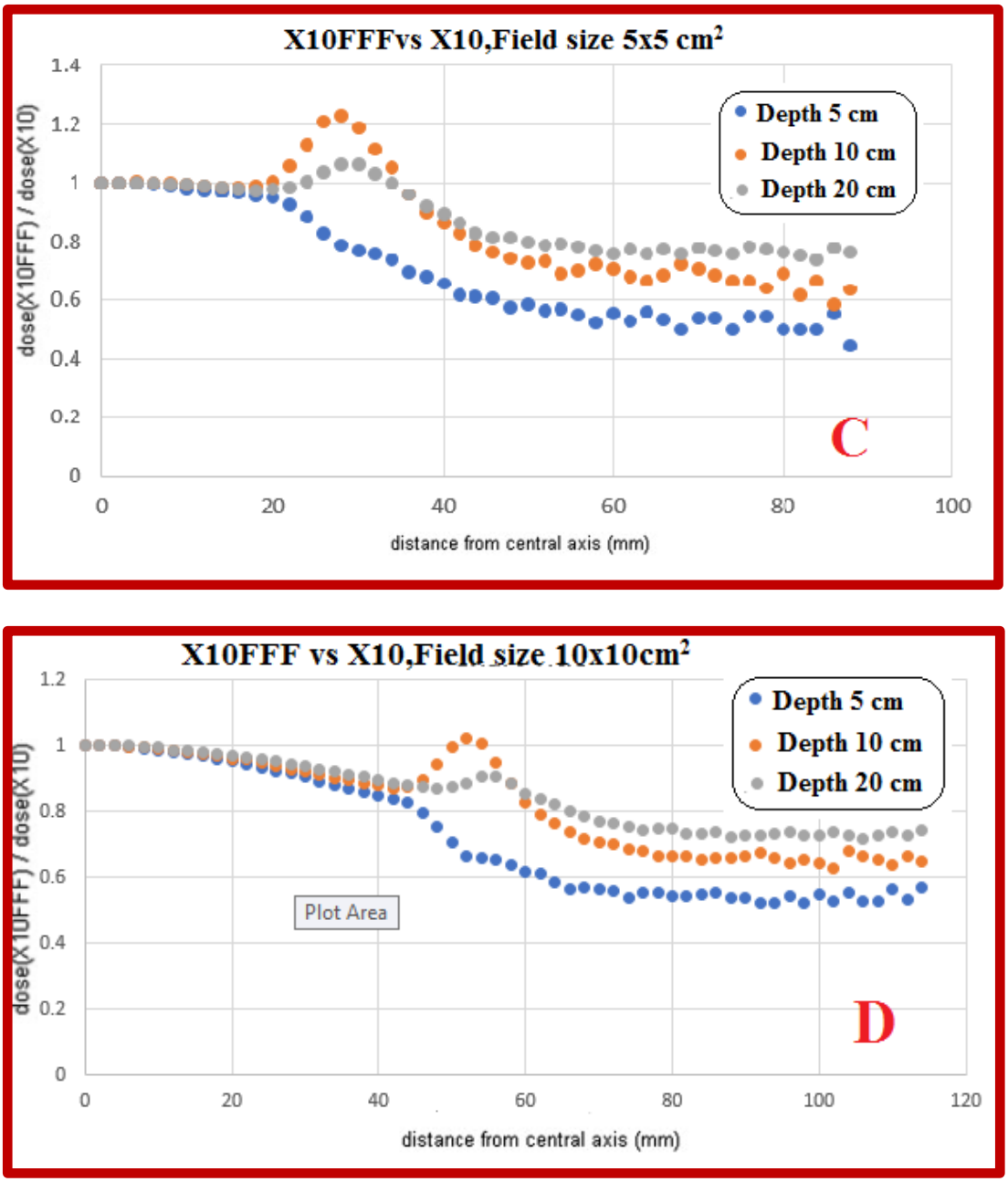

Figure 5.8: Out-of-field dose ratios for X10FFF/X10 (C, D) are shown for two selected field sizes.

5.3.6 MLC transmission

FFF beams are expected to have half the transmission of flattened beams. Off-axis softening and profile correction, as well as source sizes and weights, all have an impact on the out-of-field dose. As a result of all of these factors, the MLC transmission of FFF beams was intentionally reduced in order to get superior out-

of-field dosage models. In Monaco, the transmission characteristics of both FFF and flattened beams MLC are equal.

5.3.7. Output factors

Figure 5.9 displays the measured output factors. Compared to flattened beams, FFF beams have fewer OF variations with field size. The decreased variance in OF could be owing to the lower contaminated electron component in FFF beams, which contributes to the output variation with field size. Because documented OF corrections do not exceed 1% down to 11 cm2 for the detectors employed, the measured OF was not changed for modelling. Measured data and TPS output factors differ marginally.

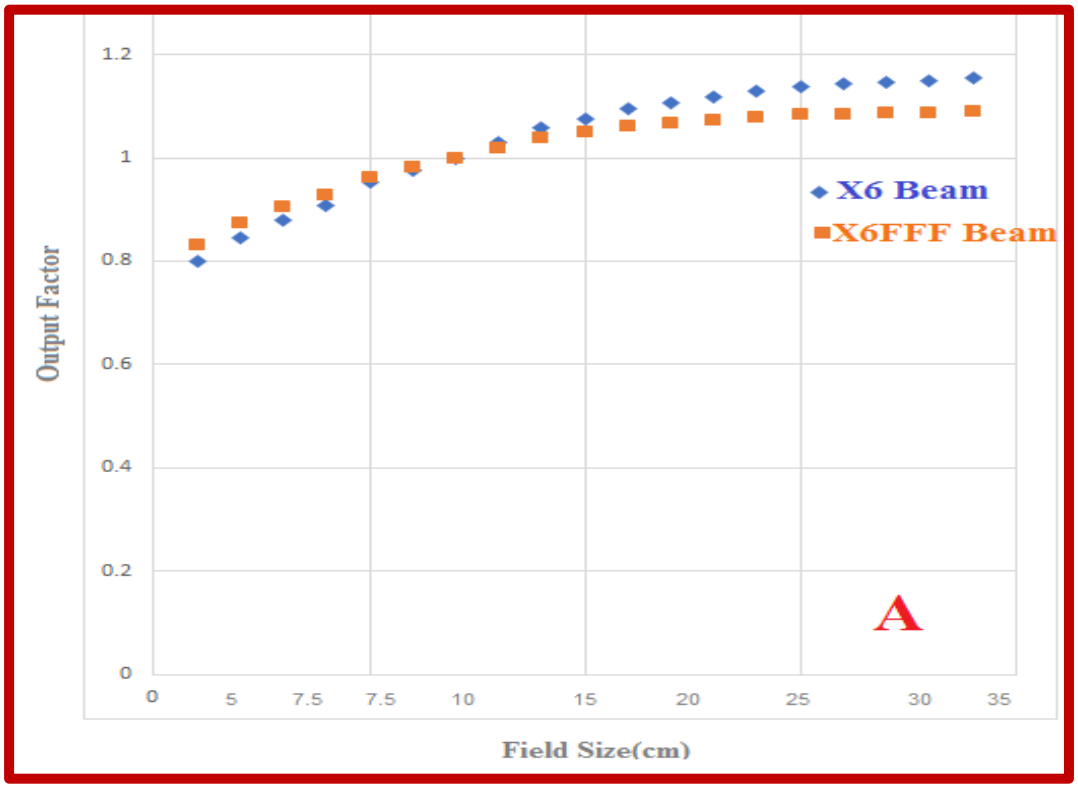

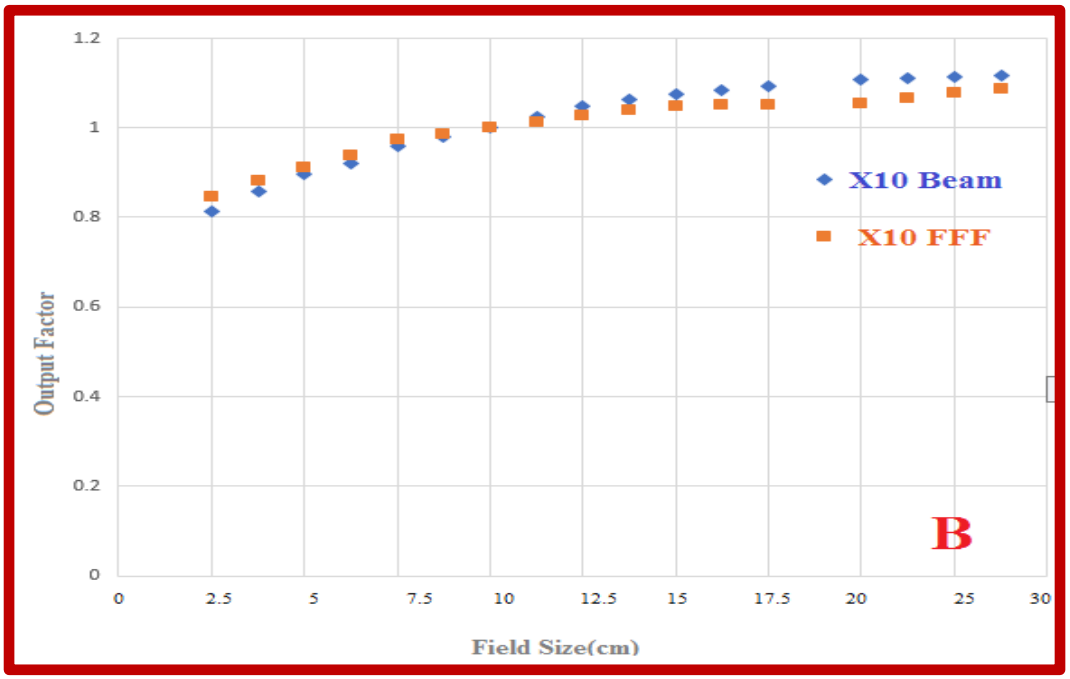

Figure 5.9: Comparison of X6FFF and X10 FFF Output factors for all field size

5.3.8 Monaco TPS Modeling

The Elekta® dedicated team assessed all beam data, PDD, Profiles, output factors, and MLC transmission in the Monaco® model, and the measured data was then validated with the modelled data by the Elekta team. 6FFF and 10 FFF are two different types of FFF. Figure 1 shows the profile of Modeled Beams PDD (5.10,5.11,5.12.5.13).

The TPS planned dose was compared to the machine delivered dose to ensure that the predicted beam data matched the measured beam data. This was accomplished by constructing TPS plans for open field and patient VMAT plans, then comparing the TPS dosage for each test field (10x10 cm2, 20x20 cm2) to the dose measured in a phantom for the same plan using Verisoft software.

VeriSoft is a piece of software that allows you to reconstruct dose fluence maps for these measurement sites. With gamma analysis, the software programme also assesses the similarity of dose fluence maps. In three dimensions, dose distributions and comparisons are analyzed numerically and graphically. 729

detector arrays were used to measure open fields and VMAT plans provided to phantom. The estimated and measured dose fluence maps were compared using VeriSoft (software).

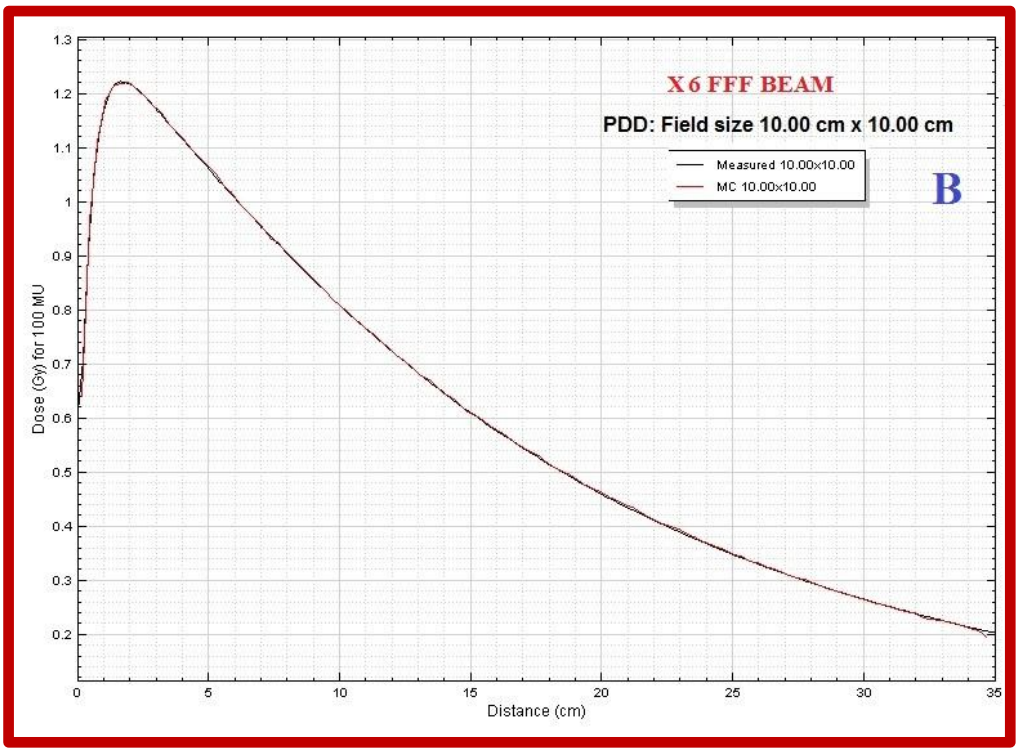

Figure 5.10: Comparison of measured and modeled (MC) depth dose curves are shown for X6FFF at for reference Field Size :5X5 cm^2 (A) and 10X10 cm^2 (B)

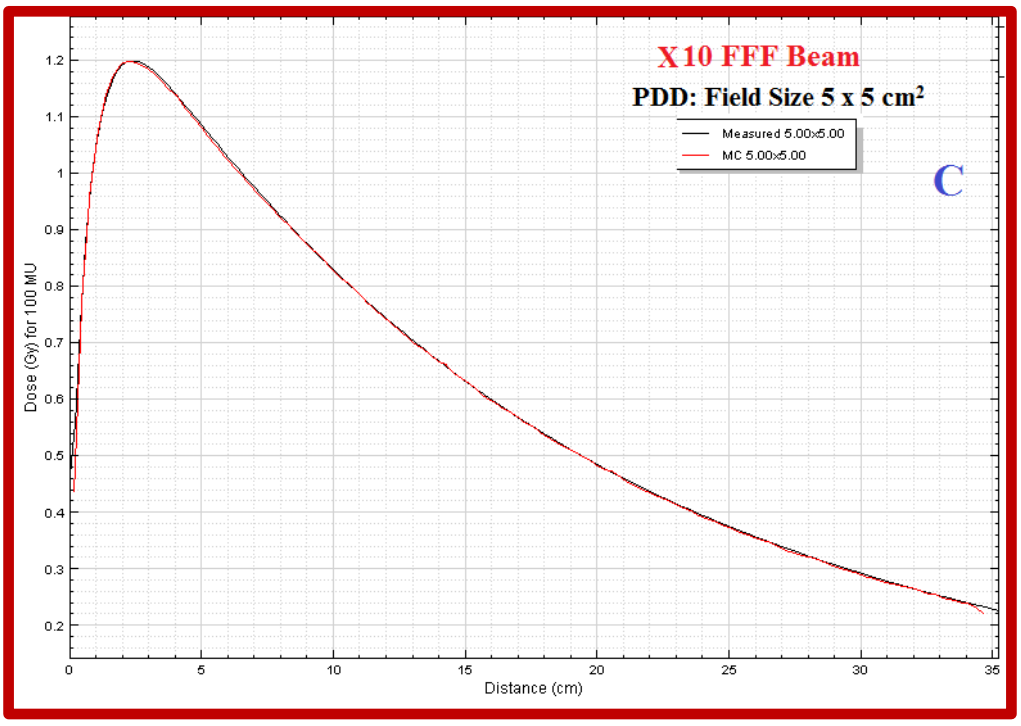

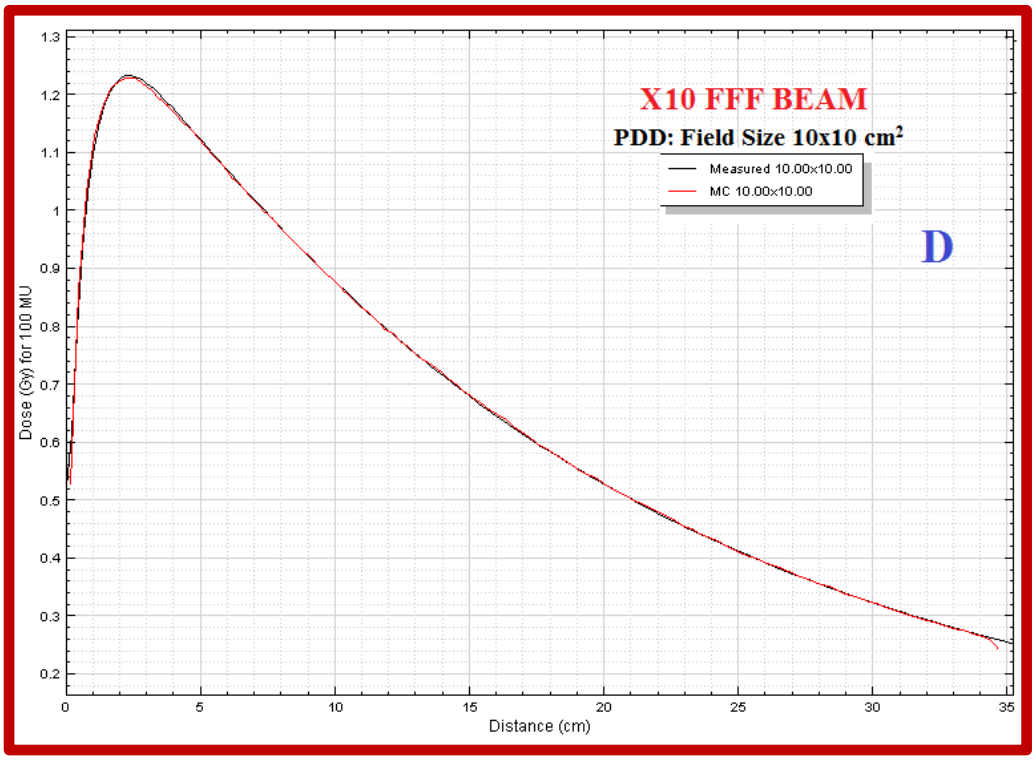

Figure 5.11: Comparison of measured and modeled (MC) depth dose curves are shown for X10 FFF at for reference Field Size :5X5 cm^2 (C) and 10X10 cm^2 (D)

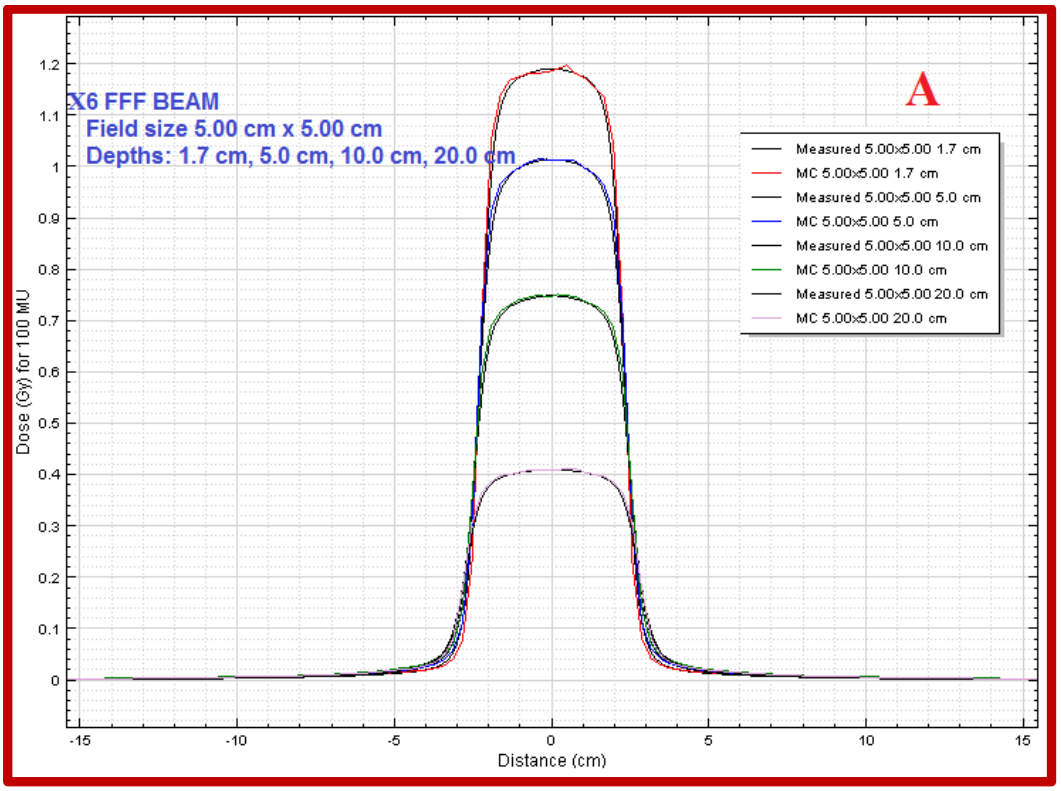

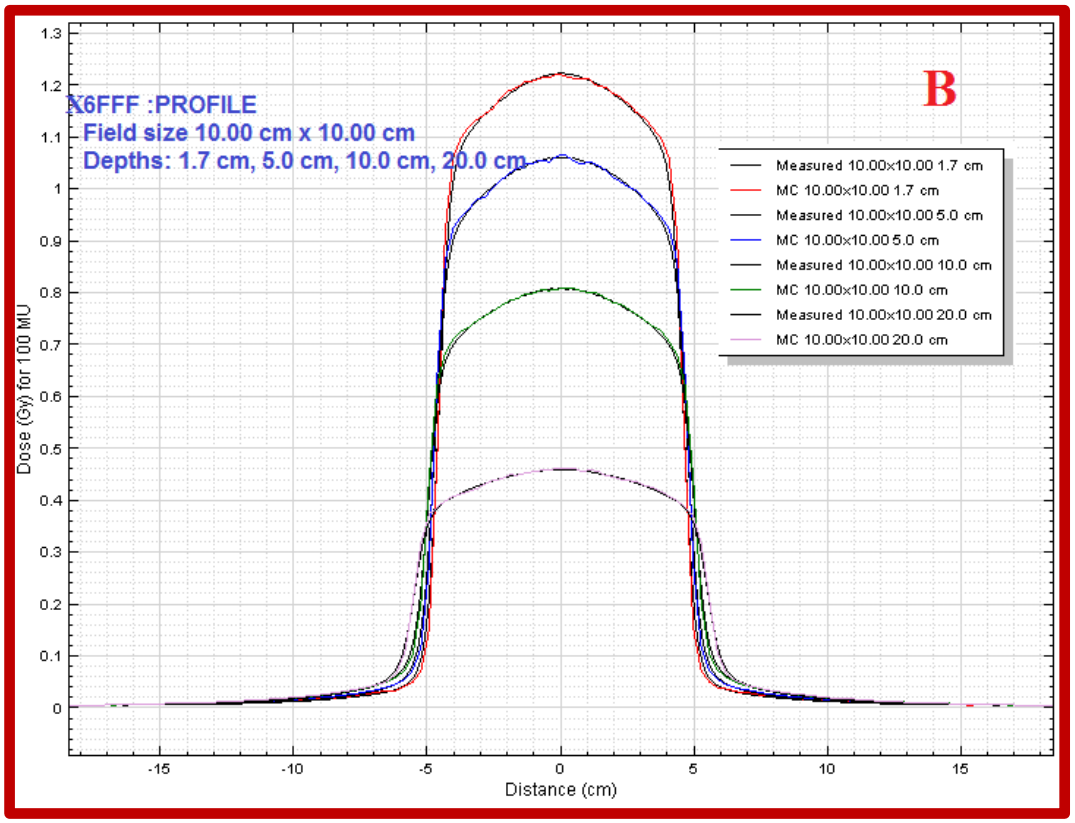

Figure 5.12: Comparison of measured and modeled (MC) Profiles are shown for X6FFF at for reference Field Size :5X5 cm^2 (A) and 10X10 cm^2 (B)

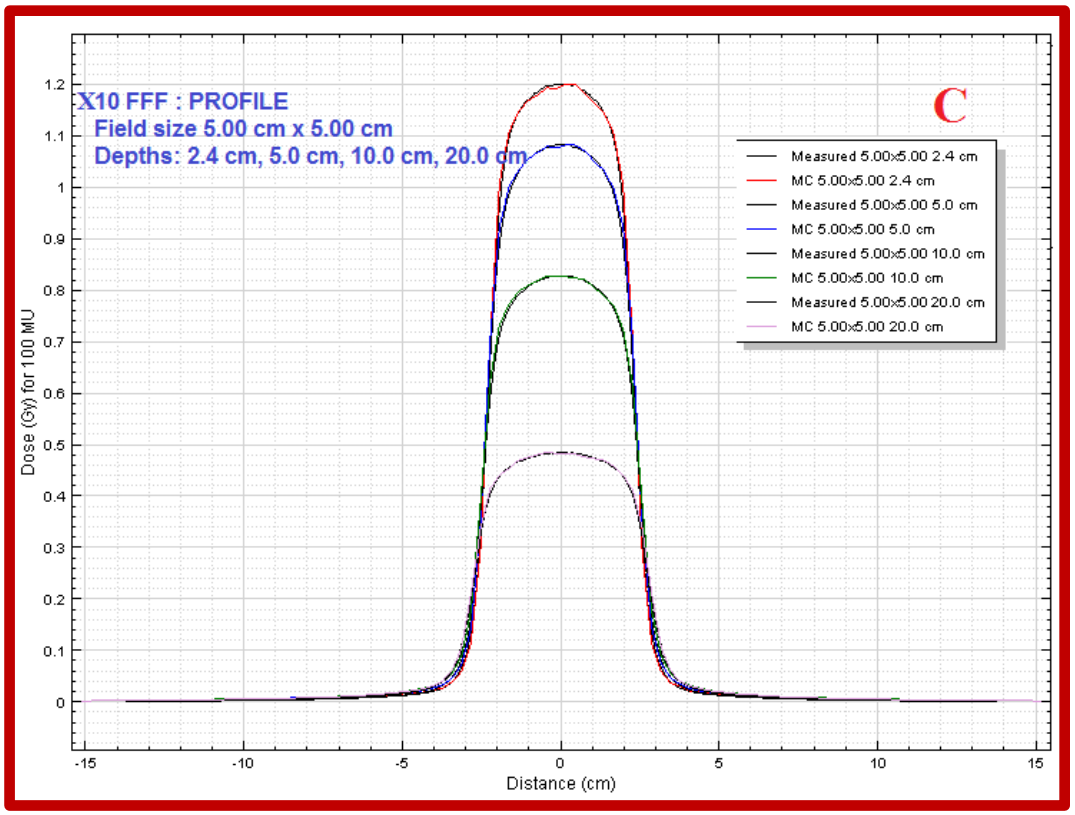

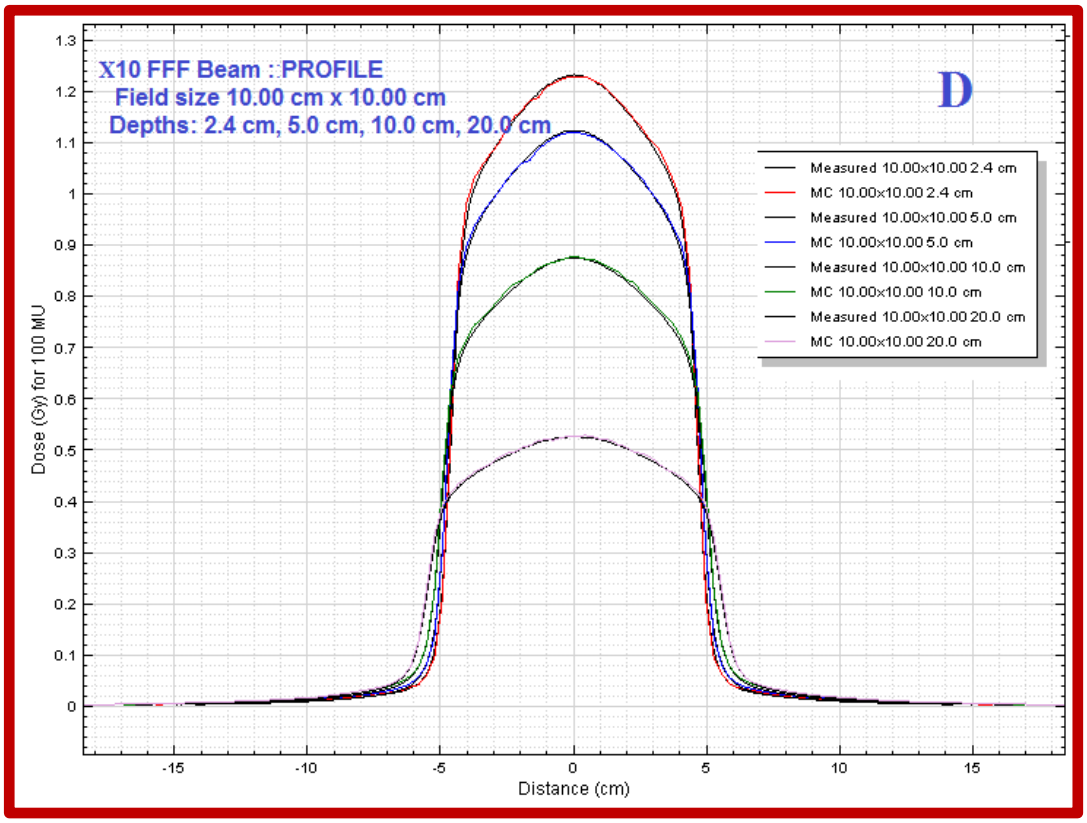

Figure 5.13: Comparison of measured and modeled (MC) Profiles are shown for X10 FFF at for reference Field Size :5X5 cm^2 (C) and 10X10 cm^2 (D)

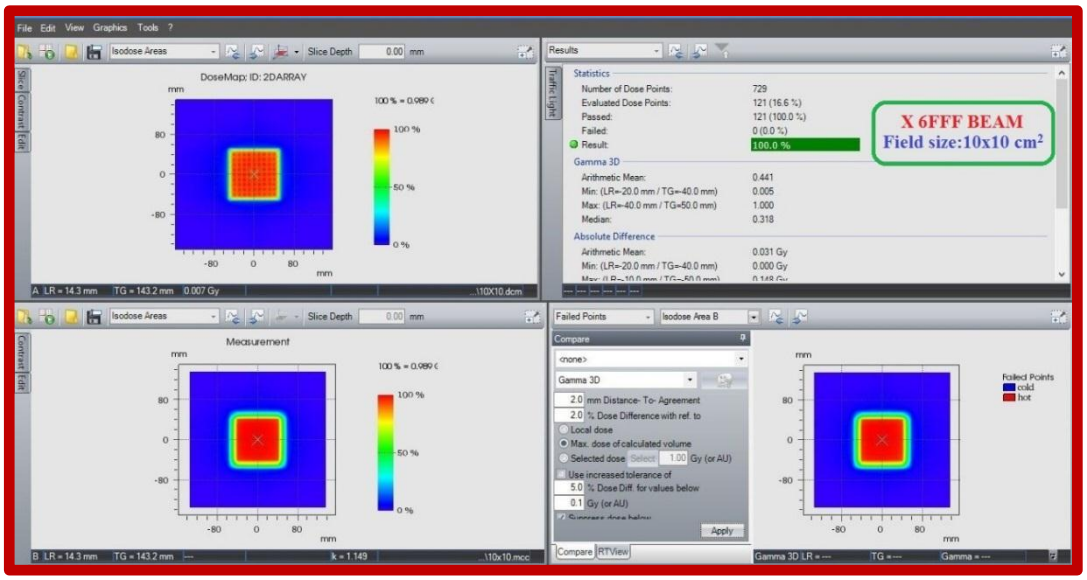

Figure 5.14: Screenshot from software for comparing X6FFF modeled TPS calculated dose and measured dose fluence maps of open field plan 10x10 cm^2

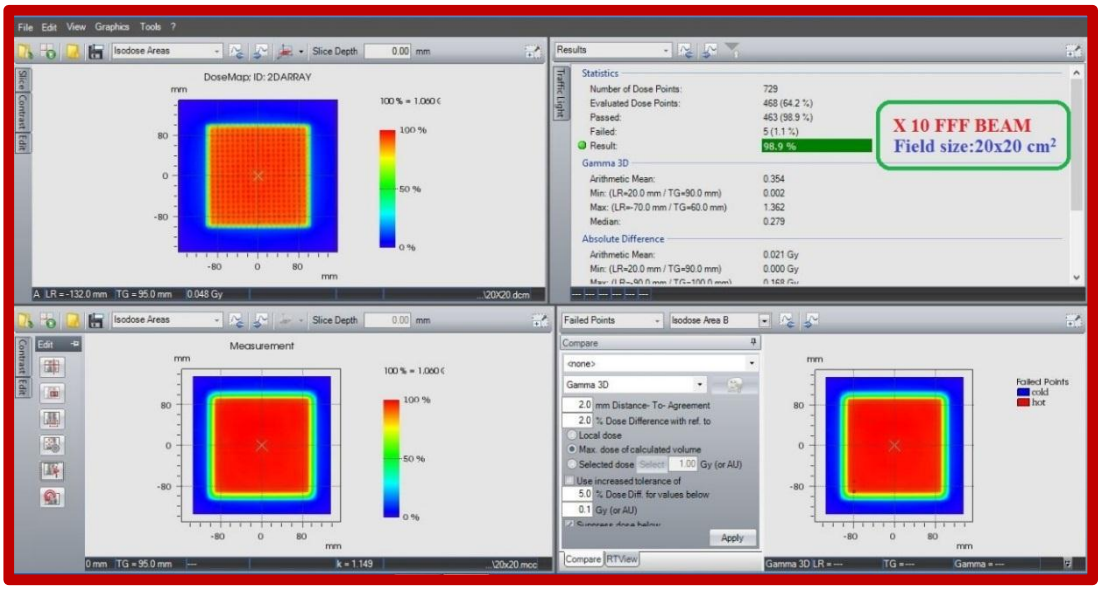

Figure 5.15: Screenshot from software for comparing X10FFF modeled TPS calculated dose and measured dose fluence maps of open field plan 20x20 cm^2

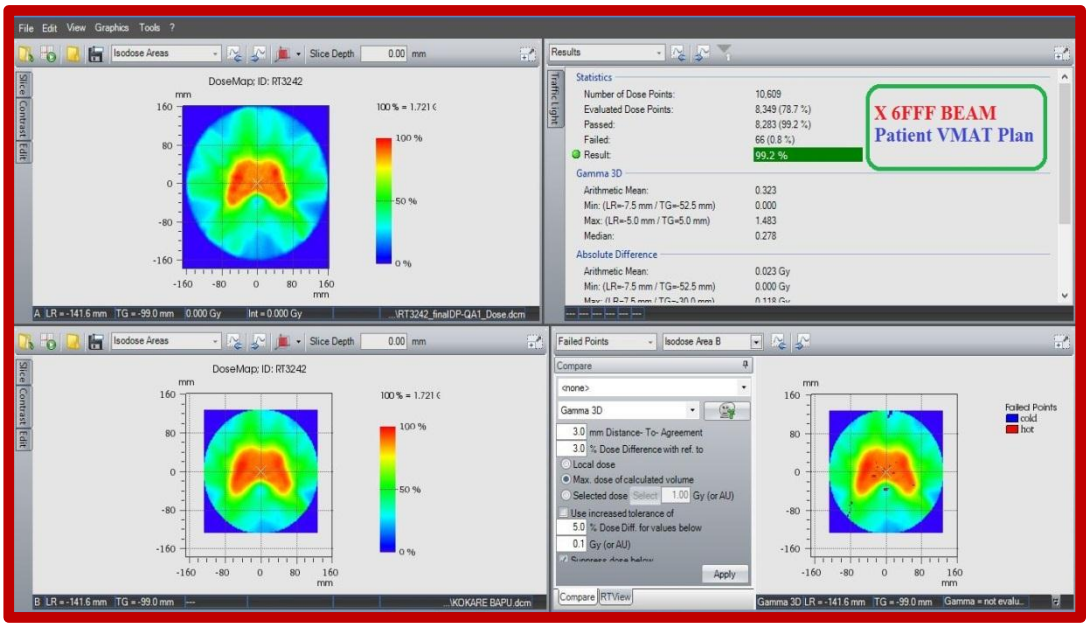

Figure 5.16: Screenshot from software for comparing X 6FFF modeled TPS calculated dose and measured dose fluence maps of Ca cervix VMAT plan.

5.3.9 Model verification: test beams and patient treatment plans

For both 6FFF and 10FFF beams, the computed dose distribution for 10x10cm2 and 20x20cm2 open fields matched the measured beam data with 100% &98.9% points passing the -test with 2mm and 2% criterion in Monaco TPS. Two dosage

distributions, one for each energy, are shown below. and TPS, are shown in Figures 5.14 and 5.15.

In Figure 5.16, you can see an example of a Ca Cervix VMAT plan with 729 detector arrays. In the coronal, sagittal, and transverse axes, different doses were compared. Plans for VMAT The passing requirements were 99.2%, a gamma index of 1 for 3mm, and a 3% difference between calculated and measured dosage points.

5.4 Discussion

Beyond zmax, FFF and flattened beam PDD results agree within 1%, but surface dosage is 0 to 3% lower for FFF beams at reference field size. The maximal dose depths for X6, 6FFF, and 10FFF beams are 1.6, 1.8, and 2.4 cm, respectively. Higher low-energy components in FFF photon beam spectra tend to increase the surface dose, but higher maximum photon energy and reduced electron contamination counteract this, pushing the dose maximum deeper. With FFF beams, Huang et al. discovered roughly 3 mm shifts in zmax [19] and found the same impact.

The non-flatness of FFF profiles grows as the probability of photon scattering into lateral directions decreases as the energy of input photons increases. Due to secondary source and beam hardening and leaking, the out-of-field dosage in flattened beams is higher than in FFF beams. The normalization method utilized has an impact on the comparison of FFF and flattened profiles, especially for larger field sizes and higher nominal energy, when the form difference between FFF and flattened profiles is more obvious.

In clinical situations, many parameters like as the target's size, location, and shape, as well as the degree of modulation and delivery method (IMRT or VMAT)

employed, and their interactions with beam characteristics, will affect dose outside the target (energy and shape of a profile). As evidenced by the statistics, small field sizes and higher energy FFF beams give the best possible dose decrease outside of a field. MLC transmission is higher in Flattened beams than in FFF beams due to the beam hardening effect.

The 6FFF and 10 FFF beams are often accurate in Monaco modelling. For both symmetric and asymmetric fields, the chosen requirements of 2% DD and 2 mm DTA look suitable and are reached in the majority of the investigated locations. The quality of the beam model, as well as defects in the measured dataset, influence the agreement with the measurement. Prior to the examination, all profiles were aligned and normalized to decrease these errors. The 1D gamma analysis algorithm used somewhat nullifies the impacts of discrete character and noise in the measured profiles.

5.5 Conclusion

Basic dosimetric properties were summarized for four photon beams of the first clinically used versa HD linear accelerator. All modeled beam data were successfully verified with measured data.

5.6 References

1. T. R. Mackie, T. Holmes, S. Swerdloff, P. Reckwerdt, J. O. Deasy, J. Yang, B. Paliwal, and T. Kinsella, "Tomotherapy: a new concept for the delivery of dynamic conformal radiotherapy," Medical physics, vol. 20, p. 1709, 1993.

2. J. Balog, G. Olivera, and J. Kapatoes, "Clinical helical tomotherapy commissioning dosimetry," Medical physics, vol. 30, p. 3097, 2003.

3. U. Titt, O. Vassiliev, F. P¨onisch, L. Dong, H. Liu, and R. Mohan, "A flattening filter free photon treatment concept evaluation with monte carlo," Medical physics, vol. 33, p. 1595, 2006.

4. O. N. Vassiliev, U. Titt, S. F. Kry, F. P¨onisch, M. T. Gillin, and R. Mohan, "Monte carlo study of photon fields from a flattening filter-free clinical accelerator," Medical physics, vol. 33, p. 820, 2006.

5. O. N. Vassiliev, U. Titt, F. P¨onisch, S. F. Kry, R. Mohan, and M. T. Gillin, "Dosimetric properties of photon beams from a flattening filter free clinical accelerator," Physics in medicine and biology, vol. 51, no. 7, p. 1907, 2006.

6. G. Kragl, S. af Wetterstedt, B. Kn¨ausl, M. Lind, P. McCavana, T. Kn¨o¨os, B. Mc-Clean, and D. Georg, "Dosimetric characteristics of 6 and 10mv unflattened photon beams," Radiotherapy and Oncology, vol. 93, no. 1, pp. 141–146, 2009.

7. J. Cashmore, "The characterization of unflattened photon beams from a 6 mv linear accelerator," Physics in medicine and biology, vol. 53, no. 7, p. 1933, 2008.

8. P. R. Almond, P. J. Biggs, B. Coursey, W. Hanson, M. S. Huq, R. Nath, and D. Rogers, "Aapm's tg-51 protocol for clinical reference dosimetry of high-energy photon and electron beams," Medical physics, vol. 26, p. 1847, 1999

9. High Dose Rate mode, available with Agility™ on Elekta's Versa HD™ linear accelerator paper].2014; Available from:http://medicalphysics web.org /cws/ article/ whitepapers/59207

10. Boda-Heggemann J, Mai S, Fleckenstein J, et al. Flattening-filter-free intensity modulated breath-hold image-guided SABR (Stereotactic ABlative Radiotherapy) can be applied in a 15-min treatment slot. Radiother Oncol. 2013;109(3):505–09.

11. F. P¨onisch, U. Titt, O. N. Vassiliev, S. F. Kry, and R. Mohan, "Properties of unflattened photon beams shaped by a multileaf collimator," Medical physics, vol. 33, p. 1738, 2006.

12. M. Schwedas, M. Scheithauer, T. Wiezorek, and T. G. Wendt, "Strahlenphysikalische einflussgr¨ossen bei der dosimetrie mit verschiedenen detektortypen," Zeitschrift f¨ur Medizinische Physik, vol. 17, no. 3, pp. 172 – 179, 2007.

13. Thompson CM, Weston SJ, Cosgrove VC, Thwaites DI. A dosimetric characterization of a novel linear accelerator collimator. Med Phys. 2014;41(3):031713.

14. International Electro technical Commission. Medical electrical equipment — Part 2.1. Particular requirements for the basic safety and essential performance of electron accelerators in the range 1 MeV to 50 MeV. IEC 60601–2-1 Ed. 3.0. Geneva, Switzerland: IEC; 2009.

15. Valdenaire, H Mailleux and P. Fau . Modeling of flattening filter free photon beams with analytical and Monte Carlo TPS. Biomed. Phys. Eng. Express 2 (2016) 035010

16. Almberg S S, Frengen J and Lindmo T 2012 Monte Carlo study of infield and out-of-field dose distributions from a linear accelerator operating with and without a flattening-filter Med. Phys. 39 5194–203

17. Cashmore J 2008 The characterization of unflattened photon beams from a 6MVlinear accelerator Phys. Med. Biol. 53 1933–46

18. Huang Y, Siochi R A and Bayouth J E 2012 Dosimetric properties of a beam quality-matched 6MVunflattened photon beam Journal of Applied Clinical Medical Physics/American College of Medical Physics 13 3701

19. Huang Y et al 2013 Equivalent-quality unflattened photon beam modeling, planning, and delivery Journal of Applied Clinical Medical Physics/American College of Medical Physics 14

CHAPTER -VI

Dosimetric comparison of flattened and flattening filter-free beams for liver stereotactic body irradiation in deep inspiration breath hold, and free breathing conditions

Chapter -VI

Dosimetric comparison of flattened and flattening filter-free beams for liver stereotactic body irradiation in deep inspiration breath hold, and free breathing conditions

6.1 Introduction:

The clinical use of the flattening filter-free (FFF) beam in linear accelerators is a subject of great interest in recent times. [1–3] Considering the physical characteristics of the FFF beam, it can be expected that the dose fall-off beyond the field sizes will be sharper than that of the flattened beam (FB). This could be attributed to the reduction in (residual) electron contamination and decline in the head scatter factor. From the clinical perspective, FFF beam could lead to a reduction in the beyond field border dose for modern therapy delivery techniques. Sharper dose fall may yield a higher dose gradient, leading to a sparing of organs at risk (OAR), enhancing the dose to the tumor. Another advantage of the FFF beam is its increased dose rate, which will in turn reduce the treatment time substantially.

This chapter has been published as a manuscript: Munirathinam N, Pawaskar PN. (2019) Dosimetric comparison of flattened and flattening filter-free beams for liver stereotactic body irradiation in deep inspiration breath hold, and free breathing conditions. Journal of Radiotherapy in Practice page 1 of 6. doi: 10.1017/ S146039691800064X. Accepted: 16 October 2018

However, it is essential to validate the FFF beam for the dosimetric outcome of the beam, to reduce the healthy tissue dose, with better or equal tumor dose coverage

Sharper dose fall may yield a higher dose gradient, leading to a sparing of organs at risk (OAR), enhancing the dose to the tumor. Another advantage of the FFF

beam is its increased dose rate, which will in turn reduce the treatment time substantially. However, it is essential to validate the FFF beam for the dosimetric outcome of the beam, to reduce the healthy tissue dose, with better or equal tumor dose coverage. Several investigators have investigated different physical characteristics of the FFF beam, such as the beam profile, etc. Therefore, the dosimetric characteristic of the FFF beam will have to be evaluated in actual clinical situations, specifically with the planning target volume (PTV) coverage and OAR sparing for different available linear accelerators. [4] A substantial amount of work has been published on Varian (Varian Medical System, Polo Alto, CA, USA) FFF; but the literature. available regarding the Elekta (Elekta AB, Stockholm, Sweden) unflattened beam is very limited. [5–10] Stereotactic body irradiation (SBRT) is an emerging field and is used for different body sites, like lung, liver and spinal metastasis. SBRT has proved its efficacy in several cases, both for primary as well as metastatic sites. Stereotactic irradiation involves the delivery of a very high dose over a number of fractions. Body stereotactic radiotherapy demands a very good motion management technique.[11–13] In particular, SBRT may be appropriate for selected patients with organ-confined, limited-volume primary tumours or oligo-metastatic disease.[14] Traditionally, SBRT was delivered using multiple three dimensional conformal radiation therapy (3DCRT) beams or intensity-modulated radiation therapy (IMRT) beams.[15,16] The disadvantage with 3DCRT is insufficient fluence modulation, yielding insufficient OAR sparing. However, IMRT gives a good fluence modulation, and hence better OAR sparing. The treatment time is considerably longer, which can lead to patient discomfort and an increase in the probability of inter fraction motion. Volumetric-modulated arc therapy (VMAT) may be a better option as it

can deliver the radiation dose within a shorter time and achieve effective OAR sparing. The potential of VMAT used for SBRT to treat liver tumour has been evaluated by a few researchers; nevertheless, these evaluations have limitations.[5,6] For example, SBRT was not evaluated using FFF, during deep inspiration breath hold (DIBH) and free breathing conditions.

6.2. Aim,

The aim of this study, therefore, was to evaluate the characteristics of the flattened and unflattened beams of the Elekta Versa HD linear accelerator, using VMAT-based liver SBRT technique, in free breathing and DIBH conditions.

6.3. Material Method:

6.3.1 Patient selection:

For a set of eight patients, diagnosed with liver-metastasis were enrolled in this prospective observational study. Volumetric modulated arc plans with 6 MV FF and 6 MV FFF were generated under the free breathing and DIBH conditions

6.3.2 CT simulation

Before CT simulation, all patients underwent two or three practice sessions of breath hold technique for procedure familiarization. All patients were immobilized with vacuum bag (vack-lock; Orfit Industries, Belgium) and The vacuum bag takes on the shape of the patient when deflated. Patient in supine position and the hands were kept above the head.

The computed tomography (CT) images were acquired for all patients in Biograph MCT-20, PET-CT (Siemens AG, Medical solutions, Germany) with 1.5 mm slice thickness; field of view 50 cm. CT was acquired in in both DIBH and free breathing conditions. Using ABC respiratory assistant instruments were used. CT

datasets were transferred to the Monaco Sim (CMS Elekta, Sunnyvale, CA, USA) workstation for contouring, using DICOM-enabled protocol.

6.3.3 Target and OAR delineation

An experience radiation oncologist contoured the gross target volume and clinical target volume, in the DIBH as well as free breathing study sets. In free breathing study set, the gross tumor volume was delineated using the minimum intensity projection that was obtained from the 20-slice Siemens positron emission tomography (PET)-CT (Biagraph MCT-20, Germany) console. DIBH and free breathing study sets were co-registered with each other, while they were obtained in the PET-CT. Therefore, they did not require any mutual information co-registration.

Target volumes (TV) and OARs were delineated for all the patients using Monaco Sim (CMS Elekta, Sunnyvale, CA, USA) Clinical Target Volume (CTV). A margin of 0.5 cm was given to CTV to generate planning target volume (PTV). The OARs viz. bowel bag, heart, bilateral kidney, bilateral lung, chest wall and Spinal cord was con-toured. OAR were contoured by the resident radiation oncologists. CT study sets, along with the contours, were transferred to the Monaco (Elekta Ltd, Crawly, UK) treatment planning system, for radiotherapy planning. Elekta Versa HD (Elekta AB, Stockholm, Sweden), a linear accelerator was used to deliver the VMAT plans. The linear accelerator is fitted with MLCs having 80 leaf pairs of 5 mm width.

6.3.4 Treatment planning system:

Monaco treatment planning system (Elekta Ltd, Crawly, UK) version 5.10.0 utilizes physical effects of radiation and biological properties of the tissue. It has three biological constraints such as Target EUD, Parallel and serial and six

physical constraints such as target penalty, quadratic overdose, overdose DVH, under dose DVH, maximum dose and quadratic under dose. The user has an option to set the cell sensitivity of the tumor in target EUD. The organ at risk can be set as serial or parallel constraints depending on the properties of the tissue.

The system uses a two-stage process of optimizing dose distribution. Generally, in stage one the ideal fluence distribution of beams is optimized to meet a user-defined prescription for given set of beams. In stage two, segmentation is done, which includes the segment shapes and weights, so that deliverable fields are obtained. In this stage system uses Monte Carlo simulation during optimization. [17]

6.3.5 Optimization strategy

In VMAT optimization, prior to stage one, system divides the beam into sectors. In stage one, at the initialization stage, the system creates the dose calculation cube around all defined structures and calculates structure volumes using cubic voxels. Then it projects the union of all target volumes with the margin defined. Numbers of static sectors are created based on arc length and user defined IGA. Beam lets for each sector are created. Width of beam let is user defined and length is equal to the length of individual MLC leaves. The system uses an enhanced pencil beam algorithm to calculate the open field dose. Then, the fluence optimization begins in which the weights (fluence) of all individual pencil beams are varied simultaneously. The unconstrained problems are solved by conjugate gradient algorithm [17]. After the unconstrained optimization finishes, if necessary the system changes each cost function relative weight to make the optimizer meet the isoconstraints and restarts the unconstrained optimization problem. Stage one optimization continues until all the constraints are met. The accuracy of dose at the

end of the stage one is limited because the algorithm is kernel based two dimensional methods, especially in the presence of heterogeneities.

In second stage, the treatment planning system considers the deliverability of accelerator. It takes each fluence map and sequences it in such a way that it is spread over the original sector it represents. The system determines leaf trajectories based on the target dose rate defined by the user. If segment shape optimization (SSO) method is selected, the system selects the optimal dose rate by its own. Then, the system converts optimized fluences into deliverable arc sequence with multiple control points and the gantry position. The gantry positions need not be equally spaced. Dose calculation is done with voxel based Monte Carlo algorithm. The user can change the calculation accuracy and time by modifying some parameters like dose rate, Monte Carlo grid spacing and variance.

6.3.6 Planning objectives

Prescribed dose to PTV was 50 Gy in 10 Fractions at 10 Gy per fraction. It was stipulated that not less than 98% volume of PTV should receive a dose less than the prescribed dose and that not more than 2% volume of PTV should receive a dose more than 105% of the prescription dose. QUANTEC Protocol 10 was used for all the OARs. The hot spot was considered as a 2% volume receiving more than 110% of the prescription dose.

6.3.7 Planning techniques

All VMAT plans were planned with the following calculation properties: Grid spacing was selected as 3 mm, and Monte Carlo variance was 3%. Monte Carlo algorithm was selected as secondary algorithm for second stage dose calculation that is final dose calculation. The dose was calculated to the medium and not to the water. For all plans, heterogeneity correction was applied

Patients were planned using a partial arc of 230° coplanar arc at table position of 0° (Gantry starts at 180° CW 200° + Gantry starts at 150° CW 30°). Two non-coplanar beams, 30° anterior and 30° posterior, were added at 270° table position. The gantry traverse for all arcs was twice the same locus. Table position– patient–gantry collision possibilities were evaluated before the actual delivery.

Planning was done using both FFF and flat 6MV photon beams. All patients were treated with a dose of 50 Gy in 10 fractions (this is a standard regime followed in SBRT liver).[18] All patients with one to three liver lesions were combined to form a lone PTV.[12,13]

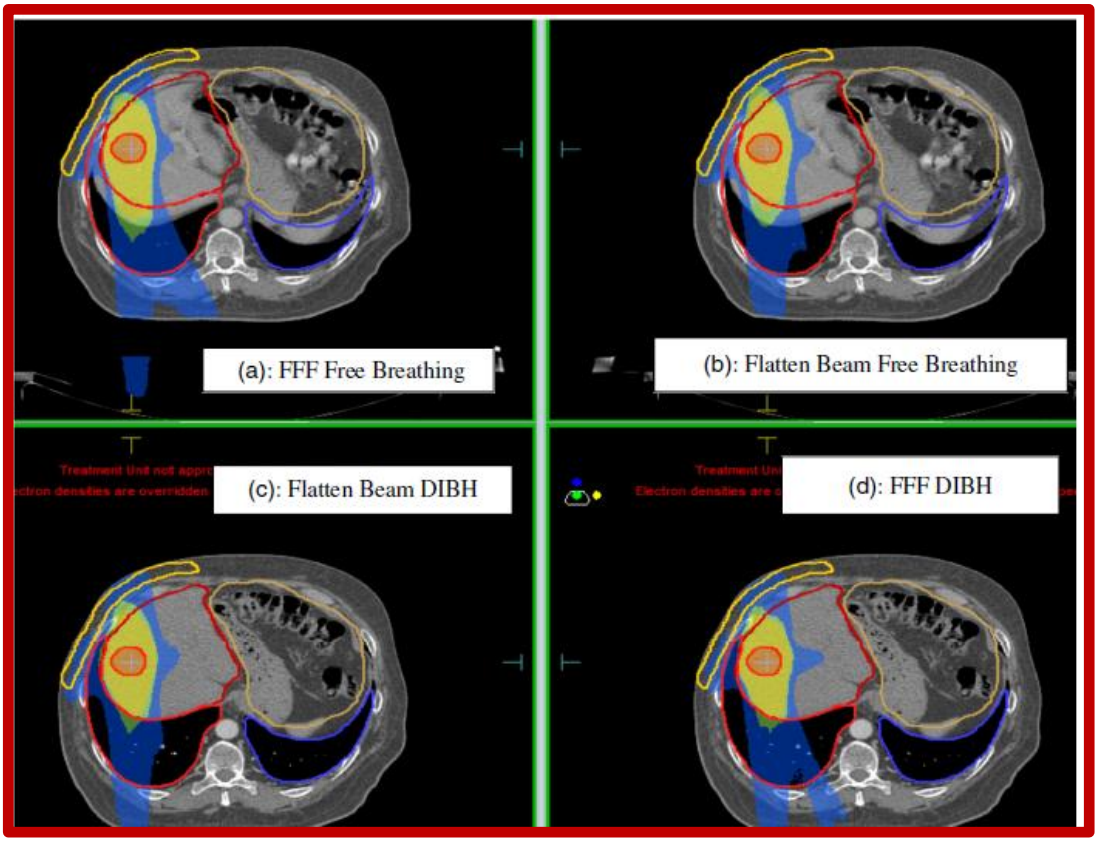

A comparison of single patient plan is presented in Figure 6.1. Panels A, B, C and D represent FFF beam in free breathing CT dataset, FB in free breathing CT dataset, FB in DIBH CT data set and FFF beam in DIBH CT dataset, respectively.

All plans were carried out using Elekta versa HD FFF 6MV photon beam, for the purpose of treatment, in DIBH study set. Subsequently, the same plan was copied onto the free breathing study set and optimization and dose calculation were carried out, without changing the optimization parameters. Two more treatment plans were created in DIBH and free breathing study sets, using an Elekta versa HD linear accelerator with FB.

6.4.0 Data collection and plan evaluation tools

6.4.1. Target volume (TV)

Quantitative and qualitative methods were used for evaluation of PTV. The references were taken from the recommendations of International Commission for Radiation Units(ICRU) Report No. 83. [19] Plans were analyzed using CT slice-by-slice isodose coverage and dose volume histograms (DVH).TV coverage and the conformity of the PTV was evaluated with isodose distribution in the transverse, sagittal and coronal planes. The criteria for dose minimum and maximum was considered as *D*98%and *D*2%, respectively. *D*98%and *D*2%wereereferred to as a dose received by 98% and 2% volume of PTV,

Results were evaluated for doses received by 98% PTV volume (D98%), maximum dose, Paddick conformity index (CI), heterogeneity index (HI) and PTV volume receiving 105% (V105%) of the prescription dose. Paddick CI and HI were defined as follows: [20]

$$CI = \frac{V_{RX}^2}{TV * V_{RI}}$$

where TV=target volume, VRX=target volume covered by 100% isodose line, VRI=volume of 100% isodose line,

$$HI = \frac{D_{5\%}}{D_{95\%}}$$

D5% and D95% were the doses received by 5 and 95% of the target

6.4.2 Organs at risk,

Total Eight dosimetric plans were generated for each patient and their specific DVHs were compared for organ-sparing. OAR doses were evaluated for mean dose, for bowel bag, heart, bilateral kidney, bilateral lung, chest wall, diaphragm and liver. Spinal cord was evaluated for the maximum dose. Spillage dose to unspecified tissues, corresponding to different beam models in DIBH and free breathing study sets, were evaluated for 5% (I-5%), 10%(I-10%), 20% (I-20%), 30% (I-30%), 40% (I-40%), 50% (I-50%), 60%(I-60%), 70% (I-70%) and 80% (I-80%) isodose volumes.

6.4.3 Treatment efficiency

Beam-on time (BOT) and TMUs were compared for all the plans FFF beam in DIBH, FB in DIBH, FFF beam in free breathing and FB in free breathing to assess the efficiency of the treatment. TPS was used to calculate MU and its average was obtained to calculate the BOT. All the plans were delivered at maximum dose rate of 600 MU/min FF Beam and 1400 MU/min FFF Beam to minimize the treatment time.

6.5. RESULTS:

6.5.1. Planning target volume (PTV)

The mean PTV volume of the liver lesions was 23·7±12·9 cm3, with no patient exhibiting more than three lesions. The graphical comparison of the dose–volume histogram for flattened and unflattened beams, on DIBH, is presented in Figure 6.2

Averaged overall patient results for dose received by 98% volume (D98%), maximum dose, Paddick CI, HI and PTV volume receiving 105% (V105%) of the prescription dose are presented, respectively, in the left and right panels of Figure 6.3.

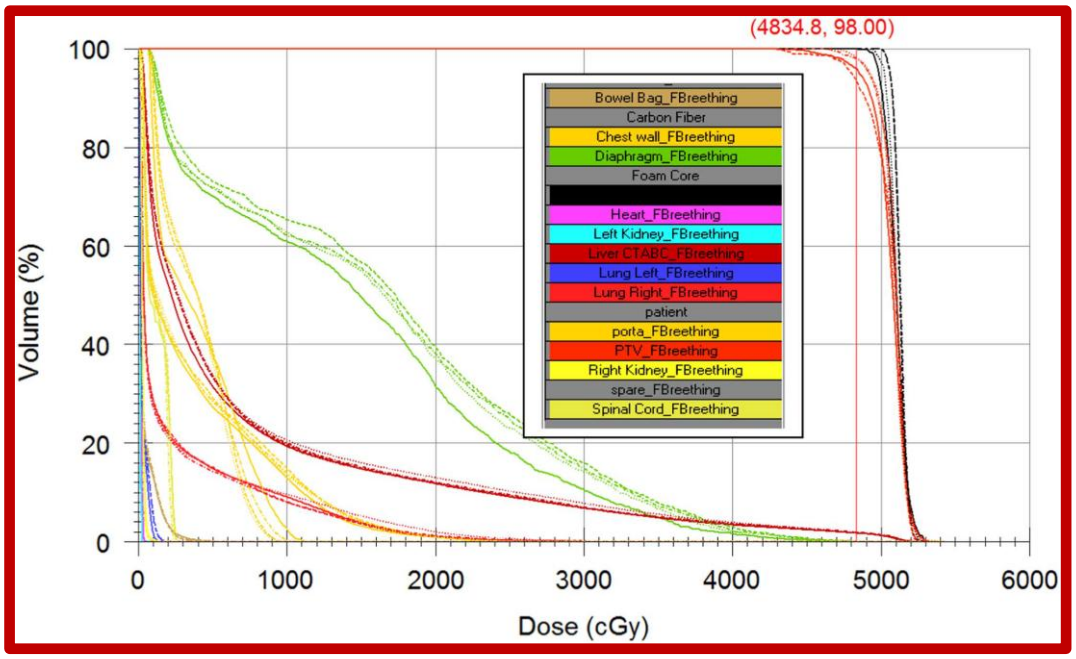

Figure 6.2. Dose–volume histogram comparison in DIBH and free breathing study sets, using flattened and unflattened beams. Abbreviation: DIBH, deep inspiration breath Hold

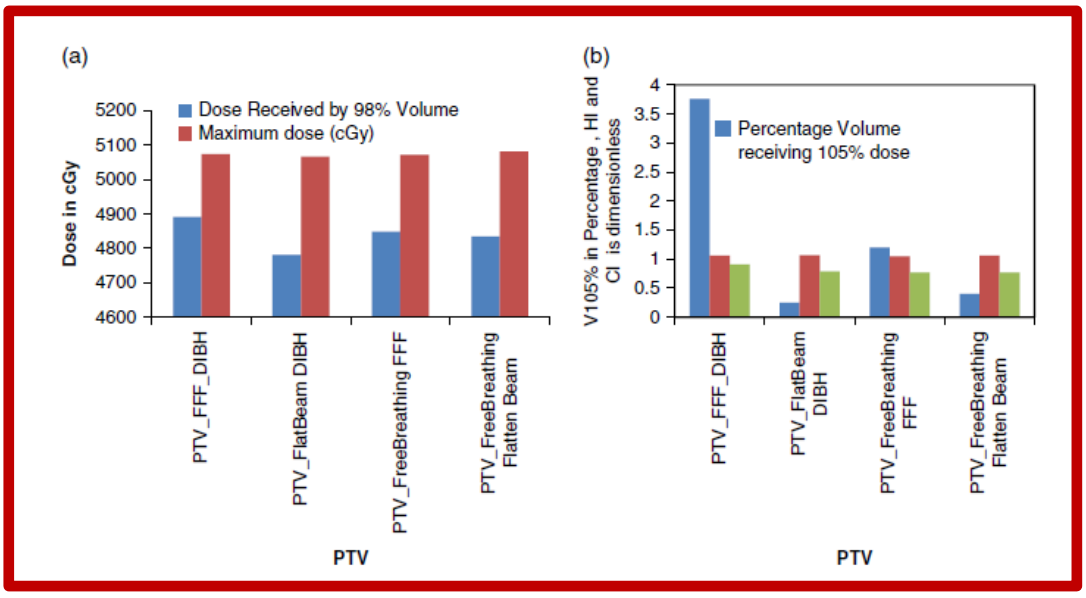

Figure 6.3. Variation of PTV coverage and hotspot related parameters, as a function of beam model in DIBH and free breathing condition. Abbreviations: DIBH, deep inspiration breath hold; PTV, planning target volume

Mean D98% for FFF in DIBH, FB DIBH, FFF in free breathing and FB in free breathing dataset were 48·9, 47·81, 48·5 and 48·3 Gy, respectively. Statistical co-relation (p) at 95% confidence interval (p), between the different beam models, was calculated using a Student's t-test. DIBH study set p, for FFF-FB, was 0·34. Free breathing study set p, for FFF-FB, was 0·69. Statistical significance p, for FFF-FB, indicates no statistical variation between the DIBH and free breathing study sets.

The average PTV maximum dose for FFF and FB for DIBH study sets, were 50·7 and 50·7 Gy, respectively. Maximum doses for free breathing study set, for the same group, were 50·7 and 50·8 Gy, respectively. PTV V105% for the same set were 3·76, 0·25, 1·2 and 0·4%, respectively. Mean HI for all study sets and beam models varies between 1·05 and 1·07. Paddik CI, using unflattened and FBs, in DIBH at 98% prescription dose were 0·91 and 0·79, respectively. The average CI of both beams, for free breathing CT set, was 0·77. The difference between the FFF and FBs for DIBH study set (statistical significance p) was <0·001.

6.5.2. Organs at risk

Average dose for OARs including the bowel bag, heart, bilateral kidneys, bilateral lung, chest wall, diaphragm, liver and maximum dose for spinal cord were presented in Figures 4a, 4b and 4c, respectively.

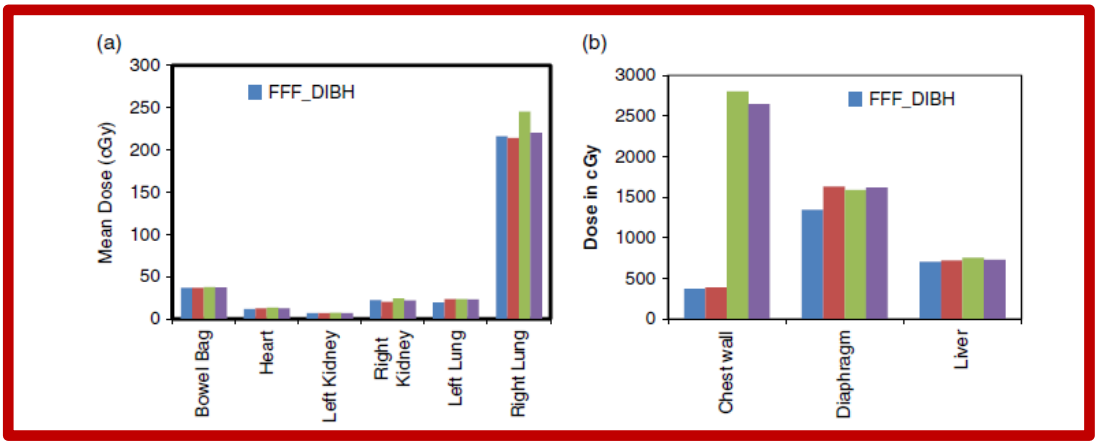

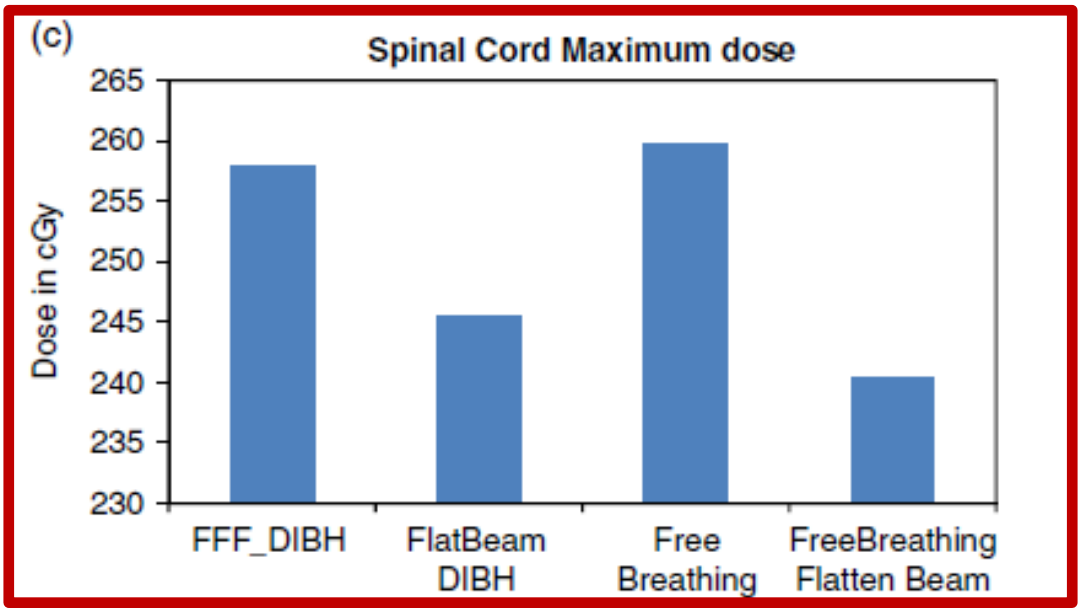

Figure 6.4. Mean dose to bowel bag, heart, bilateral kidney, bilateral lung (panel A), chest wall, diaphragm and liver (panel B) and maximum dose to the spinal cord (panel C), in DIBH and free breathing datasets using unflattened and flattened beam models. Abbreviation: DIBH, deep inspiration breath holds.

The dose administered to organs presented in panel A of Figure 6.4 is very low, as the organs are away from the target volume. Mean dose to the right lung varies between 2·2 and 2·5Gy with regard to different beam models and study sets. Bowel, bilateral kidney and left lung doses were between 0·07 and 0·37 Gy. Average doses to chest wall, for unflattened beam and FB, were 3·7 and 3·9 Gy, respectively; the same for free breathing study set were 28 and 26·5 Gy, respectively. Difference of dose on

chest wall, between DIBH and free breathing study sets, was statistically significant (p=0·03). Mean diaphragm doses for all four tested plans were comparable and varied between 13·4 and 16·3 Gy. Mean liver dose also did not yield any variation, with

respect to beam models and study sets.

The spillage doses of different beams and models (I-5% and I-10% to I-80%), are presented in Figure 6.5.

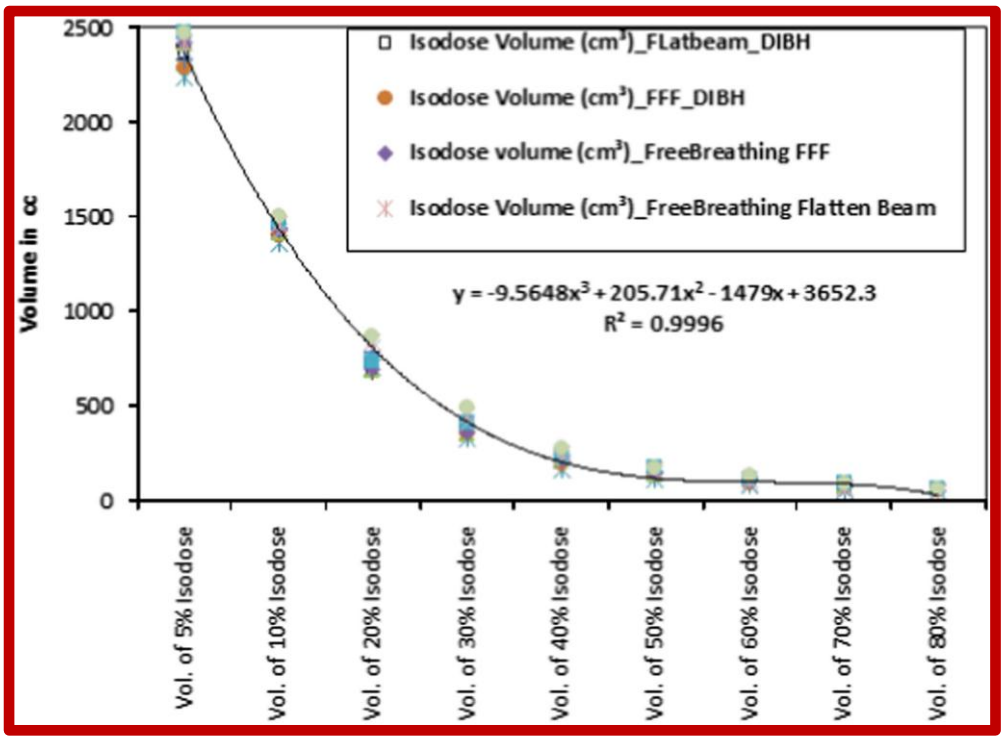

Figure 6.5. Isodose volume of 5% and 10%–80% were plotted as a function of beam model in DIBH and free breathing conditions

Figure 5 shows a negligible variation of the isodose volumes, with respect to flattened and unflattened beams, in DIBH and free breathing conditions. For example, I-5% yields a variation within the range of 2288·8–2427·2 cm3. This was noted to be the highest variation among all the isodose volumes. The variation between the isodose volumes attributed to the flattened and unflattened beams, for DIBH and free breathing conditions, diminishes with the increasing isodose values. The variation in I-80% was between 47·6 and 53·8 cm3, which is only 6·2 cm3.

6.5.3. Monitor unit

Average monitor units of FFF beam in DIBH, FB in DIBH, FFF beam in free breathing CT dataset and FB in free breathing CT dataset were 1318·6±265·1,

1940·3±287·6, 1343·3±238·1 and 2192·5±252·6 MU, respectively. The mean numbers of the breath holds were found to be 3·3±1·9 and 9·7±3·2 for unflattened beam and FB, respectively.

6.7. Discussion

Several studies of the past have investigated the planning aspect of unflattened beam, for liver and lung SBRT, esophagus, craniospinal irradiation and cranial stereotactic radiotherapy. [6–10,21–23] It is established that unflattened beam is dosimetrically comparable with the FB. Investigators have obtained a mixed result on the efficacy of the unflattened beam over the FB. For liver SBRT, many studies have been designed,

comparing flattened and unflattened beams. However, no study group has studied the influence of breath hold technique on this.

This study is the first of its kind to evaluate flattened and unflattened beams, with respect to free breathing and breath holding techniques. Reggiori et al. noted the effect of tumour volume on flattened and unflattened beams, depending on the CI. They favored unflattened beam for intermediate volume tumours (100 cm3≤PTV volume ≤300 cm3) and FB for the smaller and larger tumours. The mean target volume of the patient in this study did not exceed 50 cm3. However, we have observed an advantage of the unflattened beam over the FB in the target conformity.6

Earlier studies have noted a considerable reduction in the delivery time for unflattened beam because of the enhanced dose rate. For Elekta Versa HD linear accelerator, the dose rates are 600 and 2000–2200 MU/minute, for flattened and unflattened beams, respectively. Breath holding times do not exceed 30 seconds, with the average holding time between 20 and 25 seconds. Therefore, breath

holding technique essentially requires an unflattened beam to reduce the delivery time.

The advantage of Elekta versa HD linear accelerator is the speed of the MLC, which is as fast as 6 cm/second, which helps sustain a very high dose rate of 2000–2200 MU/minute. High dose rate delivery requires a higher MLC speed for a compatible delivery. A low MLC speed cannot sustain a high dose rate VMAT delivery. [24]

In this study, we observed a high CI with respect to the unflattened beam for breath hold technique. OAR doses to chest wall show a high dose difference between the breath hold and the free breathing techniques. Change in the CI of the unflattened beam is characteristic of the unflattened character of the beam. However, the loss of dose to the chest wall can be attributed to the fact that the chest wall in DIBH is fixed in a longer distance, for a longer time from the target. However, decrease in chest wall doses can be explained only with the unflattened characteristic of the beam.

As per the basic theory of Gaussian distribution, an unflattened beam is closer to a Gaussian distribution while a FB is a blur Gaussian. With the same characteristics, an unflattened beam should observe a better dose buildup to tumour, with a sharper fall at the periphery. However, no such phenomenon has been observed in any previous investigations so far.

Several authors have reported phase I/II clinical trials of liver metastasis, using stereotactic body irradiation.[12,13,25–27] For the large surgical series, including those primarily in patients with metastatic colorectal cancer, 5-year survival after liver resection ranges between 37 and 71%.[25–27] Patients who were not suitable for surgery and those with poor risk-prognostic factor were chosen for the

radiotherapy clinical trials, yielding a median survival of 20·5 month and a two-year local control of 100%.[12]

6.8. Conclusion

VMAT-based stereotactic body irradiation for liver metastasis shows considerable reduction in the delivery time for FFF beam, when compared to the FB. The reduction in delivery time is essential to keep the treatment time suitable for patients using the

breath holding technique. Unflattened beam shows no dosimetric advantage for unspecified tissues and OAR. However, a better conformal dose distribution was obtained for the unflattened beam. In conclusion, an unflattened beam is a good choice for liver SBRT, while using the breath hold technique.

6.8. References:

1. Kry S F, Howell R M, Titt U, Salehpour M, Mohan R, Vassiliev O N. Energy spectra, sources, and shielding considerations for neutrons generated by a flattening filter-free Clinac. Med Phys 2008; 35: 1906–1911.

2. Vassiliev O N, Kry S F, Chang J Y, Balter P A, Titt U, Mohan R. Stereotactic radiotherapy for lung cancer using a flattening filter free Clinac. J Appl Clin Med Phys 2009; 10 (1): 14–21.

3. Kry S F, Howell R M, Polf J, Mohan R, Vassiliev O N. Treatment vault shielding for a flattening filter-free medical linear accelerator. Phys Med Biol 2009; 54: 1265–1273.

4. Kragl G, Baier F, Lutz S et al. Flattening filter free beams in SBRT and IMRT: dosimetric assessment of peripheral doses. Z Med Phys 2011; 21: 91–101.

5. Mancosu P, Castiglioni S, Reggiori G et al. Stereotactic body radiation therapy for liver tumours using flattening filter free beam: dosimetric and technical considerations. Radiat Oncol 2012; 7 (1): 16.

6. Reggiori G, Mancosu P, Castiglioni S et al. Can volumetric modulated arc therapy with flattening filter free beams play a role in stereotactic body radiotherapy for liver lesions? A volume- based analysis. Med Phys 2012; 39 (2): 1112–8.

7. Nicolini G, Ghosh-Laskar S, Shrivastava S K et al. Volumetric modulation arc radiotherapy with flattening filter-free beams compared with static gantry IMRT and 3D conformal radiotherapy for advanced esophageal cancer: a feasibility study. Int J Radiat Oncol Biol Phys 2012; 84: 553–60.

8. Sarkar B, Pradhan A. Choice of appropriate beam model and gantry rotational angle for low-dose gradient-based craniospinal irradiation using volumetric modulated arc therapy. J Radiother Pract 2017; 16 (1): 53–64.

9. Navarria P, Ascolese A M, Mancosu P et al. Volumetric modulated arc therapy with flattening filter free (3F) beams for stereotactic body radiation therapy (SBRT) in patients with medically inoperable early stage non-small cell lung cancer (NSCLC). Radiother Oncol 2013; 107: 414–8.

10. Sarkar B, Pradhan A, Munshi A, Roy S, Ganesh T, Mohanti B. EP-1685:Influence of flat, flattening filter free beam model and different MLC's on VMAT based SRS/SRT. Radiother Oncol 2016; 119: S787.

11. Timmerman R D, Kavanagh B D, Cho L C, Papiez L, Xing L. Stereotactic body radiation therapy in multiple organ sites. J Clin Oncol 2007; 25: 947–952.

12. Rusthoven K E, Kavanagh B D, Cardenes H et al. Multi-institutional phase I/II trial of stereotactic body radiation therapy for liver metastases. J Clin Oncol 2009; 27 (10): 1572–8.

13. Lee M T, Kim J J, Dinniwell R et al. Phase I study of individualized stereotactic body radiotherapy of liver metastases. J Clin Oncol 2009; 2710): 1585–91

14. Macdermed D M, Weichselbaum R R, Salama J K. A rationale for the targeted treatment of oligometastases with radiotherapy. J Surg Oncol 2008; 98: 202–206.

15. Cai J, Malhotra H K, Orton C G. A 3D- conformal technique is better than IMRT or VMAT for lung SBRT. Med Phys 2014; 41 (4): 040601.

16. de Pooter J A, Romero A M, Wunderink W, Storchi P R, Heijmen B J. Automated non-coplanar beam direction optimization improves IMRT in SBRT of liver metastasis. Radiother Oncol 2008; 88 (3):376–81

17. L Nithya, N Arunai Nambi Raj, Sasikumar Rathinamuthu, Kanika Sharma, Influence of increment of gantry angle and number of arcs on esophageal volumetric modulated arc therapy planning in Monaco planning system: A planning study, JMP Year: 2014 Volume**:** 39: 4: 231-237

18. Milano M T, Katz A W, Muhs A G et al. A prospective pilot study of curative- intent stereotactic body radiation therapy in patients with 5 or fewer oligometastatic lesions. Cancer: Interdiscip Int J Am Cancer Soc 2008; 112 (3): 650–8.

19. *ICRU Report 83, Journal of the ICRU, Vol. 10, No. 1*. Oxford University Press; 2010.17.

20. Paddick I. A simple scoring ratio to index the conformity of radiosurgical treatment plans: technical note. J Neurosurg 2000; 93 (Supplement 3):219–22.

21. Dzierma Y, Bell K, Palm J, Nuesken F, Licht N, Rübe C. mARC vs. IMRT radiotherapy of the prostate with flat and flattening-filter-free beamenergies. Radiat Oncol 2014; 9 (1): 250.

22. Thomas E M, Popple R A, Prendergast B M, Clark G M, Dobelbower M C, Fiveash J B. Effects of flattening filter-free and volumetric-modulated arc therapy delivery on treatment efficiency. J Appl Clin Med Phys 2013; 14: 4328. https://doi.org/10.1120/jacmp.v14i6.4328.

23. Sarkar B, Pradhan A, Munshi A. Do technological advances in linear accelerators improve dosimetric outcomes in stereotaxy? A head-on comparison of seven linear accelerators using volumetric modulated arc therapy-based stereotactic planning. Indian J Cancer 2016; 53 (1): 166–173.

24. Manikandan A, Sarkar B, Holla R, Vivek T R, Sujatha N. Quality assurance of dynamic parameters in volumetric modulated arc therapy. Br J Radiol 2012; 85 (1015): 1002–10.

25. Fong Y, Fortner J, Sun R L, Brennan M F, Blumgart L H. Clinical score for predicting recurrence after hepatic resection for metastatic colorectal cancer: analysis of 1001 consecutive cases. Ann Surg 1999; 230 (3): 309.

26. Shah S A, Bromberg R, Coates A, Rempel E, Simunovic M, Gallinger S.Survival after liver resection for metastatic colorectal carcinoma in a large population. J Am Coll Surg 2007; 205 (5): 676–83.

27. Aloia T A, Vauthey J N, Loyer EMet al. Solitary colorectal liver metastasis: resection determines outcome. Arch Surg 2006; 141 (5): 460–7.

CHAPTER -VII

A Feasibility Study of Flattened and Flattening Filter Free Beam based Treatment Techniques for Cervical Carcinoma

Chapter -VII

A Feasibility Study of Flattened and Flattening Filter Free Beam based Treatment Techniques for Carcinoma Cervix

7.1 Introduction:

Over the last three decades, radiotherapy has played a significant role in the treatment of more than half of all cancer patients. [1]. Cervical cancer continues to be the most frequent gynecological cancer in the globe. Cervical cancer is routinely treated with radiotherapy. [2,3].

Modern LINACs can produce both FB and FFFB photon beams. The use of FFFB in radiotherapy has improved treatment delivery since removing a flattening filter from the X-ray beam's path leads to more efficient photon generation and a considerable increase in dose rate at the treatment level. Because of the shorter treatment intervals, higher dose rates diminish intra fraction motion and improve patient comfort. Furthermore, Lower scatter, leakage, and out-of-field scatter doses are among the dosimetric advantages of the FFFB. [4,5]. Radiation-induced secondary malignancies may be reduced as a result of the reduction in out-of-field doses.

The first clinical investigation on the use of the FFF beam to minimize the long treatment duration for high dosage radiosurgery was published in 1991 [6]. According to Casemore et al. [7], Whereas an FFF beam decreases scattering and related exposure to distal organs, A FFFB with the same photon intensity has a lower secondary dosage to distal nor-mal organs than an FB with the same photon intensity. Over the previous few decades, many radiation treatments have advanced dramatically. The delivery technology for radiation therapy is advancing, from 3-dimensional conformal radiotherapy (3DCRT) to intensity-modulated radiotherapy

(IMRT) and volumetric-modulated arc therapy (VMAT). [8]

Although 3-dimensional conformal radiotherapy (3DCRT) (9-11) confines the radiation dose to the PTV, intensity modulated radiotherapy (IMRT) (12-16) has the added benefit of protecting the organs at risk (OAR). It can be very tough to spare the OAR without affecting PTV coverage while using 3DCRT. Many diseases, including cervical cancer, have recently seen an increase in the use of IMRT and VMAT Techniques. IMRT has been studied extensively, however Otto et al. [16] and Palma et al. [17] found that the VMAT method achieves great target conformity and spares more organs at risk than IMRT. In terms of treatment delivery, VMAT is more efficient because it requires low monitor units (MUs) and has a shorter beam-on time.

To offer rotational IMRT with increased gantry speed, multi-leaf collimator motion, and dose rates while sparing normal tissue, VMAT and helical tomotherapy have been developed. [18-19] Compared to static beam Intensity Modulated Radiation Therapy (IMRT), VMAT requires lesser monitor units (MUs) and has a shorter treatment period [20].

When compared to 3DCRT treatment planning, VMAT and IMRT give greater target conformity and essential structure sparing, but low dose volume in normal tissue is much higher in VMAT and IMRT [21,22]. This increased low dose volume is concerning because it raises the risk of radiation-induced carcinogenesis, especially in patients who are expected to live a long time [23]. VMAT is already compared with 3DCRT and IMRT for different cancer types at different sites [4].

Although it is well proven that VMAT improves delivery efficiency over IMRT (4-5), it is questionable whether VMAT also improves plan quality for cervix cancer treatment planning when compared to 3DCRT and IMRT, as shown in Table 4.

Each of these investigations used four 3DCRT fields, 9 IMRT fixed-gantry fields, and one full arc of VMAT. In comparison to the findings of these studies, it's still unknown whether VMAT produces better plan quality for cervical cancer radiation therapy than IMRT. Furthermore, there was very little information in the published literatures about the time invested in the inverse planning process, as well as how the quality of the 3DCRT, IMRT, and VMAT plans is controlled, which have a significant impact on the planning outcomes and thus the plan quality comparison result.

The primary purpose of this research was to compare dosimetric characteristics and establish which radiation technique and beam energy was the most effective.i.e., to obtain the optimal dosimetric distribution of the target while minimizing the dose delivered to the cervix by creating three radiotherapy plans with different (FB, FFFB beam 6MV &10 MV Energy) for a specific case.

7.2. Aim,

To determine the effects of filtered and flattening filter free beams with energies of 6 and 10 MV on the cervix using various treatment techniques such as 3DCRT, IMRT, and VMAT, as well as how to create clinically appropriate FFF photon beam treatment plans and investigate their potential benefits for cervical cancer patients.

7.3. Material Method:

7.3.1 Patient selection:

We chose 30 patients with cervical carcinoma who were between the ages of 54 and 69 for our retrospective analysis. The T3N1M0 stage of cervical cancer was found in all of the participants in this investigation. [24] They'd all developed lymph nodes and were getting ready to start definite radiation treatments.

7.3.2 CT simulation

Before to CT Scanning, all patients were instructed to follow a bladder protocol, which included voiding the bladder and afterwards drink water approximately 1 liter to refill it. To guarantee bladder filling, they were told to wait 45 minutes before the planning scan. Fiducial markers were placed at the region of the pelvic brim. A vacuum cushion was used to immobilize all of the patients, which deflated into the shape of the patient. In a supine position, the patient raised his hands above his head.

CT scans were performed on all of the patients with a Biograph MCT-20, PET-CT with a 3 mm slice thickness, a field - of - view of 50 cm, and a depth of 5 cm below the ischial tuberosity. The DICOM-enabled interface was used to upload CT files to the Monaco Sim workstation for contouring.

7.3.3 Target and OAR delineation,

The GTV and CTV were contoured by a qualified radiation oncologist. For all of the patients, Clinical Target Volume was utilised to define OARs (CTV). To get the planning goal volume, CTV was given a 0.5 cm margin (PTV). The bladder, rectum, bowel, and femoral heads were contoured, among other OARs. The bladder was contoured from the apex to the dome, and the rectum was contoured from the anus (at the inferior level of the ischial tuberosity) to the recto-sigmoid junction. Up to the level of the ischial tuberosity, the contours of the bilateral femoral heads were traced. [25,26,27]

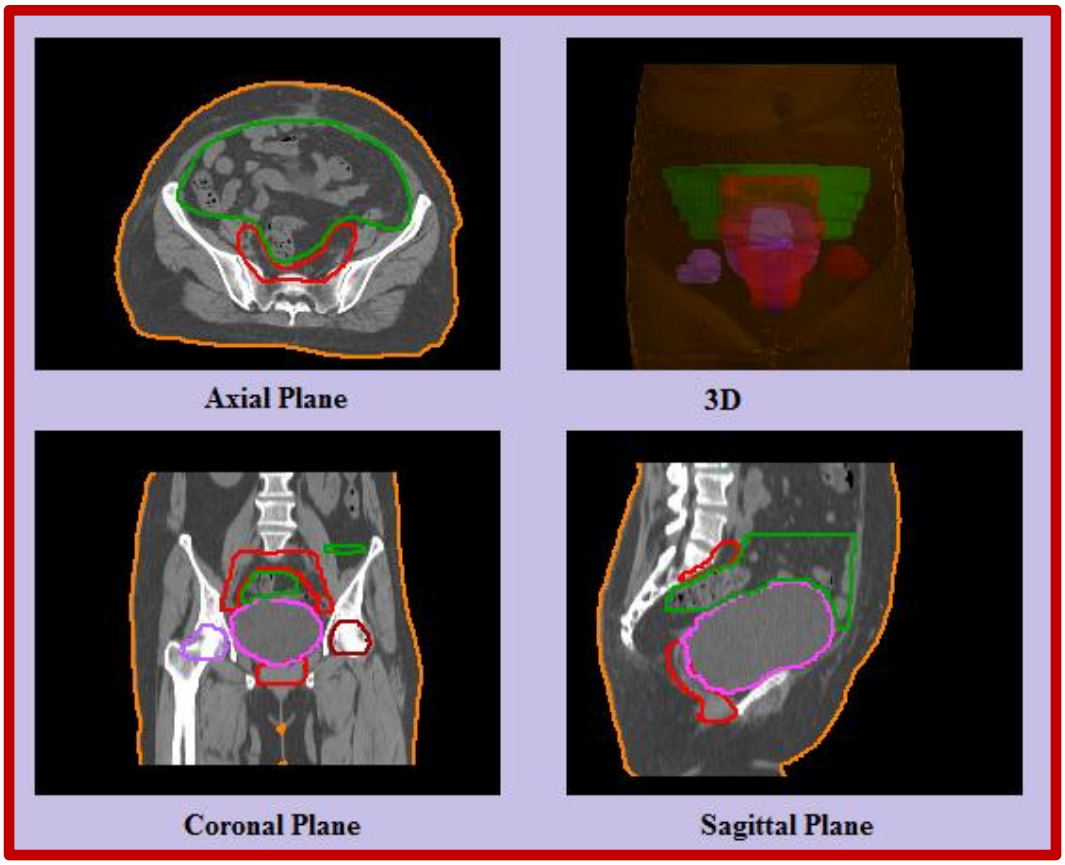

Figure 7.1 Represents the delineated Target volume and OARs in Axial/coronal/sagittal Plane/3D View

The resident radiation oncologists contoured the OAR. For radiotherapy planning, the CT study sets and outlines were sent to the Monaco TPS. Using an Elekta Versa HD linear accelerator, the VMAT designs were delivered. The linear accelerator is equipped with MLCs with 80 leaf pairs of 5 mm width.

7.3.4 Treatment planning system:

The MONACO TPS version 5.10.0 takes into account the physical effects of radiation as well as the tissue's biological features. Target EUD, serial, and parallel are three biological constraints, whereas target penalty, overdose DVH, quadratic overdose, under dosage DVH, quadratic under dose and maximum dose are six physical constraints, In target EUD, the user may adjust the tumor's cell sensitivity. The organ at risk can be limited in a serial or parallel way, depending on the tissue's properties.

The system optimizes dosage distribution in two stages. Stage one optimizes the optimal fluence distribution of beams to fit a user-defined prescription for a given group of beams. In second stage optimizes, deliverable fields are created through segmentation, which comprises segment shapes and weights. The system uses Monte Carlo simulation during the optimization stage. [14]

7.3.5 Planning objectives

PTV was given a dose of 50 Gy divided into 25 fractions of 2 Gy each [26,27]. No more than 98 percent of PTV should receive a dose less than the prescribed quantity, and no more than 2% of PTV should receive a dose greater than 105 percent of the approved dose. QUANTEC Protocol 10 was used to process all of the OARs.A hot spot was described as a 2% volume receiving more than 110% of the specified dose.

7.3.6 Planning techniques

A Monaco TPS version 5.10.0 was used to develop 240 plans for the 30 patients using 3DCRT, 9F-IMRT, and Single arc -VMAT. A 6-MV&10MV photon energy Elekta Versa HD accelerator with FF and FFF beams. The PTV was treated with a prescription of 50 Gy in 2 Gy parts. The 3DCRT plans had four box fields (anterior-posterior and Left-right) with gantry angles of about 0,90,180, and 270 degrees (no physical or dynamic wedges were utilised). Multileaf collimators (MLCs) were used to cover the bladder, rectum, and other organs at danger. If the dose distribution of the 3-dimensional plan is optimised, you can use the field in approach to reduce the dose level by 110 percent if needed. Based on Photon beam energies of 6MV and 10 MV, we produced two sets of 3DCRT- designs. With a grid size of 3mm, the doses were estimated using the PBC algorithm.

The 9 F-IMRT plans have gantry angles of 0,40,80,120,160,200,240,280, and 320 degrees. The plans were created using a robust inverse planning method. We

define a maximum of 20 control points per beam. The Multileaf collimator was programmed to move at a speed of 6 centimetres per second. The doses were estimated using the Monte Carlo Technique on a 3-mm grid, and to optimize the doses, the dose volume optimizer (DVO) method was utilized. The plans were given a dosage rate of 600 MU/min using a sliding window approach (6 & 10MV FF).

All VMAT plans featured the following calculating properties: The Monte Carlo variance was set at 3%, and the grid spacing was set to 3 mm. In the second step, For the final dose calculation, the Monte Carlo approach was chosen as the secondary methodology. Instead of water, the dose was estimated using the medium. Heterogeneity correction was applied to all plans. A single 360° gantry rotation was used to deliver the VMAT plan (clockwise from 180 to 180 degrees). MLC segmentation was accomplished using the sweep sequencer tool in the VMAT technique. Monte Carlo simulations were used to calculate the dose. To achieve the specified dose using the VMAT plan, we flattened 6 and 10MV photon beams and employed a Flatten filter-free photon beam.3DCRT, IMRT, and VMAT plans were optimized utilizing optimization parameters (Table 7.2) and calculation parameters to achieve the requisite dose limitations (Table 7.1). (Table 7.3). On 3D CT images, the radiation dosage from 3DCRT, IMRT, and VMAT plans was computed, with heterogeneous corrections applied.

Structure	Parameter	Constraints
PTV	$V_{95\%}$	> 47.5Gy
	$V_{10\%}$	< 107% of Prescribed Dose
Rectum	$V_{60\%}$	< 45 Gy
Bladder	$V_{35\%}$	< 45 Gy
Bowel	D_{Max}	< 50 Gy
Femoral Head	$V_{20\%}$	< 40 Gy

Table 7.1: Treatment Planning Objectives for 3DCRT, IMRT and VMAT:

Structure	Cost functions	Parameter	Isoconstraints
PTV	Target EUD	0.5	50 Gy
	Quadratic Overdose	51.5 Gy	0.45Gy
	Target penalty	95%	50 Gy
Rectum	Parallel	k=3	35 Gy
Bladder	Parallel	k=3	30 Gy
Bowel	Parallel	k=3	25 Gy
	Maximum dose	Shrink=3 mm	48 Gy
Femoral Head	Maximum dose	Shrink=3 mm	48 Gy
Body	Quadratic Overdose	Shrink=0 mm, 50 Gy	0.10 Gy
	Quadratic Overdose	Shrink=3 mm, 47 Gy	0.15 Gy
	Maximum dose	Shrink=5 mm	46 Gy
	Maximum dose	Shrink=10 mm	40 Gy
	Maximum dose	Shrink=15 mm	35 Gy
	Maximum dose	Shrink=25 mm	25 Gy

EUD-Equivalent Uniform Dose; k=Power law exponent

Table 7.2. The cost functions for optimization of IMRT and VMAT plans in cervical cancer

Calculations Properties	
Grid Spacing	0.3 cm
Dose Deposition to	Medium
Algorithm	Monte Carlo photon
Statistical Uncertainty	1% / calculation

Table: 7.3 For 3DCRT, IMRT and VMAT Calculations Properties

7.4.0 Plan quality indices and plan evaluation tools

7.4.1. Target volume (TV)

PTV was evaluated using both quantitative and qualitative methods. The references were taken from the International Commission for Radiation Units (ICRU) Report No. 83's recommendations. CT slice-by-slice isodose coverage and dose volume histograms were used to assess the plans (DVH). Isodose distribution in the transverse, sagittal, and coronal planes was used to measure TV coverage and PTV conformance.

For various approaches such as 3 DCRT, IMRT, and VMAT, 95 percent isodose lines were used to calculate CI, HI, DGI, and TC. In addition, the exposure to OARs was calculated using a dose–volume histogram. Using the equations (1–3), the conformity index (CI), homogeneity index (HI), and dose gradient were calculated:

$$CI = \frac{(TV_{RI})^2}{(TV \times V_{RI})}, \quad (1)$$

where TV=target volume, VRX=target volume covered by 100% isodose line, VRI=volume of 100% isodose line,

$$HI = \frac{(D_{2\%} - D_{98\%})}{D_{50\%}}, \quad (2)$$

Maximum dose received by 2% of PTV (D2%), minimum dose received by 98% of PTV (D98%), dose received by 50% of PTV (D50%)

$$DGI = \frac{V_{RI}}{V_{HRI}}. \quad (3)$$

Total volume encompassed in half of the prescription dose ($_{VHRI}$) and corresponding RI

In Equation (1), total volume included in prescription dosage (VRI) was replaced for volume of PTV receiving prescription dose (TVRI), volume of PTV (TV), and total volume encompassed in prescription dose (TVRI). Equation (2) was used to compute HI by substituting the maximum dose received by 2% of PTV (D2%), the lowest dose received by 98 percent of PTV (D98%), and the dose received by 50% of PTV (D50%).

By substituting total volume included in half of the prescription dose (VHRI) and corresponding VRI, equation (3) was utilised to calculate DGI.

7.4.2 Organs at risk,

For a total of 30 patients, 240 dosimetric plans were created, and their unique DVHs were compared for organ spare. OAR doses were evaluated for dose for bladder (D15%, D25%, D35%, D50%) rectum (D15%, D25%, D35%, D50%), bowel (V15Gy (%,), V30Gy (%), V45Gy (%)) and femoral heads (V25Gy (%), V45Gy (%)Mean dose (Gy), Max. dose (Gy)) and. The maximal dose was assessed in the spinal cord.

7.4.3 Treatment efficiency

TMUs were compared for all three treatment plans (3DCRT, IMRT, and VMAT) to determine therapy efficacy. TPS was used to determine MU, and the BOT was calculated using its average. To reduce treatment time, all plans were provided at a maximal dose rate of 600,1200,2400 MU/min 6 & 10MV FB and FFFB.

The 6 MV FB VMAT design was employed as a baseline for statistical comparison. Each of the other treatment approach designs was re-normalized to deliver the same mean dose to PTV, as in, to eliminate any bias or rescaling impacts. A paired-sample t-test was used to compare plan quality metrics and dosage to OARs; The difference was significant with a p-value of 0.05 [29].

7.5. RESULTS:

7.5.1. Planning target volume (PTV)

Flattened and flattened filter free beam of 6 and 10 MV were used to construct clinically acceptable and equivalent 3DCRT, IMRT, and VMAT plans. Table 4 summarizes the dosimetric parameters for PTV coverage derived by 3DCRT, IMRT, and VMAT plans utilizing FB and FFFB of 6 and 10 MV. In comparison to 3DCRT and IMRT plans, HI is greatly enhanced in VMAT (FB and FFFB of 6 and 10 MV) plans. Plans using VMAT and IMRT produced a highly conformal dosage and were greatly improved. For all VMAT plans using FB and FFFB photon beam energy, HI, CI, DG, and TC are comparable (6 MV and 10 MV). For FB and FFFB of 6 and 10 MV, which were shown to be significantly different (p 0.05). MUs were lower in 10 MV VMAT plans and greater in FFF VMAT plans. Figure 2 illustrates the isodose distribution for the same patient using FB and FFFB of 6 and 10 MV in the axial planes in 3DCRT, IMRT, and VMAT designs. Figure 3 shows DVH form 3DCRT, IMRT, and VMAT layouts with 6 and 10 MV FB and FFFB.

These DVH demonstrate no significant changes in PTV coverage for VMAT plans using FB and FFFB of 6 and 10 MV, even in a high dosage site. FB VMAT produces a more uniform and conformal dose distribution to the PTV than FFFB VMAT, 3DCRT, or IMRT.

7.5.2. Dose to OAR's

Table 4 presents the dosimetric data for OARs, which were calculated using FB and FFFB of 6 and 10 MV for 3DCRT, IMRT, and VMAT plans. As the VMAT and IMRT plans modulate the intensity to spare critical organs and having more number beams, DG is worsened. Dose to Bladder, Bowel, rectum and femoral heads was significantly reduced with VMAT (FB & FFFB) plans compare to 3DCRT and IMRT. Dose to bladder (V15%, V25%, V35% and V50%) was comparable with FF VMAT plans and significantly higher in FFF VMAT plans. Dose to bowel (Mean, V15%, V30% and V45%) was comparable with FF VMAT plans and significantly higher in FFF VMAT plans. Dose to rectum (V15%, V25%, V35% and V50%) was comparable with FF VMAT plans and significantly higher in FFF VMAT plans. Dose to femoral heads (V25%, V40%, Mean and Max) were comparable for all the VMAT plans using FF and FFF photon beams.

7.5.3. Monitor units (MUs)

The treatment efficiency of 3DCRT, IMRT, and VMAT plans using FB and FFFB of 6 and 10 MV was evaluated using total numbers of monitor units. The number of Monitor Units (MUs) for FB VMAT and FB IMRT 6 and 10 MV did not differ significantly. In comparison to IMRT and VMAT, the total MUs in 3DCRT plans are much lower.

The number of Monitor Units (MUs) was significantly different for FB and FFFB 6 and 10 MV (p 0.05). FFFB requires a statistically significant (p 0.05) increase in

the number of monitor units when compared to FB. Table 4 compares total monitor units (MUs) for individual patients using FB and FFFB of 6 and 10 MV in 3DCRT, IMRT, and VMAT designs. When FFFBs of 6 and 10 MV were compared to FBs of 6 and 10 MV, Mus increased by 10.5 percent and 30%, respectively.

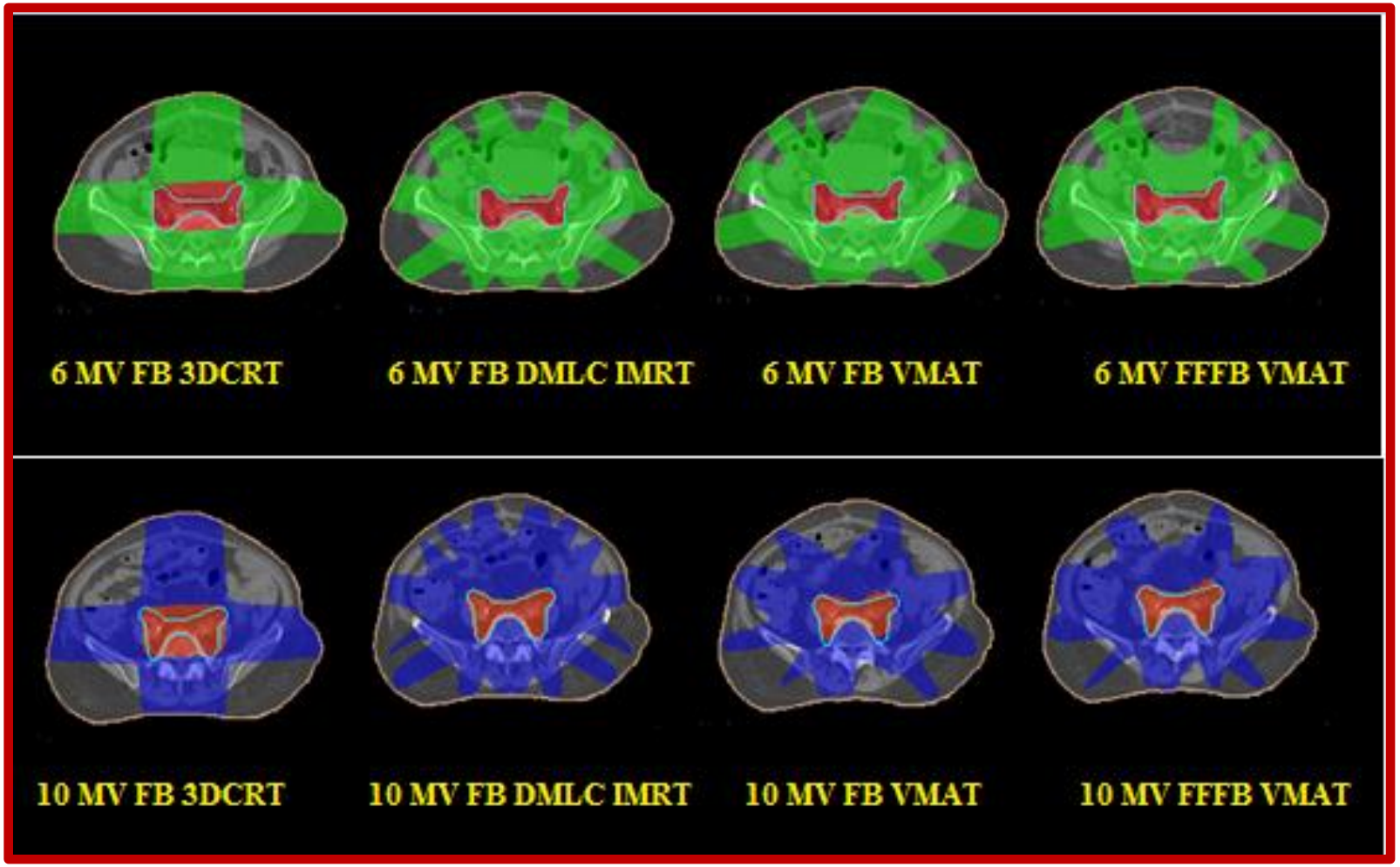

Fig. 7.2 – Comparison of isodose distribution utilizing FB and FFFB of 6 MV and 10MV from 3DCRT, IMRT, and VMAT designs.

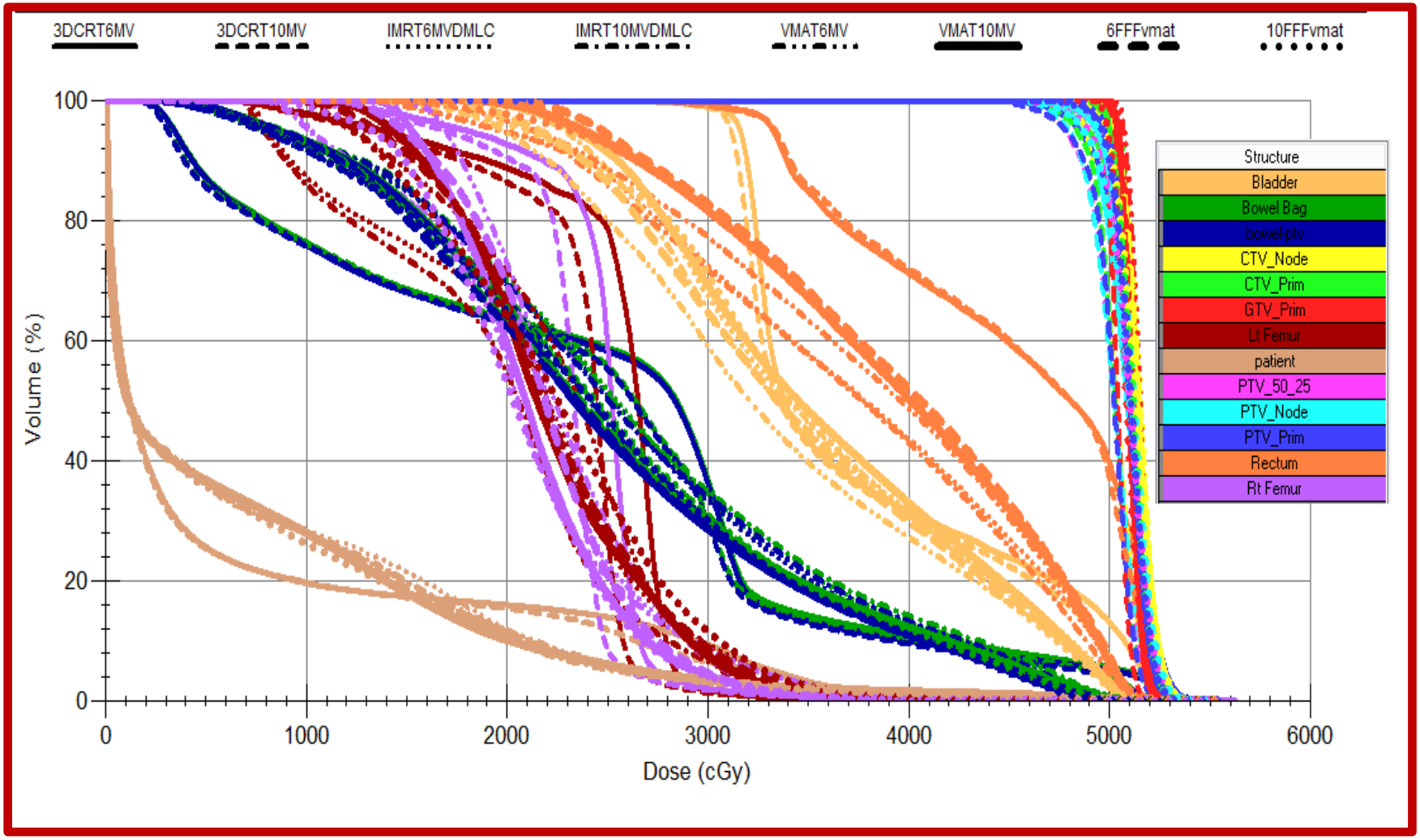

Figure-3: DVH comparison of target coverage and OARs for 3DCRT, IMRT, and VMAT plans utilizing 6 MV and 10MV FB and FFFB

Structure	Parameter	6MV 3DCRT	10 MV 3DCRT	6 MV DMLC IMRT	10 MV DMLC IMRT	6MV VMAT	10 MV VMAT	6 MV FFF VMAT	10 MV FFF VMAT	p-Value						
										6 MV 3DCRT	10 MV 3DCRT	6 MV DMLC IMRT	10 MV DMLC IMRT	10 MV VMAT	6 MV FFF VMAT	10 MV FFF VMAT
PTV	HI	0.11±0.03	0.09±0.07	0.04±0.28	0.05±0.01	0.07±0.01	0.07±0.02	0.07±0.01	0.07±0.01	0.00	0.00	0.00	0.00	0.60	0.75	0.69
	CI	0.62±0.09	0.61±0.08	0.79±0.06	0.77±0.06	0.8±0.05	0.8±0.05	0.79±0.06	0.79±0.05	0.00	0.00	0.36	0.11	0.83	0.52	0.48
	DG	0.22±0.04	0.23±0.04	0.35±0.03	0.37±0.03	0.32±0.03	0.32±0.04	0.33±0.03	0.33±0.03	0.00	0.00	0.00	0.00	0.78	0.12	0.14
	TC	0.97±0.01	0.96±0.02	1±0.00	1±0.00	1±0	0.99±0.01	1±0	1±0	0.00	0.00	0.65	0.62	0.63	0.79	0.77
	MU	294.92±13	257.0±13	1020.6±10	992.54±89	1068.1±11	951.52±70	1262.2±13	1265.1±13	0.00	0.00	0.00	0.00	0.00	0.00	0.00
Bladder	V15%	48.09±3.15	47.49±3.03	45.07±3.63	45.17±3.33	43.94±4.94	43.68±5.02	44.85±4.1	45.06±3.62	0.00	0.00	0.00	0.00	0.56	0.00	0.00
	V25%	44.22±5.67	43.98±5.55	41.2±4	41.26±3.73	39.72±5.85	39.88±5.9	41±5.12	41.16±4.57	0.00	0.00	0.00	0.00	0.67	0.00	0.00
	V35%	40.27±7.79	39.98±7.71	37.76±3.92	38.43±4.32	35.9±5.84	36.48±5.65	37.17±5.29	37.39±4.82	0.00	0.00	0.00	0.00	0.00	0.00	0.00

	V50%	35.18±6.98	35.42±7.59	33.29±3.22	33.47±3.2	31.18±5.02	31.29±5.21	32.08±4.74	32.37±4.28	0.00	0.00	0.00	0.00	0.38	0.00	0.00
Bowel	**Mean (Gy)**	24.33±3.29	24.67±3.71	25.11±2.4	25.23±2.58	23.9±2.47	23.77±2.99	24.23±2.48	24.35±2.35	0.00	0.00	0.00	0.00	0.21	0.00	0.00
	V15 Gy %	69.16±14.9	69.25±15.42	84.72±5.28	85.03±5.86	80.61±7.28	77.99±10.74	80.14±8.64	79.53±8.51	0.00	0.00	0.00	0.00	0.00	0.26	0.00
	V30 Gy %	31.44±7.24	31.52±8.58	28.25±8.4	28.55±8.9	26.71±7.6	26.8±8	27.53±7.11	28.18±6.52	0.00	0.00	0.00	0.00	0.12	0.00	0.00
	V45 Gy %	11.99±5.32	12.5±5.27	5.22±2.05	5.55±2.21	5.17±2.02	5.45±1.98	5.3±2.04	5.58±2.12	0.00	0.00	0.20	0.12	0.00	0.00	0.00
Rectum	**V15%**	51.42±1.08	50.99±1.33	48.08±1.74	48.22±1.78	48.4±2.15	48.44±2.08	48.81±1.38	48.64±1.68	0.00	0.00	0.13	0.26	0.62	0.07	0.10
	V25%	50.92±1.23	50.35±1.45	45.16±2.62	45.23±2.7	46.02±3.39	45.99±3.23	46.5±2.45	46.31±2.82	0.00	0.00	0.36	0.41	0.61	0.12	0.34
	V35%	50.13±1.29	49.5±1.51	41.87±3.14	41.89±3.15	43.29±4.03	43.23±3.75	44.04±3.16	43.72±3.48	0.00	0.00	0.00	0.00	0.53	0.00	0.04
	V50%	47.12±2.58	47.01±2.29	36.57±3.11	36.7±3.37	38.56±4.02	38.35±3.88	39.56±3.12	39.31±3.85	0.00	0.00	0.00	0.00	0.09	0.00	0.00
Femoral Head Rt	**V25%**	25.03±5.6	24.5±5.86	22.41±3.14	22.6±2.98	21.43±2.62	21.74±2.77	21.27±2.35	21.71±2.77	0.00	0.00	0.05	0.05	0.12	0.05	0.16

	V40%	23.28±6.11	23.09±6.07	20.46±2.84	20.17±2.61	19.74±2.39	19.94±2.54	19.6±2.12	20.11±2.51	0.00	0.00	0.13	0.14	0.07	0.01	0.00
	Mean (Gy)	21.35±5.91	21.12±6.15	19.93±2.59	19.52±2.48	19.46±2.47	19.56±2.71	19.29±2.1	19.71±2.49	0.00	0.00	0.22	0.53	0.01	0.00	0.00
	Max (Gy)	36.27±8.52	37.01±8.5	35.71±7.88	36.68±8.16	36±7.43	36.51±7.34	32.34±9.67	36.05±6.77	0.45	0.12	0.00	0.42	0.13	0.00	0.12
Femoral Head Lt	**V25%**	24.39±5.5	24.73±5.56	23±2.79	22.78±2.73	24.7±3.45	24.29±2.92	24.01±3.31	24±3.75	0.13	0.34	0.00	0.00	0.21	0.00	0.00
	V40%	23.56±6.84	23.11±6.93	20.99±2.47	20.58±2.52	22.86±3.39	22.43±2.8	22.01±3.01	21.93±3.69	0.00	0.00	0.00	0.00	0.12	0.00	0.00
	Mean (Gy)	21.84±7.2	21.49±7.4	20.31±2.68	19.98±2.82	21.34±3.39	20.88±3.02	20.68±3.14	20.42±3.63	0.24	0.37	0.00	0.00	0.00	0.00	0.00
	Max (Gy)	39.72±6.38	40.05±6.07	36.5±5.02	36.53±5.31	36.56±5	35.45±3.96	37.13±5.35	36.06±5.57	0.00	0.00	0.66	0.62	0.00	0.00	0.12

Table 4 summarizes the dosimetric parameters for PTV coverage & OAR's derived by 3DCRT, IMRT, and VMAT plans utilizing FB and FFFB of 6 and 10 MV

7.6. Discussion:

According to our observations, for deep-seated tumours like the Ca Cervix, more beam energy should be used. To deliver the optimal dose at any depth, the Elekta versa HD comes with photon energies of 6 MV, 10 MV, and 15 MV for FF and 6 MV & 10 MV for FFF.As highlighted by et al. [30], Over 15 MV photon energy, there is no significant improvement in dose distribution or integral dosage, and the neutron is created by a 15 MV photon beam. Neutron dosage is more essential than photon exposure because of their high relative biological effectiveness (RBE) and a radiation weighting factor of 20, resulting in higher biological damage. [31].We did not include 15 MV in this investigation for the same reason. For 3DCRT approaches, FFFB is not viable, especially for large tumours. VMAT enables for better conformity of the high dosage volume to the PTV as compared to three-dimensional conformal therapies like IMRT. This could assist to reduce the danger of secondary malignancies emerging in high-dose areas in the field. For prostate malignancies, Alvarez Moret et al. [32] established the same fact. VMAT has already been compared to IMRT for several cancer types at various sites [4]. Although it is commonly known that VMAT outperforms IMRT in terms of delivery efficiency [4-5],

3DCRT, IMRT, and VMAT plans employing FB and FFFB of 6 and 10 MV radiation planning in the instance of dosimetric impact of varied photon energy on cervix carcinomas. In terms of PTV coverage, there were no statistically significant variations between the 6, 10 plans, although 3DCRT Techniques produces less OAR sparing, HI, and CI when compared to IMRT and VMAT. Although the number of MUs exposing normal tissues to low doses was substantially higher in 6 MV plans than in 10 MV plans, these disadvantages can be tolerated because the

risk of secondary cancers caused by photo neutron generation is higher in 10 and 15 MV designs [33].

In the framework of a detailed dosimetric analysis on cervical carcinomas, 3DCRT, IMRT and VMAT plans using FB and FFFB of 6 and 10 MV radiation planning When comparing VMAT plans to 3DCRT and IMRT plans, there are a few things to keep in mind., HI is much better. The dosage conformity of VMAT and IMRT designs was greatly improved. The severity of DG is worsening as VMAT and IMRT programmes modify the intensity to spare important organs and have more beams. In VMAT and IMRT designs, the target coverage ratio is much higher. Even with the larger energy, MUs are much lower in 3DCRT layouts. The VMAT plans greatly lowered the dose to the bladder (V15 percent, V25 percent, V35 percent, and V50 percent). VMAT plans dramatically reduced dose to bowel (Mean, V30 percent and V45 percent). The rectum dose was considerably reduced with the VMAT and IMRT systems (V15 percent, V25 percent, V35 percent, and V50 percent). The radiation to the femoral heads was considerably reduced according to IMRT techniques (V25 percent, V40 percent, and Mean).

In the case of dosimetric effects of filtered and flattening filter free photon beams on VMAT plans employing FB and FFFB of 6 and 10 MV radiotherapy planning Table 4 shows that the HI, CI, DG, and TC for all VMAT plans employing FF and FFF photon beams are comparable. In 10 MV VMAT, MUs were lower, while in Vmat plans with FFF, they were higher. V15 percent, V25 percent, V35 percent, and V50 percent dose to bladder were equivalent in FF VMAT plans but much greater in FFF VMAT plans. The dose to bowel (Mean, V15 percent, V30 percent, and V45 percent) was equivalent across FF and FFF VMAT plans, but much greater in FFF VMAT plans. V15 percent, V25 percent, V35 percent, and V50

percent dose to rectum were equivalent in FF VMAT plans but much greater in FFF VMAT plans. For all VMAT plans using FF and FFF photon beams, the dose to femoral heads (V25 percent, V40 percent, Mean, and Max) was comparable.

VMAT plans that use FFFB offer similar target coverage, however for the same coverage, FB spares more bladder and rectum than FFFB for both photon energies. This reduces the amount of toxicity that patients experience after receiving radiation. In comparison to FFFB, FB creates VMAT plans that are more conformal and homogeneous. This study discovered that FB is superior to FFFB for cervix VMAT radiation planning.

7.7. Conclusion:

This comprehensive study established a feasible planning strategy for the treatment of carcinoma of the cervix. It demonstrates VMAT's capacity to develop highly conformal and homogenous treatment plans in cervix radiotherapy when compared to 3DCRT and IMRT.

The greatest dosages to OARs after VMAT were 1 to 3 times lower than after 3DCRT, according to our research. VMAT had lower mean doses, maximum doses, and volume for OARs than the other techniques (6&10MV FB and FFFB). In comparison to IMRT and 3DCRT, VMAT dramatically reduces the risk of subsequent cancer in the relevant OARs (6&10MV FB and FFFB).

The VMAT (6 MV FB) approaches, according to this study, may provide better results for a cervical cancer patient. More data from more patients must be collected and analyzed to make this an evidence-based theory.

7.8 References:

1. Duan J, Kim RY, Elassal S, Lin HY, Shen S. Conventional high-dose-rate brachytherapy with concomitant complementary IMRT boost: a novel approach for improving cervical tumor dose coverage. Int J Radiat Oncol Biol Phys 2008; 71 (3): 765–771.

2. Georg P, Georg D, Hillbrand M, Kirisits C, Pötter R. Factors influencing bowel sparing in intensity modulated whole pelvic radiotherapy for gynaecological malignancies. Radiother Oncol 2006; 80 (1): 19–26.

3. Portelance L, Chao KS, Grigsby PW, Bennet H, Low D. Intensity-modulated radiation therapy (IMRT) reduces small bowel, rectum, and bladder doses in patients with cervical cancer receiving pelvic and para-aortic irradiation. Int J Radiat Oncol Biol Phys 2001; 51 (1): 261–266.

4. Otto K. Volumetric modulated arc therapy: IMRT in a single gantry arc. Med Phys 2008; 35 (1): 310–317.

5. Teoh M, Clark CH, Wood K, Whitaker S, Nisbet A. Volumetric modulated arc therapy: a review of current literature and clinical use in practice. Br J Radiol 2011; 84 (1007): 967–996

6. Vanetti E, Clivio A, Nicolini G, et al. Volumetric modulated arc radiotherapy for carcinomas of the oro-pharynx, hypo-pharynx and larynx: a treatment planning comparison with fixed field IMRT. Radiother Oncol 2009; 92 (1): 111–117.

7. Palma D, Vollans E, James K, et al. Volumetric modulated arc therapy for delivery of prostate radiotherapy: comparison with intensity-modulated radiotherapy and three-dimensional conformal radiotherapy. Int J Radiat Oncol Biol Phys 2008; 72 (4): 996–1001.

8. Zhang P, Happersett L, Hunt M, Jackson A, Zelefsky M, Mageras G. Volumetric modulated arc therapy: planning and evaluation for prostate cancer cases. Int J Radiat Oncol Biol Phys 2010; 76 (5): 1456–1462.

9. Yin L, Wu H, Gong J, et al. Volumetric-modulated arc therapy vs. c-IMRT in esophageal cancer: a treatment planning comparison. World J Gastroenterol 2012; 18 (37): 5266–5275.

10. Abbas AS, Moseley D, Kassam Z, Kim SM, Cho C. Volumetric-modulated arc therapy for the treatment of a large planning target volume in thoracic esophageal cancer. J Appl Clin Med Phys 2013; 14 (3): 192–202.

11. Masi L, Doro R, Favuzza V, Cipressi S, Livi L. Impact of plan parameters on the dosimetric accuracy of volumetric modulated arc therapy. Med Phys 2013; 40 (7): 071718.

12. Treutwein M, Hipp M, Koelbl O, Dobler B. Searching standard parameters for volumetric modulated arc therapy (VMAT) of prostate cancer. Radiat Oncol 2012; 7: 108.

13. Wang Y, Chen L, Zhu F, Guo W, Zhang D, Sun W. A study of minimum segment width parameter on VMAT plan quality, delivery accuracy, and efficiency for cervical cancer using Monaco TPS. J Appl Clin Med Phys 2018; 19 (5): 609–615.

14. Nithya L, Raj NA, Rathinamuthu S, Sharma K, Pandey MB. Influence of increment of gantry angle and number of arcs on esophageal volumetric modulated arc therapy planning in Monaco planning system: a planning study. J Med Phys 2014; 39 (4): 231–237.

15. Chen A, Li Z, Chen L, et al. The influence of increment of gantry on VMAT plan quality for cervical cancer. J Radiat Res Appl Sci 2019; 12 (1): 447–454.

16. Edge SB, Compton CC. The American Joint Committee on Cancer: the 7th edition of the AJCC cancer staging manual and the future of TNM. Ann Surg Oncol 2010; 17 (6): 1471–1474.

17. Lim K, Small,WJr, Portelance L, et al. Consensus guidelines for delineation of clinical target volume for intensity-modulated pelvic radiotherapy for the definitive treatment of cervix cancer. Int J Radiat Oncol Biol Phys 2011; 79 (2): 348–355.

18. Forrest J, Presutti J, Davidson M, Hamilton P, Kiss A, Thomas G. A dosimetric planning study comparing intensity-modulated radiotherapy with four-field conformal pelvic radiotherapy for the definitive treatment of cervical carcinoma. Clin Oncol (R Coll Radiol) 2012; 24 (4): e63–e70.

19. Vrdoljak E, Omrcen T, Novakovi´c ZS, et al. Concomitant chemobrachy radiotherapy with ifosfamide and cisplatin followed by consolidation chemotherapy for women with locally advanced carcinoma of the uterine cervix–final results of a prospective phase II-study. Gynecol Oncol 2006; 103 (2): 494–499.

20. R Development Core Team (2016). R: A Language and Environment for Statistical Computing. R Foundation for Statistical Computing, Vienna, Austria. http://www.R-project.org. Accessed on 10th August 2020.

21. Haciislamoglu E, Colak F, Canyilmaz E, et al. The choice of multi-beam IMRT for whole breast radiotherapy in early-stage right breast cancer. *SpringerPlus*. 2016;5(1):688. doi:10.1186/s40064-016-2314-2.

22. Navarria P, Pessina F, Cozzi L, et al. Can advanced new radiation therapy technologies improve outcome of high grade glioma (HGG) patients? analysis of 3D-conformal radiotherapy (3DCRT) versus volumetric-modulated arc therapy

(VMAT) in patients treated with surgery, concomitant and adjuvant chemo-radiotherapy. *BMC Cancer*. 2016; 16:362. doi:10.1186/s12885-016-2399-6.

23. Newhauser WD, Durante M. Assessing the risk of second malignancies after modern radiotherapy. *Nature reviews Cancer*. 2011; 11(6): 438-448. doi: 10.1038/nrc3069.

24. Edge SB, Compton CC. The American Joint Committee on Cancer: the 7th edition of the AJCC cancer staging manual and the future of TNM. Ann Surg Oncol 2010; 17 (6): 1471–1474.

25. Lim K, Small,WJr, Portelance L, et al. Consensus guidelines for delineation of clinical target volume for intensity-modulated pelvic radiotherapy for the definitive treatment of cervix cancer. Int J Radiat Oncol Biol Phys 2011; 79 (2): 348–355.

26. Stephen B Edge, Carolyn C Compton. The American Joint Committee on Cancer: the 7th edition of the AJCC cancer staging manual and the future of TNM. Ann Surg Oncol.2010 Jun;17(6):1471-4.

27.Lim K, Small W Jr, Portelance L, Creutzberg C, Jurgenliemk-Schulz IM, Mund t A, et al. Consensus guidelines for delineation of clinical target volume for intensity modulated pelvic radiotherapy for the definitive treatment of cervix cancer. Int J Radiat Oncol Biol Phys 2011; 79: 348–55.

28.Paddick I. A simple scoring ratio to index the conformity of radio surgical treatment plans: technical note. Journal of neurosurgery. 2000 Dec;93(Supplement 3):219-22

29. R Development Core Team (2016). R: A language and environment for statistical computing. R Foundation for Statistical Computing, Vienna, Austria. URL http://www.R-project.org

30. Das IJ, Kase KR. Higher energy: is it necessary, is it worth thecost for radiation

oncology? *Med Phys* 1992;**19**:917–25.

31. Bethesda, Maryland: NCRP; 1987. NCRP. NCRP Report No. 79: Neutron Contamination for Medical Electron Accelerators.

32. Alvarez Moret J, Koelbl O, Bogner L. Quasi-IMAT techniqueand secondary cancer risk in prostate cancer. Strahlenther Onkol 2009; **185:248**–53.

33.. Lalit Kumar, Girigesh Yadav, Kothanda Raman, Manindra Bhushan, and Manoj Pal: The dosimetric impact of different photon beam energy on RapidArc radiotherapy planning for cervix carcinoma J Med Phys. 2015 Oct-Dec; 40(4): 207–213.

CHAPTER -VIII

Dosimetric characteristics of VMAT plans with respect to a different increment of gantry angle size for Ca cervix

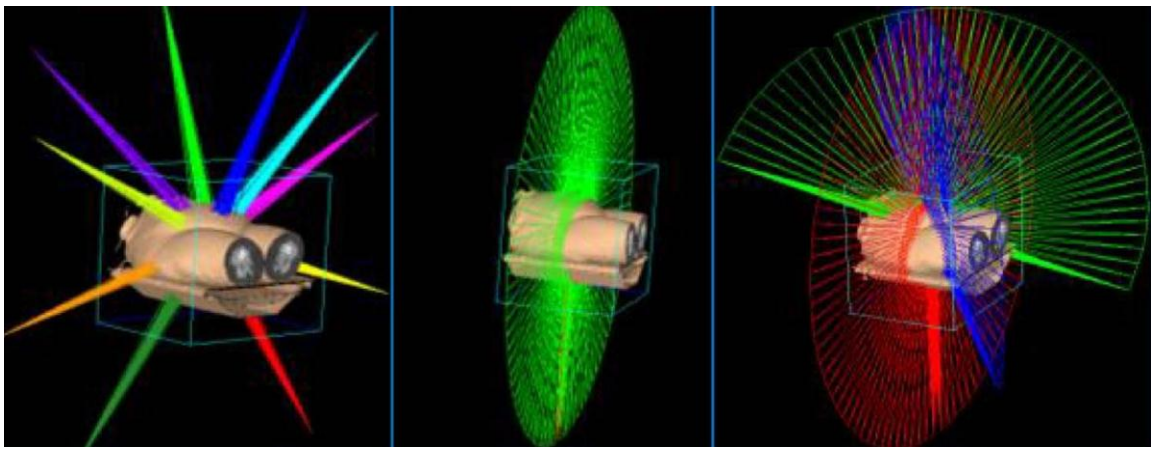

Chapter -VIII

Dosimetric characteristics of VMAT plans with respect to a different increment of gantry angle size for Ca cervix

8.1 Introduction:

External beam radiotherapy (EBRT) followed by intracavitary brachytherapy is the primary treatment protocol for cervical cancer. [1] Conventional EBRT irradiates the whole pelvis region either from anterior or posteriorly or/and laterally. Thus, critical organs at risk (OARs) are exposed to radiation and severe radiation-induced toxicities are observed. Over the last decade, interest in the use of intensity-modulated radiotherapy (IMRT) to treat cervical cancer has increased.

This chapter has been published as a manuscript: Natraj M, Pawaskar PN, and Chairmadurai A. (2020) Dosimetric characteristics of VMAT plans with respect to a different increment of gantry angle size for Ca cervix. Journal of Radiotherapy in Practice page 1 of 5. doi: 10.1017/S146039692000093X. Accepted: 2 October 2020

IMRT technique has the benefit over conventional whole-pelvis irradiation; potentially improves the target dose coverage and reduces the toxicity to OARs). [2,3] IMRT typically involves 5–9 beams placed around the patient at equal angular spacing and the uniform radiation intensities from open fields are modulated by multileaf collimators (MLCs). A novel radiation technique has evolved by replacing 5–9 fixed beam angles in IMRT, with a single gantry arc of up to 360°, known as volumetric-modulated arc therapy (VMAT). [4,5]

VMAT has been introduced to overcome some of the limitations associated with fixed-field IMRT. It allows continuous delivery of radiation by simultaneously

varying the dose rate, position of MLCs and gantry rotation speed. VMAT has achieved highly conformal dose distributions, with improved target dose coverage and sparing of normal tissues, as compared to conventional radiotherapy and IMRT techniques. [6–8] VMAT also has the potential to reduce monitor unit (MU) usage and ultimately reduce the treatment delivery time. Each arc is divided into multiple equal sectors in VMAT technique and MLC modulates the open radiation field by to-and-fro movement between successive sectors. Sector angle is defined by the parameter

'Increment of Gantry Angle' (IGA) and the number of sectors is given by arc length divided by IGA. The number of sectors and IGA has the tendency to influence the quality of treatment plan [9,10] along with the number of arcs and arc lengths. [11–13] Influence of smaller and larger IGA was reported as negligible in oesophageal cancer [14] and contrarily, larger IGA yielded significantly better plans in cervical cancer. [15] In this study, we have investigated the influence in VMAT plans by a sequence of IGAs in definitive radiotherapy treatment for cervical cancer.

The plans are quantitatively analyzed in terms of conformity index (CI), heterogeneity index (HI), dose–gradient index (DGI), target coverage (TC) by prescription dose, MU usage, control points (CPs) and dose to organs.

8.2. Aim,

The aim of this study, to investigate feasible increment size parameters for VMAT Planning. The plans are quantitatively analyzed in terms of conformity index (CI), heterogeneity index (HI), dose–gradient index (DGI), target coverage (TC) by prescription dose, monitor unit (MU) usage, control points (CPs) and dose to organs. and the ultimate goal is providing an efficient increment size for VMAT planning

in Monaco planning system.

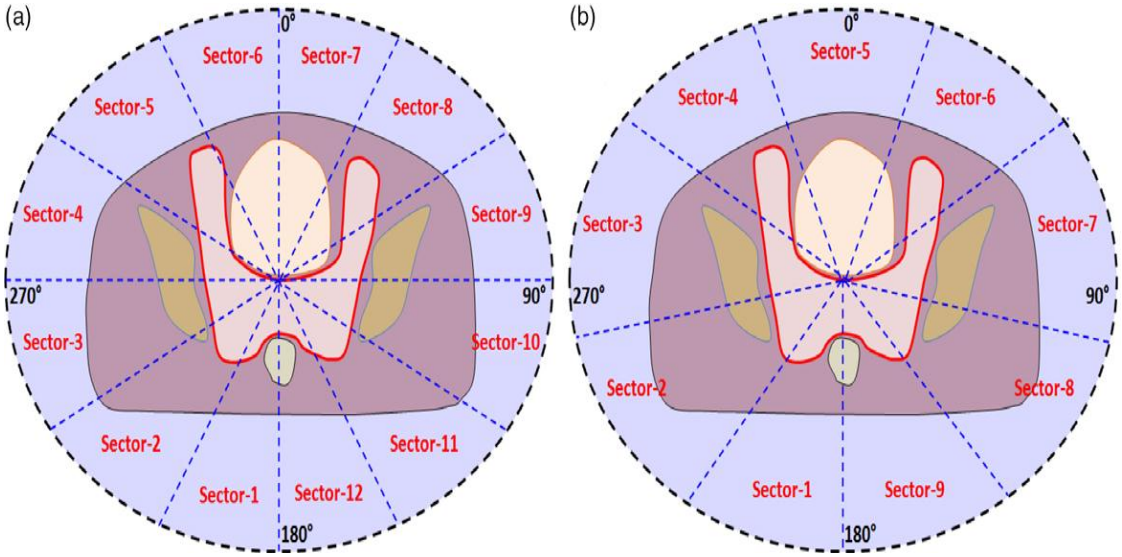

Figure 8.1. Comparison between the single arc of 360°, VMAT plans with IGA (a) 30° and (b) 40° in cervical cancer.

8.3. Material Method:

8.3.1 Patient selection:

In this retrospective study, we selected 27 patients with carcinoma cervix cancer having aged between 54 and 69. All the patients enrolled in this study were at T3N1M0 stage of cervical cancer. [16] Each of them had evolved lymph nodes and were preparing to undergo definitive radiotherapy treatment.

8.3.2 CT simulation

Before CT all Patients were instructed to follow a bladder protocol, in which each patient was asked to void the bladder and then drink approximately1 liter of water to fill the bladder. They were asked to wait for around 45 min before planning scan to ensure bladder filling. Fiducial markers were kept at the level of pubic symphysis. All patients were immobilized with vacuum bag (vack-lock; Orfit Industries, Belgium) and the vacuum bag takes on the shape of the patient when deflated. Patient in supine position and the hands were kept above the head.

The computed tomography (CT) images were acquired for all patients in Biograph MCT-20, PET-CT (Siemens AG, Medical solutions, Germany) with 3 mm slice thickness; field of view 50 cm and from the L1–L2 Vertebral level to 5 cm below the ischial tuberosity. CT datasets were transferred to the Monaco Sim (CMS Elekta, Sunnyvale, CA, USA) workstation for contouring, using DICOM-enabled protocol.

8.3.3 Target and OAR delineation,

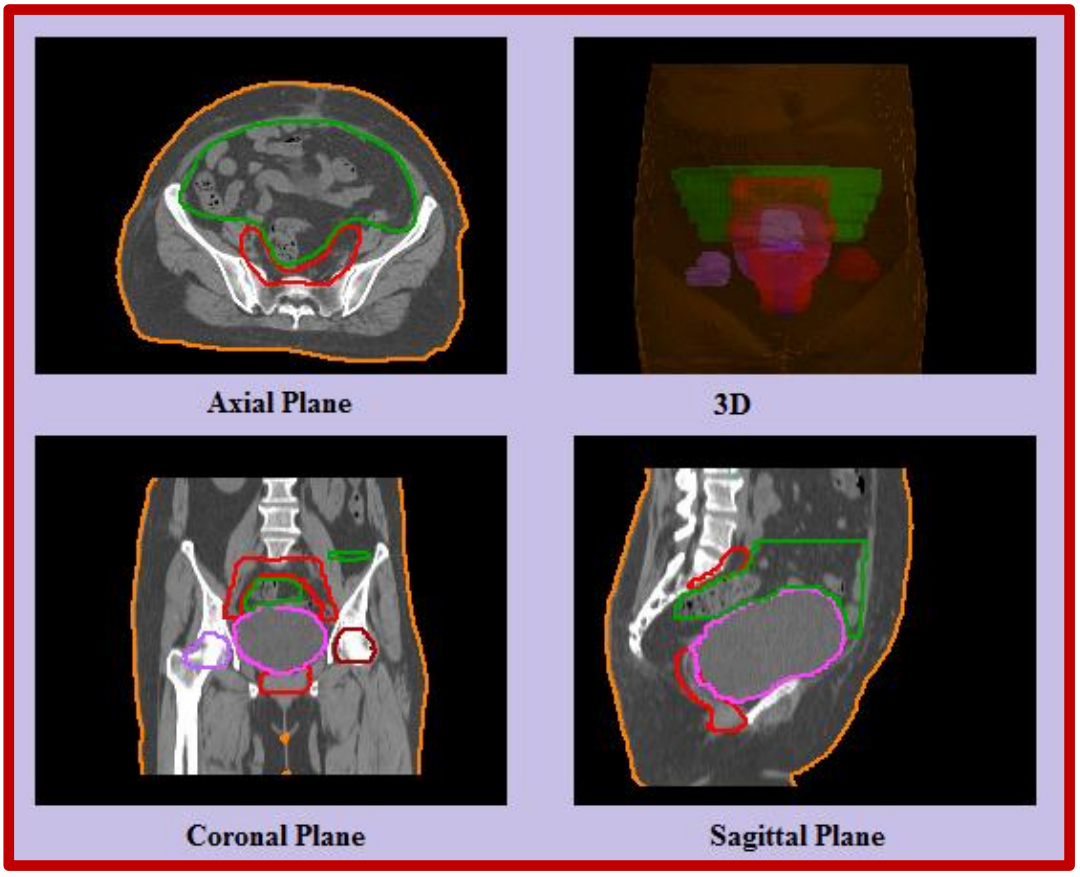

Figure 8.2. Represents the delineated Target volume and OARs in Axial/coronal/sagittal Plane/3D View

An experience radiation oncologist contoured the gross target volume and clinical target volume OARs were delineated for all the patients using Monaco Sim (CMS Elekta, Sunnyvale, CA, USA) Clinical Target Volume (CTV). A margin of 0.5 cm was given to CTV to generate planning target volume (PTV). The OARs viz. bladder, rectum, bowel and femoral heads were con-toured. Contour of the bladder

from apex to dome was drawn while the rectum was contoured from the anus (at inferior level of ischial tuberosity) to recto-sigmoid junction. Contours of the bilateral femoral heads were drawn up to the level of ischial tuberosity [17].

OAR were contoured by the resident radiation oncologists. CT study sets, along with the contours, were transferred to the Monaco (Elekta Ltd, Crawly, UK) treatment planning system, for radiotherapy planning. Elekta Versa HD (Elekta AB, Stockholm, Sweden), a linear accelerator was used to deliver the VMAT plans. The linear accelerator is fitted with MLCs having 80 leaf pairs of 5 mm width.

8.3.4 Treatment planning system:

Monaco treatment planning system (Elekta Ltd, Crawly, UK) version 5.10.0 utilizes physical effects of radiation and biological properties of the tissue. It has three biological constraints such as Target EUD, Parallel and serial and six physical constraints such as target penalty, quadratic overdose, overdose DVH, under dose DVH, maximum dose and quadratic under dose. The user has an option to set the cell sensitivity of the tumor in target EUD. The organ at risk can be set as serial or parallel constraints depending on the properties of the tissue.

The system uses a two-stage process of optimizing dose distribution. Generally, in stage one the ideal fluence distribution of beams is optimized to meet a user-defined prescription for given set of beams. In stage two, segmentation is done, which includes the segment shapes and weights, so that deliverable fields are obtained. In this stage system uses Monte Carlo simulation during optimization. [14].

8.3.5 Optimization strategy

In VMAT optimization, prior to stage one, system divides the beam into sectors. In stage one, at the initialization stage, the system creates the dose calculation cube around all defined structures and calculates structure volumes using cubic voxels. Then it projects the union of all target volumes with the margin defined. Numbers of static sectors are created based on arc length and user defined IGA. Beam lets for each sector are created. Width of beam let is user defined and length is equal to the length of individual MLC leaves. The system uses an enhanced pencil beam algorithm to calculate the open field dose. Then, the fluence optimization begins in which the weights (fluence) of all individual pencil beams are varied simultaneously. The unconstrained problems are solved by conjugate gradient algorithm [14]. After the unconstrained optimization finishes, if necessary the system changes each cost function relative weight to make the optimizer meet the isoconstraints and restarts the unconstrained optimization problem. Stage one optimization continues until all the constraints are met. The accuracy of dose at the end of the stage one is limited because the algorithm is kernel based two dimensional methods, especially in the presence of heterogeneities.

In second stage, the treatment planning system considers the deliverability of accelerator. It takes each fluence map and sequences it in such a way that it is spread over the original sector it represents. The system determines leaf trajectories based on the target dose rate defined by the user. If segment shape optimization (SSO) method is selected, the system selects the optimal dose rate by its own. Then, the system converts optimized fluence into deliverable arc sequence with multiple control points and the gantry position. The gantry positions need not be equally spaced. Dose calculation is done with voxel based Monte Carlo algorithm.

The user can change the calculation accuracy and time by modifying some parameters like dose rate, Monte Carlo grid spacing and variance.

8.3.6 Planning objectives

Prescribed dose to PTV was 50 Gy in 25 Fractions at 2 Gy per fraction. It was stipulated that not less than 98% volume of PTV should receive a dose less than the prescribed dose and that not more than 2% volume of PTV should receive a dose more than 105% of the prescription dose. QUANTEC Protocol 10 was used for all the OARs. The hot spot was considered as a 2% volume receiving more than 110% of the prescription dose.

8.3.7 Planning techniques

All VMAT plans were planned with the following calculation properties: Grid spacing was selected as 3 mm, and Monte Carlo variance was 3%. Monte Carlo algorithm was selected as secondary algorithm for second stage dose calculation that is final dose calculation. The dose was calculated to the medium and not to the water. For all plans, heterogeneity correction was applied. VMAT plan was delivered in a single arc of 360° gantry rotation (clockwise direction from 180 to −180°). Sweep sequencer tool was used for MLC segmentation in VMAT technique. On contrary to static fields in IMRT, the intensity of photon field is modulated in a gantry arc in VMAT plan. The planned arc of VMAT was divided into uniform sectors using the parameter ‘IGA’ (Figure 1). Intensity modulation was facilitated by MLC; MLC segments move from right to left in a sector and return back from left to right in the following sector during continuous irradiation. Thereby, intensity modulations were done in a to-and-fro movement between successive sectors. 6 MV flattened photon beam was used to deliver the prescribed dose using VMAT plan. VMAT plans were optimized by varying the parameter

'IGA' (as 10, 20, 30 and 40°) and the plans were named as VMAT,10 VMAT,20 VMAT,30 and VMAT,40 respectively.

VMAT plans were optimized to achieve the required dose constraints (Table 8.1) using the optimization parameters (Table 8.2) and calculation parameters (Table 8.3). The radiation dose from VMAT plan was calculated on 3D CT images and heterogeneous corrections were applied.

Structure	Parameter	Constraints
PTV	$V_{95\%}$	> 47.5Gy
	$V_{10\%}$	< 107% of Prescribed Dose
Rectum	$V_{60\%}$	< 45 Gy
Bladder	$V_{35\%}$	< 45 Gy
Bowel	D_{Max}	< 50 Gy
Femoral Head	$V_{20\%}$	< 40 Gy

Table 8.1. Treatment planning objectives for VMAT

Structure	Cost functions	Parameter	Isoconstraints
PTV	Target EUD	0.5	50 Gy
	Quadratic Overdose	51.5 Gy	0.45Gy
	Target penalty	95%	50 Gy
Rectum	Parallel	k=3	35 Gy
Bladder	Parallel	k=3	30 Gy
Bowel	Parallel	k=3	25 Gy
	Maximum dose	Shrink=3 mm	48 Gy
Femoral Head	Maximum dose	Shrink=3 mm	48 Gy

Body	Quadratic Overdose	Shrink=0 mm, 50 Gy	0.10 Gy
	Quadratic Overdose	Shrink=3 mm, 47 Gy	0.15 Gy
	Maximum dose	Shrink=5 mm	46 Gy
	Maximum dose	Shrink=10 mm	40 Gy
	Maximum dose	Shrink=15 mm	35 Gy
	Maximum dose	Shrink=25 mm	25 Gy

EUD-Equivalent Uniform Dose; k=Power law exponent

Table 8.2. The cost functions for optimization of VMAT plans in cervical cancer

Sequencing Parameters	
Max number of Arcs	1
Max. control points per Arc	200
Min. Segment Width	0.5 cm
Fluence Smoothing	Medium
Calculations Properties	
Grid Spacing	0.3 cm
Dose Deposition to	Medium
Algorithm	Monte Carlo photon
Statistical Uncertainty	1% / calculation

Table 8.3. Sequencing parameters and calculation properties for VMAT plans

8.4.0 Plan quality indices and plan evaluation tools

8.4.1. Target volume (TV)

Quantitative and qualitative methods were used for evaluation of PTV. The references were taken from the recommendations of International Commission for Radiation Units(ICRU) Report No. 83. [19] Plans were analyzed using CT slice-by-slice isodose coverage and dose volume histograms (DVH).TV coverage and the conformity of the PTV was evaluated with isodose distribution in the transverse, sagittal and coronal planes.

CI, HI, DGI and TC by 95% isodose line were derived to compare the dosimetric characteristics of the VMAT plans optimized with different 'IGA'.15,20 In addition to that, dose to OARs were obtained from dose–volume histogram. The plan quality indices were calculated using the following Equations (1–3):

$$CI = \frac{(TV_{RI})^2}{(TV \times V_{RI})}, \quad (1)$$

where TV=target volume, VRX=target volume covered by 100% isodose line, VRI=volume of 100% isodose line,

$$HI = \frac{(D_{2\%} - D_{98\%})}{D_{50\%}}, \quad (2)$$

Maximum dose received by 2% of PTV (D2%), minimum dose received by 98% of PTV (D98%), dose received by 50% of PTV (D50%)

$$DGI = \frac{V_{RI}}{V_{HRI}}. \quad (3)$$

Total volume encompassed in half of the prescription dose ($_{VHRI}$) and corresponding RI

Volume of PTV receiving prescription dose (TVRI), volume of PTV (TV) and total volume encompassed in prescription dose (VRI) were substituted in Equation (1) to calculate CI. Maximum dose received by 2% of PTV (D2%), minimum dose received by 98% of PTV (D98%), dose received by 50% of PTV (D50%) were substituted in Equation (2) to calculate HI. Total volume encompassed in half of the prescription dose (VHRI) and corresponding VRI were substituted in Equation (3) to calculate DGI.

Physical parameters such as total MU and CPs were recorded. CPs per 10° were calculated to understand the physical constraints in MLC for PTV coverage. The width of PTV required to scale-up by MLC is given at 10° increment for a cervical and oesophageal cancer (Figure 3). IGA 30 had yielded better VMAT plans in earlier

studies, [14,15] and so VMAT30 plan was considered as a reference for statistical comparison. Each of the VMAT plans was renormalized to provide the same mean dose to PTV, as in VMAT30 to avoid any bias or rescaling effects.

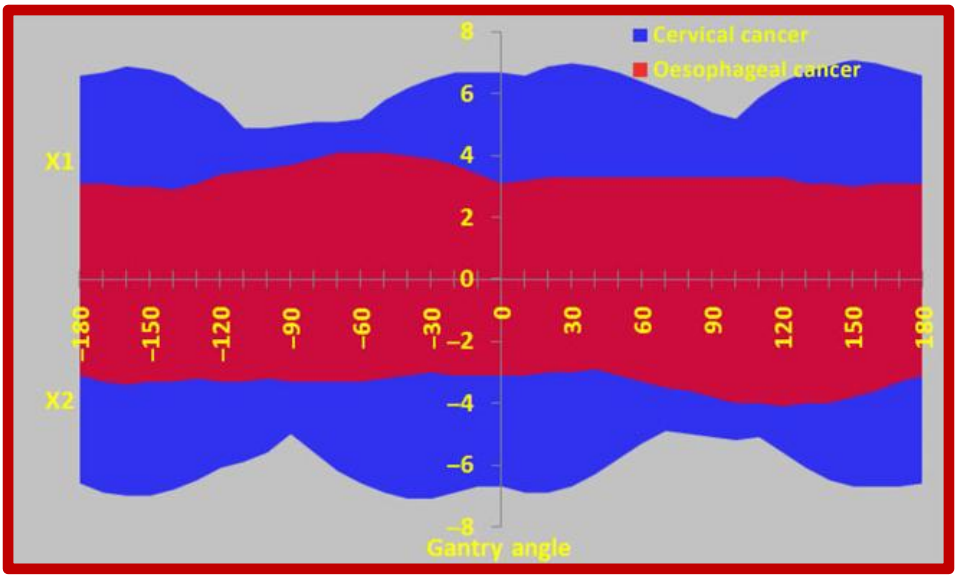

Figure 8.3. Comparison between the width of PTV in beam's eye view at 10° increment for a cervical and esophageal cancer.

8.6.2 Organs at risk,

Total 27 patients dosimetric plans were generated for each patient and their specific DVHs were compared for organ-sparing. OAR doses were evaluated for dose for bladder (D15%, D25%, D35%, D50%) rectum (D15%, D25%, D35%, D50%), bowel (V15Gy (%,), V30Gy (%), V45Gy (%)) and femoral heads (V25Gy (%), V45Gy (%)Mean dose (Gy), Max. dose (Gy)) and. Spinal cord was evaluated for the maximum dose.

8.6.3 Treatment efficiency

Beam-on time (BOT) and TMUs were compared for all the plans (IGA-10, IGA-20, IGA-30, IGA-40) to assess the efficiency of the treatment. TPS was used to calculate MU and its average was obtained to calculate the BOT. All the plans were delivered at maximum dose rate of 600 MU/min FF to minimize the treatment time.

8.5. RESULTS:

8.5.1. Planning target volume (PTV)

Table 8.4 compares the plan quality indices of VMAT plans for the range of IGAs. CI indicates the degree of confining prescription dose within PTV and it was worsened with larger IGA (30 and 40°). HI indicates the degree of difference between the minimum and maximum dose within PTV and it was enhanced with larger IGA (30 and 40°). DGI indicates the degree of dose–gradient in falloff region and it was worsened with larger IGA (30 and 40°). TC was worst in VMAT10 plan and comparable elsewhere (20, 30 and 40°). Plan quality indices were significantly different ($p < 0{\cdot}05$) with smaller IGA (10 and 20°) and remained unaltered beyond 30°.

8.5.2. Organs at risk

Dose to OARS and comparison with VMAT plans are given in Table 8.4. Overall, dose to OARs were reduced with smaller IGA (10 and 20°) and were comparable with 40°; the differences were significant ($p < 0{\cdot}05$). The dose received by 50% of the volume (D50%) in the bladder was worsened up to 6 Gy with larger IGA (30 and 40°). Dose to rectum (D15%, D25%, D35% and D50%) were comparable among all the plans. The volume receiving 15 Gy (V15Gy) in bowel was worsened up to 10% with larger IGA (30 and 40°). Smaller IGA (10 and 20°), worsened V25Gy up to 3% in the femoral head.

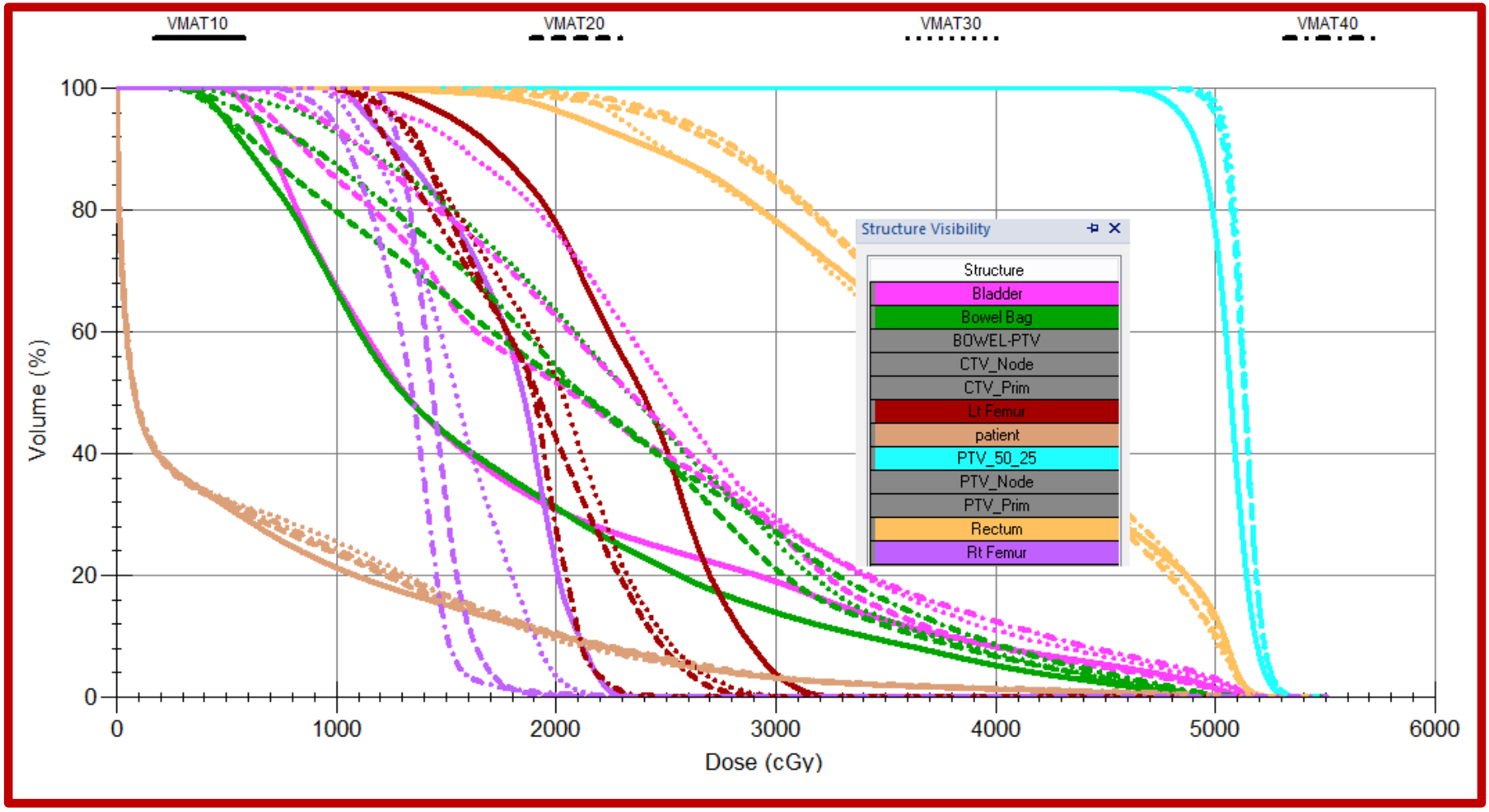

Figure.8.4 DVH comparison for target coverage and OARs for range of IGAs VMAT plans.

Structure	Parameter	$VMAT^{10}$	$VMAT^{20}$	$VMAT^{30}$	$VMAT^{40}$	*p*-value ($VMAT^{30}$)		
						$VMAT^{10}$	$VMAT^{20}$	$VMAT^{40}$
PTV	CI	0.83±0.03	0.82±0.05	0.80±0.05	0.80±0.05	0.00	0.00	0.75
	HI	0.12±0.02	0.08±0.02	0.07±0.01	0.07±0.01	0.00	0.01	0.66
	DG	0.28±0.04	0.30±0.04	0.32±0.03	0.33±0.04	0.00	0.00	0.00
	TC	0.95±0.03	0.99±0.01	1.00±0.00	1.00±0.00	0.00	0.04	0.81
Bladder	$D_{15\%}$	42.89±3.96	44.64±4.26	45.54±4.01	45.45±3.77	0.00	0.00	0.62
	$D_{25\%}$	37.38±5.42	40.69±4.79	41.54±4.91	41.63±4.84	0.00	0.00	0.70
	$D_{35\%}$	32.33±6.15	36.66±4.93	37.66±4.95	37.81±5.12	0.00	0.00	0.65
	$D_{50\%}$	26.37±5.91	31.23±5.01	32.69±4.21	32.66±4.71	0.00	0.00	0.93
Rectum	$D_{15\%}$	48.36±1.35	48.44±1.42	49.00±1.45	49.33±1.27	0.00	0.00	0.01
	$D_{25\%}$	46.24±1.83	46.08±1.92	47.08±2.30	47.33±1.99	0.00	0.00	0.18

	$D_{35\%}$	43.25±2.01	43.27±2.17	44.60±2.78	44.75±2.44	0.00	0.00	0.46
	$D_{50\%}$	37.65±1.84	38.46±2.48	39.82±2.99	39.94±2.47	0.00	0.00	0.66
Bowel	V_{15Gy} (%)	71.07±11.44	80.22±7.7	82.84±4.92	82.44±7.43	0.00	0.01	0.58
	V_{30Gy} (%)	22.57±5.65	27.66±5.83	29.36±5.39	29.25±5.13	0.00	0.00	0.74
	V_{45Gy} (%)	3.91±1.46	5.36±1.91	5.88±1.57	6.16±1.78	0.00	0.03	0.09
	Mean Dose (Gy)	22.28±2.56	24.53±2.15	25.02±1.72	24.96±2.01	0.00	0.01	0.61
Femoral Head	V_{25Gy} (%)	25.58±2.57	24.43±2.98	22.83±4.13	22.18±2.61	0.00	0.00	0.21
	V_{40Gy} (%)	23.85±2.40	22.43±2.79	21.9±2.80	20.75±2.57	0.00	0.00	0.00
	Mean Dose (Gy)	22.57±2.49	20.72±2.87	20.98±2.75	20.14±2.90	0.00	0.01	0.00
	Max. Dose (Gy)	38.31±4.33	38.81±5.41	39.96±6.10	38.29±7.10	0.06	0.11	0.01

Table 8.4. Plan quality indices of VMAT plans for the range of IGAs

8.5.3. Monitor unit& Control Points

Table 8.5 compares the number of sectors, MU and CP of VMAT plans (10, 20, 30 and 40°). MUs required to deliver prescribed doses were reduced with a decrease in the number of sectors. Meanwhile, CPs were increased with a decrease in the number of sectors. The differences were significant ($p < 0{\cdot}05$).

Parameter	IG-10	IG-20	IG-30	IG-40	*p*-value ($VMAT^{30}$)		
					$VMAT^{10}$	$VMAT^{20}$	$VMAT^{40}$
Sector	**36**	**18**	**12**	**9**	**-**	**-**	**-**
MU	**1124.3±138.2**	**1055.47±115.35**	**1057.93±124.9**	**932.93±79.79**	**0.00**	**0.88**	**0.00**
CPs	**142.26±10.16**	**169.33±10.3**	**178.15±3.43**	**176.11±3.17**	**0.00**	**0.00**	**0.03**
CPs/10°	**3.95±0.28**	**4.7±0.29**	**4.95±0.1**	**4.89±0.09**	**0.00**	**0.00**	**0.04**

Table 8.5. Monitor unit& Control Points of VMAT plans for the range of IGAs

8.6. Discussion

In this retrospective study, VMAT plans were analyzed by varying the parameter IGA. Initial optimizer in VMAT technique creates an optimal dose–fluence for the required dose constraints. MLC segmentation/CPs are created to achieve the optimal dose–fluence by 'sweep sequencer tool' as per the IGA (10, 20, 30 and 40°). In a similar study, comparing IGA (15, 20, 30 and 40°) in VMAT for esophageal cancer didn't yield any significant differences in plan quality indices.[14] Larger IGA (30 and 40°) yielded better plan than smaller IGA (10 and 20°) in post-operative cervical cancer; the results had a correlation with MLC movements created under reduced freedom of optimization by 'sweep sequencer tool' for smaller IGA (10 and 20°).[15] The controversial results from previous publications[14,15] could be due to a larger volume of PTV in cervical cancer than esophageal cancer and are explained in the present study (Figure 3). The dimension of PTV (Figure 3) in lateral directions (−90 and þ90°) were smaller than in anterior or posterior directions (180 and 0°). For sector 3 (−80 to −120°) and sector 7 (60–100°) in VMAT40 (Figure 1b), the sweep sequencer had to sharply decrease the field size initially, followed by a gradual

increase (Figure 3). This fluctuation could be the reason for the superiority of plan quality indices in VMAT.30 Notably, VMAT30 had an even number of sectors and were highly symmetrical (Figure 1a).

IGA 30° yielded better plans as per target dose indices but the dose fall-off region was compromised (more dose to lung) in esophageal cancer [14] and this trend is even resembled with the present study; dose to bladder, rectum and bowel were higher with larger IGA. Eventually, dose–gradient in fall-off region was worsened with larger IGA (30 and 40°); the reason could be due to larger dimension of PTV

(Figure 3) in this study (cervical cancer versus esophageal cancer). Homogenous dose distribution within PTV was enhanced with larger IGA in this study; more number of CPs was generated by 'sweep sequencer tool' to improve the parameter. Eventually, the number of MUs was reduced by finer resolution of MLC segments for the optimal dose–fluence generated in initial optimization of VMAT by Monaco TPS. Similar

enhancement of homogenous dose distribution was observed within PTV of both esophageal [14] and cervical [15] cancers with larger IGA (30 and 40°). Increase in the number of CPs enhanced the homogeneity of delivering prescribed dose within PTV but failed to confine the prescribed dose just around the PTV. As a result, confinement of prescribed dose within PTV and dose gradient in dose fall-off regions was compromised to a small extent.

VMAT40 had reduced the MU usage but the CI and DGI was compromised due to large MLC field segments. Though the difference was significant, the conformal dose to PTV was quite comparable in this study, and also observed both in esophageal [14] and cervical [15] cancers. Thus, the CI remained unaffected with a change in the size of PTV. TC was affected with smaller IGA (10°) up to 5%, in this study of definitive radiotherapy treatment for cervical cancer, which had a resemblance to a worst of 6% in cervical cancer. [15]

8.7. Conclusion:

In VMAT technique, defining the IGA remains vital in acquiring better plan quality indices. The current study demonstrates that the strategy of VMAT30 and VMAT40 have the potential to enhance plan quality indices/therapeutic gain. This study recommends that the larger IGA (30°) could yield better results when the number of

sectors are even, for a cervical cancer patient. However, more data from more patients need to be obtained and analyzed to make this an evidence-based hypothesis.

8.8 References:

1. Duan J, Kim RY, Elassal S, Lin HY, Shen S. Conventional high-dose-rate brachytherapy with concomitant complementary IMRT boost: a novel approach for improving cervical tumor dose coverage. Int J Radiat Oncol Biol Phys 2008; 71 (3): 765–771.

2. Georg P, Georg D, Hillbrand M, Kirisits C, Pötter R. Factors influencing bowel sparing in intensity modulated whole pelvic radiotherapy for gynaecological malignancies. Radiother Oncol 2006; 80 (1): 19–26.

3. Portelance L, Chao KS, Grigsby PW, Bennet H, Low D. Intensity-modulated radiation therapy (IMRT) reduces small bowel, rectum, and bladder doses in patients with cervical cancer receiving pelvic and para-aortic irradiation. Int J Radiat Oncol Biol Phys 2001; 51 (1): 261–266.

4. Otto K. Volumetric modulated arc therapy: IMRT in a single gantry arc. Med Phys 2008; 35 (1): 310–317.

5. Teoh M, Clark CH, Wood K, Whitaker S, Nisbet A. Volumetric modulated arc therapy: a review of current literature and clinical use in practice. Br J Radiol 2011; 84 (1007): 967–996

6. Vanetti E, Clivio A, Nicolini G, et al. Volumetric modulated arc radiotherapy for carcinomas of the oro-pharynx, hypo-pharynx and larynx: a treatment planning comparison with fixed field IMRT. Radiother Oncol 2009; 92 (1): 111–117.

7. Palma D, Vollans E, James K, et al. Volumetric modulated arc therapy for delivery of prostate radiotherapy: comparison with intensity-modulated radiotherapy and three-dimensional conformal radiotherapy. Int J Radiat Oncol Biol Phys 2008; 72 (4): 996–1001.

8. Zhang P, Happersett L, Hunt M, Jackson A, Zelefsky M, Mageras G. Volumetric modulated arc therapy: planning and evaluation for prostate cancer cases. Int J Radiat Oncol Biol Phys 2010; 76 (5): 1456–1462.

9. Yin L, Wu H, Gong J, et al. Volumetric-modulated arc therapy vs. c-IMRT in esophageal cancer: a treatment planning comparison. World J Gastroenterol 2012; 18 (37): 5266–5275.

10. Abbas AS, Moseley D, Kassam Z, Kim SM, Cho C. Volumetric-modulated arc therapy for the treatment of a large planning target volume in thoracic esophageal cancer. J Appl Clin Med Phys 2013; 14 (3): 192–202.

11. Masi L, Doro R, Favuzza V, Cipressi S, Livi L. Impact of plan parameters on the dosimetric accuracy of volumetric modulated arc therapy. Med Phys 2013; 40 (7): 071718.

12. Treutwein M, Hipp M, Koelbl O, Dobler B. Searching standard parameters for volumetric modulated arc therapy (VMAT) of prostate cancer. Radiat Oncol 2012; 7: 108.

13. Wang Y, Chen L, Zhu F, Guo W, Zhang D, Sun W. A study of minimum segment width parameter on VMAT plan quality, delivery accuracy, and efficiency for cervical cancer using Monaco TPS. J Appl Clin Med Phys 2018; 19 (5): 609–615.

14. Nithya L, Raj NA, Rathinamuthu S, Sharma K, Pandey MB. Influence of increment of gantry angle and number of arcs on esophageal volumetric modulated arc therapy planning in Monaco planning system: a planning study. J Med Phys 2014; 39 (4): 231–237.

15. Chen A, Li Z, Chen L, et al. The influence of increment of gantry on VMAT plan quality for cervical cancer. J Radiat Res Appl Sci 2019; 12 (1): 447–454.

16. Edge SB, Compton CC. The American Joint Committee on Cancer: the 7th edition of the AJCC cancer staging manual and the future of TNM. Ann Surg Oncol 2010; 17 (6): 1471–1474.

17. Lim K, Small,WJr, Portelance L, et al. Consensus guidelines for delineation of clinical target volume for intensity-modulated pelvic radiotherapy for the definitive treatment of cervix cancer. Int J Radiat Oncol Biol Phys 2011; 79 (2): 348–355.

18. Forrest J, Presutti J, Davidson M, Hamilton P, Kiss A, Thomas G. A dosimetric planning study comparing intensity-modulated radiotherapy with four-field conformal pelvic radiotherapy for the definitive treatment of cervical carcinoma. Clin Oncol (R Coll Radiol) 2012; 24 (4): e63–e70.

19. Vrdoljak E, Omrcen T, Novakovi´c ZS, et al. Concomitant chemobrachy radiotherapy with ifosfamide and cisplatin followed by consolidation chemotherapy for women with locally advanced carcinoma of the uterine cervix–final results of a prospective phase II-study. Gynecol Oncol 2006; 103 (2): 494–499.

20. Paddick I. A simple scoring ratio to index the conformity of radio surgical treatment plans. Technical note. J Neurosurg 2000; 93 (Suppl. 3): 219–222.

21. R Development Core Team (2016). R: A Language and Environment for Statistical Computing. R Foundation for Statistical Computing, Vienna, Austria. http://www.R-project.org. Accessed on 10th August 2020.

CHAPTER -IX

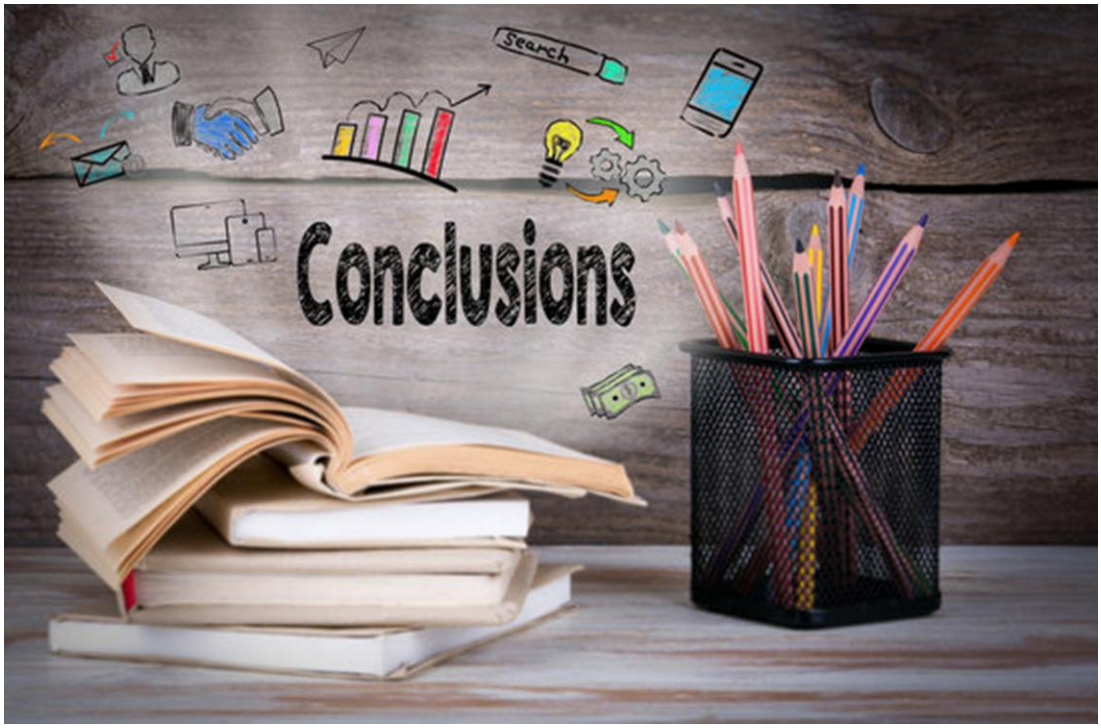

CHAPTER-IX

Summary and conclusion of the Research Work:

9.1 Commissioning and validation of FFF beam

More recently, the linear accelerators have been manufactured without flattening filters to increase the dose rate. This first chapter offers a report on the precise commissioning and examination of the dosimetric properties of flattening (FF) and flattening filter free (FFF) photon beams generated at 6 MV and 10 MV by an Elekta versa HD medical accelerator. The percentage deep dosage, dose rate, beam profile, out-of-field, energy spectra, scatter factor, surface dose, and the accuracy of commissioning/Modeling Elekta versa HD photon beam energies in the Monaco TPS using a Monte Carlo dose calculation technique are among these qualities.

New Flattening filter free (FFF) beams can be delivered by modern medical linear particle accelerators (linacs), allowing for larger dosage rates. Flattened beams appear to be unnecessary in intensity modulated radiation treatment (IMRT) and small-field stereotactic procedures. It is critical to accurately quantify and estimate the dosage distribution delivered by such beams before they can be implemented. A flattening filter-free beam has been successfully integrated into the Monaco treatment planning system, and the beam's dose calculation accuracy has been evaluated using a 2D array detector (Octavius seven29 array detector).

For 3D validation of FFF therapies, the Octavius has been found to be effective. We successfully compared measured FFF beam data to modelled data and found that the calculated dose distribution for both 6FFF and 10FFF beams, 10x10cm2 and 20x20cm2 open fields, matched the measured beam data with 100% &98.9% points passing the -test with 2mm and 2% criteria.

In summary, The stability of FFF similar to FF beams. The FFF beams improve the treatment outcomes through the availability of very high dose rates (1400 for 6FFF and 2400 MU/minute for 10FFF) and shortened treatment time especially with SRS and SBRT treatment technique.

9.2 Implementation of FFF & FF beam in liver SBRT

In second study we have chosen 10 patients (20 treatment plans) for a short course Stereotactic Body Radiation Therapy (SBRT) with VMAT plans with 6MV both flattened beam (6XFB) and flattening filter free (6XFFF) beam for liver cancer patients. VMAT-based stereotactic body irradiation for liver metastasis shows considerable reduction in the delivery time for FFF beam, when compared to the FB. The reduction in delivery time is essential to keep the treatment time suitable for patients using the breath holding technique. Unflattened beam shows no dosimetric advantage for unspecified tissues and OAR. However, a better conformal dose distribution was obtained for the unflattened beam. In conclusion, an unflattened beam is a good choice for liver SBRT, while using the breath hold technique

9.3 Treatment Techniques for Carcinoma Cervix using Flattened and Flattening Filter Free Beams: A planning Study

In the third study, we selected 30 patients to finish the research (250 treatment plans). This study included patients with cervical cancer who received external beam radiation using various modalities (3DCRT, IMRT, and VMAT). We used FB and FFFB to compare the dosimetry of 3DCRT, IMRT, and VMAT/ plans for Cervix cancer patients (6& 10MV).

This extensive study revealed a suitable treatment planning technique for cervical carcinoma. When compared to 3DCRT and IMRT, it reveals VMAT's ability to produce highly conformal and homogeneous treatment plans in cervix radiotherapy.

According to our research, the maximum doses to OARs after VMAT were 1 to 3 times lower than after 3DCRT. In comparison to the other approaches, VMAT had lower mean doses, maximum doses, and volume for OARs (6&10MV FB and FFFB). VMAT significantly reduces the risk of future cancer in the relevant OARs when compared to IMRT and 3DCRT (6&10MV FB and FFFB).

According to this study, the VMAT (6 MV FB) techniques may deliver better results for a cervical cancer patient. To make this an evidence-based theory, more data from more patients must be collected and examined.

9.4 The important role of Angular space/increment size parameters in VMAT technique

In order to complete the studies, we selected 27 patients with carcinoma cervix cancer having aged between 54 and 69. All the patients enrolled in this study were at T3N1M0 stage of cervical cancer. [16] Each of them had evolved lymph nodes and were preparing to undergo definitive radiotherapy treatment.

VMAT plan was delivered in a single arc of 360° gantry rotation (clockwise direction from 180 to −180°). Sweep sequencer tool was used for MLC segmentation in VMAT technique.6 MV flattened photon beam was used to deliver the prescribed dose using VMAT plan. VMAT plans were optimized by varying the parameter 'IGA' (as 10, 20, 30 and 40°) and the plans were named as VMAT,10 VMAT,20 VMAT,30 and VMAT,40 respectively.

In VMAT technique, defining the angular space/increment size remains vital in acquiring better plan quality indices. The current study demonstrates that the strategy

of VMAT30 and VMAT40 have the potential to enhance plan quality indices/therapeutic gain. This study recommends that the larger IGA (30°) could yield better results when the number of sectors are even, for a cervical cancer patient. However, more data from more patients need to be obtained and analyzed to make this an evidence-based hypothesis.

CHAPTER -X

RECOMMENDATIONS

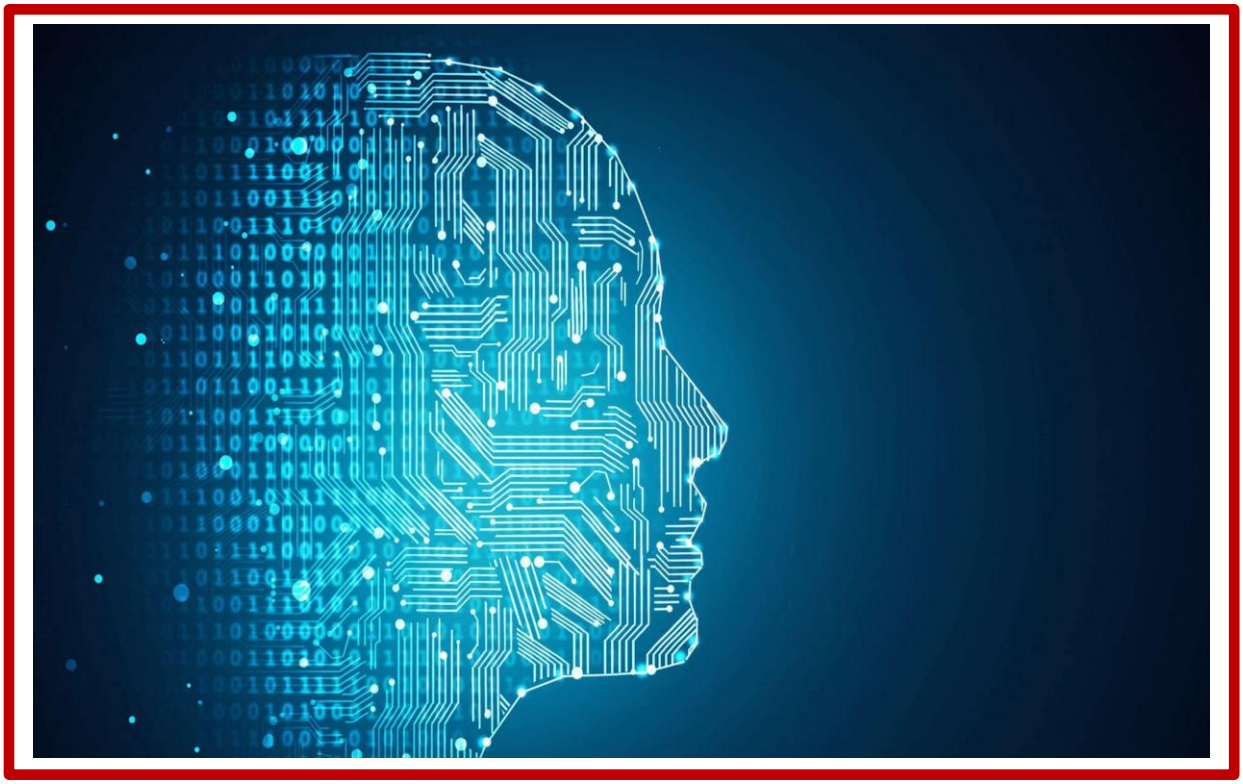

CHAPTER-X

SCOPE OF FUTURE WORK:

As we know Cancer remains leading cause of death globally. The International Agency for Research on Cancer (IARC) recently estimated that 7.6 million deaths worldwide were due to cancer with 12.7 million new cases per year being reported worldwide. Radiation remains an important modality for cancer treatment with ongoing efforts towards designing new radiation treatment modalities and techniques which continue to improve the survival and quality of life of cancer patients. With the improved clinical outcomes of cancer treatment, minimizing radiation therapy related toxicities has also become a priority. The emergence of mechanistic biological studies together with improvements in radiation technology has improved the sparing of normal cells/tissues through dose fractionation and conformal radiation techniques.

All these studies were performed in eclipse planning system with Monte Carlo algorithms but in future we suggest the researcher to perform with latest Acurous XB (AXB) algorithm which may show higher dosimetric result for cervix cancer planning. Similarly, Monte Carlo algorithms are giving better accurate dose calculation. But in present scenario limited study is available for flattened beam (FB& FFFB) IMRT and VMAT planning for cervix cancer but for FFF beams is lacking. It is time to study the dosimetric evaluation for Cervix cancer treatment plans with Monte Carlo algorithm for FFF beams.

The toxicities of normal tissues may be a concern while adopting high dose rates with FFF and need to be further studied through organized clinical protocols. Potential benefits of FFF beam might be of interest in future in the case of respiratory gated treatment where the trade-off of low duty cycle be efficiently compensated.

Although the study focused on photon therapy, proton therapy (charge particle therapy) is also another option to treat prostate cancer in external beam radiotherapy. Proton therapy can produce excellent dose distribution because protons have finite range and sharp distal fall-off at the end of proton beam path. When compared to photon therapy, proton therapy is better at sparing the rectum and bladder. At the moment, proton therapy is not available everywhere in India, but it will be a major research focus in the future.

Further we need research work of dosimetric study and clinical dosimetric outcome for other sites cancer like, head and neck, prostate, lungs, esophagus and brain etc with different various modern techniques in external beam radiotherapy specially with FFF beams.

Journal of Radiotherapy in Practice

cambridge.org/jrp

Original Article

Cite this article: Munirathinam N, Pawaskar PN. (2019) Dosimetric comparison of flattened and flattening filter-free beams for liver stereotactic body irradiation in deep inspiration breath hold, and free breathing conditions. *Journal of Radiotherapy in Practice* page 1 of 6. doi: 10.1017/S146039691800064X

Received: 18 April 2018
Revised: 4 October 2018
Accepted: 16 October 2018

Key words:
deep inspiration breath hold (DIBH); flatten beam; volumetric modulated arc therapy (VMAT); flattening filter-free (FFF) beam; free breathing

Author for correspondence:
N. Munirathinam, The Department of Medical Physics, Centre for Interdisciplinary Research, D.Y. Patil Education Society (Deemed to be) University, Kolhapur-416006, Maharashtra, India. Tel: +91-7709316668. Fax: 00231 260 1235. E-mail: munimedphy@gmail.com

Dosimetric comparison of flattened and flattening filter-free beams for liver stereotactic body irradiation in deep inspiration breath hold, and free breathing conditions

N. Munirathinam and P. N. Pawaskar

The Department of Medical Physics, Centre for Interdisciplinary Research, D.Y. Patil University, Kolhapur, Maharashtra, India

Abstract

Aim: The aim of this study is to evaluate the influence of flattened and flattening filter-free (FFF) beam 6 MV photon beam for liver stereotactic body radiation therapy by using volumetric modulated arc therapy (VMAT) technique in deep inspiration breath hold (DIBH) and free breathing condition. *Materials and methods:* Eight liver metastasis patients (one to three metastasis lesions) were simulated in breath hold and free breathing condition. VMAT-based treatment plans were created for a prescription dose of 50 Gy in 10 fractions, using a 230° coplaner arc and 60° non-coplanar arc for both DIBH and free breathing study set. Treatment plans were evaluated for planning target volume (PTV) dose coverage, conformity and hot spots. Parallel and serial organs at risk were compared for average and maximum dose, respectively. Dose spillages were evaluated for different isodose volumes from 5 to 80%. *Result:* Mean $D_{98\%}$ (dose received by 98% target volume) for FFF in DIBH, flattened beam in DIBH, FFF in free breathing and flatten beam in free breathing dataset were 48·9, 47·81, 48·5 and 48·3 Gy, respectively. $D_{98\%}$ was not statistically different between FFF and flatten beam ($p = 0{\cdot}34$ and 0·69 for DIBH and free breathing condition). PTV $V_{105\%}$ (volume receiving 105% dose) for the same set were 3·76, 0·25, 1·2 and 0·4%, respectively. Mean heterogeneity index for all study sets and beam models varies between 1·05 and 1·07. Paddik conformity index using unflattened and flattened beam in DIBH at 98% prescription dose were 0·91 and 0·79, respectively. Maximum variation of isodose volume was observed for I-5%, which was ranging between 2288·8 and 2427·2 cm^3. Increase in isodose value shows a diminishing difference in isodose volumes between different techniques. DIBH yields a significant reduction in the chest wall dose compared with free breathing condition. Average monitor units for FFF beam in DIBH, flattened beam in DIBH, FFF beam in free breathing CT dataset and flattened beam in free breathing CT dataset were $1318{\cdot}6 \pm 265{\cdot}1$, $1940{\cdot}3 \pm 287{\cdot}6$, $1343{\cdot}3 \pm 238{\cdot}1$ and $2192{\cdot}5 \pm 252{\cdot}6$ MU. *Conclusion:* DIBH and FFF is a good combination to reduce the treatment time and to achieve better tumour conformity. No other dosimetric gain was observed for FFF in either DIBH or free breathing condition.

Introduction

The clinical use of the flattening filter-free (FFF) beam in linear accelerators is a subject of great interest in recent times.[1–3] Considering the physical characteristics of the FFF beam, it can be expected that the dose fall-off beyond the field sizes will be sharper than that of the flattened beam (FB). This could be attributed to the reduction in (residual) electron contamination and decline in the head scatter factor.

From the clinical perspective, FFF beam could lead to a reduction in the beyond field border dose for modern therapy delivery techniques. Sharper dose fall may yield a higher dose gradient, leading to a sparing of organs at risk (OAR), enhancing the dose to the tumor.

Another advantage of the FFF beam is its increased dose rate, which will in turn reduce the treatment time substantially. However, it is essential to validate the FFF beam for the dosimetric outcome of the beam, to reduce the healthy tissue dose, with better or equal tumor dose coverage. Several investigators have investigated different physical characteristics of the FFF beam, such as the beam profile, etc.

Therefore, the dosimetric characteristic of the FFF beam will have to be evaluated in actual clinical situations, specifically with the planning target volume (PTV) coverage and OAR sparing for different available linear accelerators.[4] A substantial amount of work has been published on Varian (Varian Medical System, Polo Alto, CA, USA) FFF; but the literature

CAMBRIDGE UNIVERSITY PRESS

available regarding the Elekta (Elekta AB, Stockholm, Sweden) unflattened beam is very limited.[5–10]

Stereotactic body irradiation (SBRT) is an emerging field and is used for different body sites, like lung, liver and spinal metastasis. SBRT has proved its efficacy in several cases, both for primary as well as metastatic sites. Stereotactic irradiation involves the delivery of a very high dose over a number of fractions. Body stereotactic radiotherapy demands a very good motion management technique.[11–13] In particular, SBRT may be appropriate for selected patients with organ-confined, limited-volume primary tumours or oligo-metastatic disease.[14] Traditionally, SBRT was delivered using multiple three-dimensioanl conformal radiation therapy (3DCRT) beams or intensity-modulated radiation therapy (IMRT) beams.[15,16] The disadvantage with 3DCRT is insufficient fluence modulation, yielding insufficient OAR sparing. However, IMRT gives a good fluence modulation, and hence better OAR sparing. The treatment time is considerably longer, which can lead to patient discomfort and an increase in the probability of inter fraction motion. Volumetric-modulated arc therapy (VMAT) may be a better option as it can deliver the radiation dose within a shorter time and achieve effective OAR sparing. The potential of VMAT used for SBRT to treat liver tumours has been evaluated by a few researchers; nevertheless, these evaluations have limitations.[5,6] For example, SBRT was not evaluated using FFF, during deep inspiration breath hold (DIBH) and free breathing conditions. The aim of this study, therefore, was to evaluate the characteristics of the flattened and unflattened beams of the Elekta agility linear accelerator, using VMAT-based liver SBRT technique, in free breathing and DIBH conditions.

Materials and Methods

For a set of eight liver-metastasis patients, computed tomography (CT) scans were taken using DIBH as well as free breathing conditions. Before CT simulation, all patients underwent two practice sessions of breath hold technique for procedure familiarisation. Patients were immobilised using a vacuum bag (vack-lock; Orfit Industries, Belgium).

The vacuum bag takes on the shape of the patient when deflated. An axial section of 1·5 mm axial CT slices was obtained in both DIBH and free breathing conditions. CT datasets were transferred to the Monaco Sim (CMS Elekta, Sunnyvale, CA, USA) workstation for contouring, using DICOM-enabled protocol.

An experience radiation oncologist contoured the gross target volume and clinical target volume, in the DIBH as well as free breathing study sets. In free breathing study set, the gross tumor volume was delineated using the minimum intensity projection that was obtained from the 20-slice Siemens positron emission tomography (PET)-CT (Biagraph MCT-20, Germany) console. DIBH and free breathing study sets were co-registered with each other, while they were obtained in the PET-CT. Therefore, they did not require any mutual information co-registration. OAR were contoured by the resident radiation oncologists. CT study sets, along with the contours, were transferred to the Monaco (CMS Elekta) treatment planning system, for radiotherapy planning. Elekta versa HD (Elekta AB) is a linear accelerator with 80 pairs of multi-leaf collimators (MLC) of 5 mm uniform width. It is capable of delivering both flattened and unflattened beams.

Planning was done using both FFF and flat 6 MV photon beams. All patients were treated with a dose of 50 Gy in 10 fractions (this is a standard regime followed in SBRT liver).[17] All patients with one to three liver lesions were combined to form a lone PTV.[12,13]

A comparison of single patient plan is presented in Figure 1. Panels A, B, C and D represent FFF beam in free breathing CT dataset, FB in free breathing CT dataset, FB in DIBH CT dataset and FFF beam in DIBH CT dataset, respectively.

Patients were planned using a partial arc of 230° coplanar arc at table position of 0° (Gantry starts at 180° CW 200° + Gantry starts at 150° CW 30°). Two non-coplanar beams, 30° anterior and 30° posterior, were added at 270° table position. The gantry traverse for all arcs was twice the same locus. Table position–patient–gantry collision possibilities were evaluated before the actual delivery.

All plans were carried out using Elekta versa HD FFF 6 MV photon beam, for the purpose of treatment, in DIBH study set. Subsequently, the same plan was copied onto the free breathing study set and optimisation and dose calculation were carried out, without changing the optimisation parameters. Two more treatment plans were created in DIBH and free breathing study sets, using an Elekta versa HD linear accelerator with FB.

Results were evaluated for doses received by 98% PTV volume ($D_{98\%}$), maximum dose, Paddick conformity index (CI), heterogeneity index (HI) and PTV volume receiving 105% (V105%) of the prescription dose. Paddick CI and HI were defined as follows:[18]

$$\mathrm{CI} = \frac{V_{RX}^2}{TV * V_{RI}}, \quad \mathrm{HI} = \frac{D_{5\%}}{D_{95\%}}$$

where TV = target volume, V_{RX} = target volume covered by 100% isodose line, V_{RI} = volume of 100% isodose line, and $D_{5\%}$ and $D_{95\%}$ were the doses received by 5 and 95% of the target volume.

OAR doses were evaluated for mean dose, for bowel bag, heart, bilateral kidney, bilateral lung, chest wall, diaphragm and liver. Spinal cord was evaluated for the maximum dose. Spillage dose to unspecified tissues, corresponding to different beam models in DIBH and free breathing study sets, were evaluated for 5% (I-5%), 10% (I-10%), 20% (I-20%), 30% (I-30%), 40% (I-40%), 50% (I-50%), 60% (I-60%), 70% (I-70%) and 80% (I-80%) isodose volumes.

Results

The mean PTV volume of the liver lesions was $23{\cdot}7 \pm 12{\cdot}9\ \mathrm{cm}^3$, with no patient exhibiting more than three lesions. The graphical comparison of the dose–volume histogram for flattened and unflattened beams, on DIBH, is presented in Figure 2.

Averaged overall patient results for dose received by 98% volume ($D_{98\%}$), maximum dose, Paddick CI, HI and PTV volume receiving 105% ($V105\%$) of the prescription dose are presented, respectively, in the left and right panels of Figure 3.

Mean $D_{98\%}$ for FFF in DIBH, FB DIBH, FFF in free breathing and FB in free breathing dataset were 48·9, 47·81, 48·5 and 48·3 Gy, respectively. Statistical co-relation (p) at 95% confidence interval (p), between the different beam models, was calculated using a Student's t-test. DIBH study set p, for FFF-FB, was 0·34. Free breathing study set p, for FFF-FB, was 0·69. Statistical significance p, for FFF-FB, indicates no statistical variation between the DIBH and free breathing study sets. The average PTV maximum dose for FFF and FB for DIBH study sets, were 50·7 and

https://doi.org/10.1017/S146039691800064X

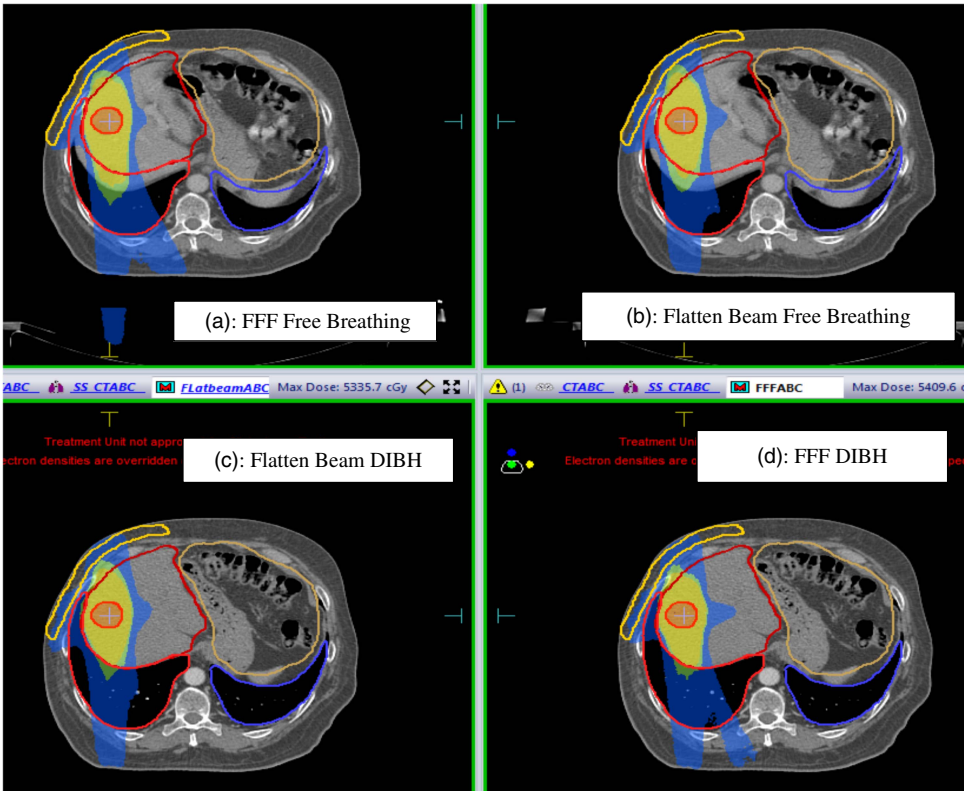

Figure 1. Treatment plans using moderate hypo-fractionated (50 Gy in 10 fractions) for liver SBRT. Panel A: FFF beam in free breathing CT dataset. Panel B: Flatten beam in free breathing CT dataset. Panel C: Flatten beam in DIBH CT dataset. Panel D: FFF beam in DIBH CT dataset. *Abbreviations*: SBRT, stereotactic body radiation therapy; FFF, flattened filter-free.

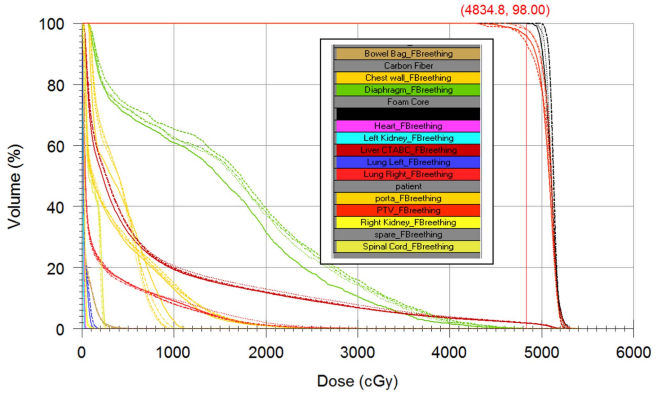

Figure 2. Dose–volume histogram comparison in DIBH and free breathing study sets, using flattened and unflattened beams. *Abbreviation*: DIBH, deep inspiration breath hold.

50·7 Gy, respectively. Maximum doses for free breathing study set, for the same group, were 50·7 and 50·8 Gy, respectively. PTV $V_{105\%}$ for the same set were 3·76, 0·25, 1·2 and 0·4%, respectively. Mean HI for all study sets and beam models varies between 1·05 and 1·07. Paddik CI, using unflattened and FBs, in DIBH at 98% prescription dose were 0·91 and 0·79, respectively. The average CI of both beams, for free breathing CT set, was 0·77. The difference between the FFF and FBs for DIBH study set (statistical significance p) was <0·001.

Average dose for OARs including the bowel bag, heart, bilateral kidneys, bilateral lung, chest wall, diaphragm, liver and maximum dose for spinal cord were presented in Figures 4a, 4b and 4c, respectively.

The dose administered to organs presented in panel A of Figure 4 is very low, as the organs are away from the target volume. Mean dose to the right lung varies between 2·2 and 2·5 Gy with regard to different beam models and study sets. Bowel, bilateral kidney and left lung doses were between 0·07 and 0·37 Gy. Average doses to chest wall, for unflattened beam and FB, were 3·7 and 3·9 Gy, respectively; the same for free breathing study set were 28 and 26·5 Gy, respectively. Difference of dose on chest wall, between DIBH and free breathing study sets, was statistically significant ($p = 0·03$). Mean diaphragm doses for all four tested plans were comparable and varied between 13·4 and 16·3 Gy. Mean liver dose also did not yield any variation, with respect to beam models and study sets.

The spillage doses of different beams and models (I-5% and I-10% to I-80%), are presented in Figure 5.

Figure 5 shows a negligible variation of the isodose volumes, with respect to flattened and unflattened beams, in DIBH and free breathing conditions. For example, I-5% yields a variation within the range of 2288·8–2427·2 cm^3. This was noted to be the highest variation among all the isodose volumes. The variation between the isodose volumes attributed to the flattened and unflattened beams, for DIBH and free breathing conditions, diminishes with the increasing isodose values. The variation in I-80% was between 47·6 and 53·8 cm^3, which is only 6·2 cm^3.

Monitor unit

Average monitor units of FFF beam in DIBH, FB in DIBH, FFF beam in free breathing CT dataset and FB in free breathing CT dataset were 1318·6 ± 265·1, 1940·3 ± 287·6, 1343·3 ± 238·1 and 2192·5 ± 252·6 MU, respectively. The mean numbers of the breath

https://doi.org/10.1017/S146039691800064X

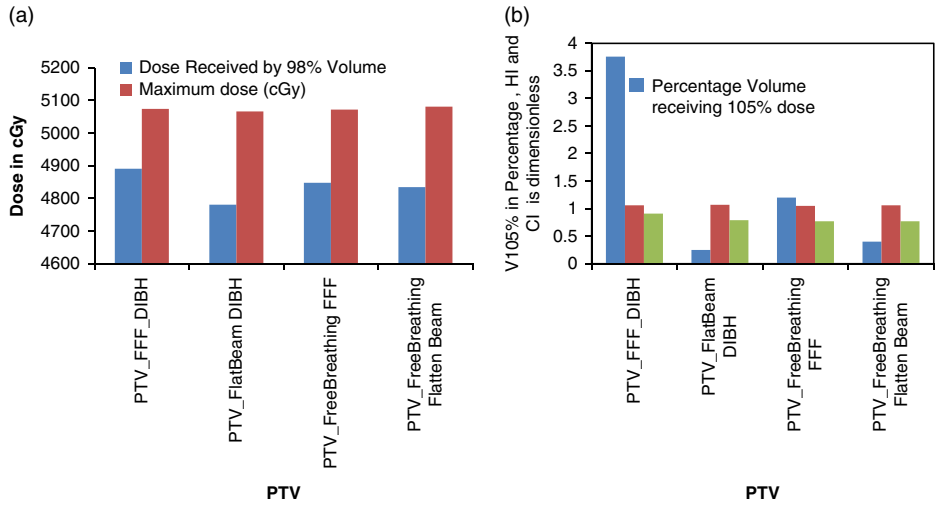

Figure 3. Variation of PTV coverage and hotspot related parameters, as a function of beam model in DIBH and free breathing condition. *Abbreviations*: DIBH, deep inspiration breath hold; PTV, planning target volume.

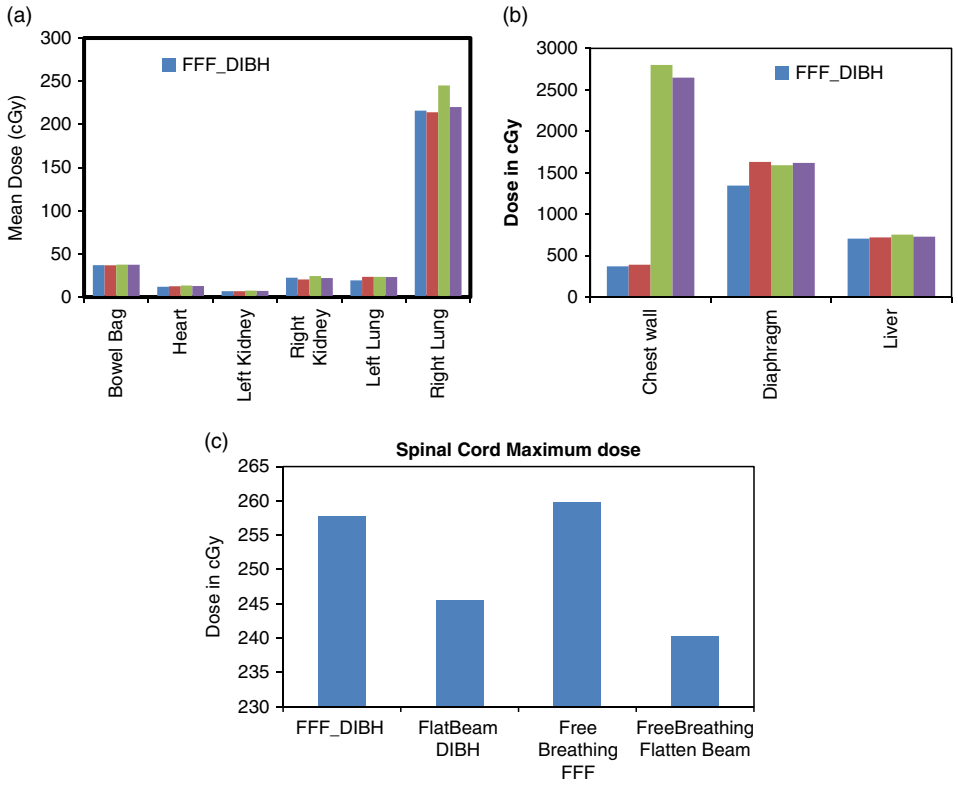

Figure 4. Mean dose to bowel bag, heart, bilateral kidney, bilateral lung (panel A), chest wall, diaphragm and liver (panel B) and maximum dose to the spinal cord (panel C), in DIBH and free breathing datasets using unflattened and flattened beam models. *Abbreviation*: DIBH, deep inspiration breath hold.

holds were found to be $3{\cdot}3 \pm 1{\cdot}9$ and $9{\cdot}7 \pm 3{\cdot}2$ for unflattened beam and FB, respectively.

Discussion

Several studies of the past have investigated the planning aspect of unflattened beam, for liver and lung SBRT, esophagus, craniospinal irradiation and cranial stereotactic radiotherapy.[6–10,19–21] It is established that unflattened beam is dosimetrically comparable with the FB. Investigators have obtained a mixed result on the efficacy of the unflattened beam over the FB. For liver SBRT, many studies have been designed, comparing flattened and unflattened beams. However, no study group has studied the influence of breath hold technique on this. This study is the first of its kind to evaluate flattened and unflattened beams, with respect to free breathing and breath holding techniques.

Reggiori et al. noted the effect of tumour volume on flattened and unflattened beams, depending on the CI. They favored

https://doi.org/10.1017/S146039691800064X

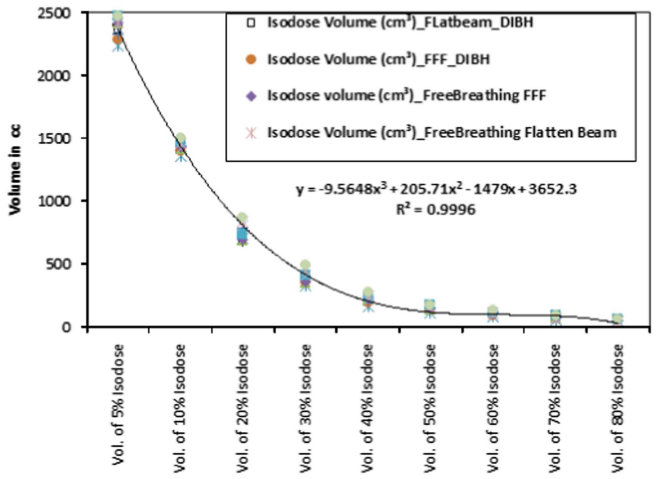

Figure 5. Isodose volume of 5% and 10%–80% were plotted as a function of beam model in DIBH and free breathing conditions.

unflattened beam for intermediate volume tumours ($100\,cm^3 \leq$ PTV volume $\leq 300\,cm^3$) and FB for the smaller and larger tumours. The mean target volume of the patient in this study did not exceed $50\,cm^3$. However, we have observed an advantage of the unflattened beam over the FB in the target conformity.[6]

Earlier studies have noted a considerable reduction in the delivery time for unflattened beam because of the enhanced dose rate. For Elekta linear accelerator, the dose rates are 600 and 2000–2200 MU/minute, for flattened and unflattened beams, respectively. Breath holding times do not exceed 30 seconds, with the average holding time between 20 and 25 seconds. Therefore, breath holding technique essentially requires an unflattened beam to reduce the delivery time.

The advantage of Elekta versa HD linear accelerator is the speed of the MLC, which is as fast as 6 cm/second, which helps sustain a very high dose rate of 2000–2200 MU/minute. High dose rate delivery requires a higher MLC speed for a compatible delivery. A low MLC speed cannot sustain a high dose rate VMAT delivery.[22]

In this study, we observed a high CI with respect to the unflattened beam for breath hold technique. OAR doses to chest wall show a high dose difference between the breath hold and the free breathing techniques. Change in the CI of the unflattened beam is characteristic of the unflattened character of the beam. However, the loss of dose to the chest wall can be attributed to the fact that the chest wall in DIBH is fixed in a longer distance, for a longer time from the target. However, decrease in chest wall doses can be explained only with the unflattened characteristic of the beam.

As per the basic theory of Gaussian distribution, an unflattened beam is closer to a Gaussian distribution while a FB is a blur Gaussian. With the same characteristics, an unflattened beam should observe a better dose buildup to tumour, with a sharper fall at the periphery. However, no such phenomenon has been observed in any previous investigations so far.

Several authors have reported phase I/II clinical trials of liver metastasis, using stereotactic body irradiation.[12,13,23–25] For the large surgical series, including those primarily in patients with metastatic colorectal cancer, 5-year survival after liver resection ranges between 37 and 71%.[23–25] Patients who were not suitable for surgery and those with poor risk-prognostic factor were chosen for the radiotherapy clinical trials, yielding a median survival of 20·5 month and a two-year local control of 100%.[12]

Conclusion

VMAT-based stereotactic body irradiation for liver metastesis shows considerable reduction in the delivery time for FFF beam, when compared to the FB. The reduction in delivery time is essential to keep the treatment time suitable for patients using the breath holding technique. Unflattened beam shows no dosimetric advantage for unspecified tissues and OAR. However, a better conformal dose distribution was obtained for the unflattened beam. In conclusion, an unflattened beam is a good choice for liver SBRT, while using the breath hold technique.

Acknowledgements. The patient treatment plans were performed at Aditya Birla Memorial Hospital, Pune. The authors are very much thankful for treatment planning system analysis by Dr Rajeev Srivastav, Dr Birendra kumar Rout and Dr Govindaraj.

References

1. Kry S F, Howell R M, Titt U, Salehpour M, Mohan R, Vassiliev O N. Energy spectra, sources, and shielding considerations for neutrons generated by a flattening filter-free Clinac. Med Phys 2008; 35: 1906–1911.
2. Vassiliev O N, Kry S F, Chang J Y, Balter P A, Titt U, Mohan R. Stereotactic radiotherapy for lung cancer using a flattening filter free Clinac. J Appl Clin Med Phys 2009; 10 (1): 14–21.
3. Kry S F, Howell R M, Polf J, Mohan R, Vassiliev O N. Treatment vault shielding for a flattening filter-free medical linear accelerator. Phys Med Biol 2009; 54: 1265–1273.
4. Kragl G, Baier F, Lutz S et al. Flattening filter free beams in SBRT and IMRT: dosimetric assessment of peripheral doses. Z Med Phys 2011; 21: 91–101.
5. Mancosu P, Castiglioni S, Reggiori G et al. Stereotactic body radiation therapy for liver tumours using flattening filter free beam: dosimetric and technical considerations. Radiat Oncol 2012; 7 (1): 16.
6. Reggiori G, Mancosu P, Castiglioni S et al. Can volumetric modulated arc therapy with flattening filter free beams play a role in stereotactic body radiotherapy for liver lesions? A volume-based analysis. Med Phys 2012; 39 (2): 1112–8.
7. Nicolini G, Ghosh-Laskar S, Shrivastava S K et al. Volumetric modulation arc radiotherapy with flattening filter-free beams compared with static gantry IMRT and 3D conformal radiotherapy for advanced esophageal cancer: a feasibility study. Int J Radiat Oncol Biol Phys 2012; 84: 553–60.
8. Sarkar B, Pradhan A. Choice of appropriate beam model and gantry rotational angle for low-dose gradient-based craniospinal irradiation using volumetric-modulated arc therapy. J Radiother Pract 2017; 16 (1): 53–64.
9. Navarria P, Ascolese A M, Mancosu P et al. Volumetric modulated arc therapy with flattening filter free (3F) beams for stereotactic body radiation therapy (SBRT) in patients with medically inoperable early stage non-small cell lung cancer (NSCLC). Radiother Oncol 2013; 107: 414–8.
10. Sarkar B, Pradhan A, Munshi A, Roy S, Ganesh T, Mohanti B. EP-1685: Influence of flat, flattening filter free beam model and different MLC's on VMAT based SRS/SRT. Radiother Oncol 2016; 119: S787.
11. Timmerman R D, Kavanagh B D, Cho L C, Papiez L, Xing L. Stereotactic body radiation therapy in multiple organ sites. J Clin Oncol 2007; 25: 947–952.
12. Rusthoven K E, Kavanagh B D, Cardenes H et al. Multi-institutional phase I/II trial of stereotactic body radiation therapy for liver metastases. J Clin Oncol 2009; 27 (10): 1572–8.
13. Lee M T, Kim J J, Dinniwell R et al. Phase I study of individualized stereotactic body radiotherapy of liver metastases. J Clin Oncol 2009; 27 (10): 1585–91.

https://doi.org/10.1017/S146039691800064X

14. Macdermed D M, Weichselbaum R R, Salama J K. A rationale for the targeted treatment of oligometastases with radiotherapy. J Surg Oncol 2008; 98: 202–206.
15. Cai J, Malhotra H K, Orton C G. A 3D-conformal technique is better than IMRT or VMAT for lung SBRT. Med Phys 2014; 41 (4): 040601.
16. de Pooter J A, Romero A M, Wunderink W, Storchi P R, Heijmen B J. Automated non-coplanar beam direction optimization improves IMRT in SBRT of liver metastasis. Radiother Oncol 2008; 88 (3): 376–81.
17. Milano M T, Katz A W, Muhs A G et al. A prospective pilot study of curative-intent stereotactic body radiation therapy in patients with 5 or fewer oligometastatic lesions. Cancer: Interdiscip Int J Am Cancer Soc 2008; 112 (3): 650–8.
18. Paddick I. A simple scoring ratio to index the conformity of radiosurgical treatment plans: technical note. J Neurosurg 2000; 93 (Supplement 3): 219–22.
19. Dzierma Y, Bell K, Palm J, Nuesken F, Licht N, Rübe C. mARC vs. IMRT radiotherapy of the prostate with flat and flattening-filter-free beam energies. Radiat Oncol 2014; 9 (1): 250.
20. Thomas E M, Popple R A, Prendergast B M, Clark G M, Dobelbower M C, Fiveash J B. Effects of flattening filter-free and volumetric-modulated arc therapy delivery on treatment efficiency. J Appl Clin Med Phys 2013; 14: 4328. https://doi.org/10.1120/jacmp.v14i6.4328.
21. Sarkar B, Pradhan A, Munshi A. Do technological advances in linear accelerators improve dosimetric outcomes in stereotaxy? A head-on comparison of seven linear accelerators using volumetric modulated arc therapy-based stereotactic planning. Indian J Cancer 2016; 53 (1): 166–173.
22. Manikandan A, Sarkar B, Holla R, Vivek T R, Sujatha N. Quality assurance of dynamic parameters in volumetric modulated arc therapy. Br J Radiol 2012; 85 (1015): 1002–10.
23. Fong Y, Fortner J, Sun R L, Brennan M F, Blumgart L H. Clinical score for predicting recurrence after hepatic resection for metastatic colorectal cancer: analysis of 1001 consecutive cases. Ann Surg 1999; 230 (3): 309.
24. Shah S A, Bromberg R, Coates A, Rempel E, Simunovic M, Gallinger S. Survival after liver resection for metastatic colorectal carcinoma in a large population. J Am Coll Surg 2007; 205 (5): 676–83.
25. Aloia T A, Vauthey J N, Loyer E M et al. Solitary colorectal liver metastasis: resection determines outcome. Arch Surg 2006; 141 (5): 460–7.

Journal of Radiotherapy in Practice

cambridge.org/jrp

Dosimetric characteristics of VMAT plans with respect to a different increment of gantry angle size for Ca cervix

Munirathinam Natraj[1], P. N. Pawaskar[1] and Arun Chairmadurai[2]

[1]Department of Medical Physics, Centre for interdisciplinary Research, D.Y. Patil University, Kolhapur, India and [2]Department of Radiation Oncology, Jaypee Hospital, Noida, India

Original Article

Cite this article: Natraj M, Pawaskar PN, and Chairmadurai A. (2020) Dosimetric characteristics of VMAT plans with respect to a different increment of gantry angle size for Ca cervix. *Journal of Radiotherapy in Practice* page 1 of 5. doi: 10.1017/S146039692000093X

Received: 10 August 2020
Revised: 30 September 2020
Accepted: 2 October 2020

Key words:
cervical cancer; increment of gantry angle; sector angle; volumetric-modulated arc therapy

Author for correspondence:
Dr. Padmaja N. Pawaskar, Department of Medical Physics, Centre for interdisciplinary Research, D.Y. Patil University, Kolhapur, India.
Tel: +91 9028074295.
E-mail: samgrish@gmail.com

Abstract

Aim: We have investigated the influence in volumetric-modulated arc therapy (VMAT) plans by a sequence of increment of gantry angle (IGA) in definitive radiotherapy treatment for cervical cancer. The plans are quantitatively analysed in terms of conformity index (CI), heterogeneity index (HI), dose–gradient index (DGI), target coverage (TC) by prescription dose, monitor unit (MU) usage, control points (CPs) and dose to organs.

Materials and Methods: In this retrospective study, we selected 27 patients with cervical cancer having aged between 54 and 69. All the patients enrolled in this study were at T3N1M0 stage of cervical cancer. The prescription dose to planning target volume (PTV) was 50 Gy and was administered in 2 Gy/fraction through VMAT technique. VMAT plans were optimised by varying the parameter 'IGA' as 10, 20, 30 and 40°.

Results: Homogenous dose distribution within PTV and TC by prescription dose was significantly enhanced ($p < 0{\cdot}05$) with larger IGA. The difference between volume receiving 15 Gy (V_{15Gy}) in bowel was up to 10% with larger IGA (30 and 40°) and V_{25Gy} in femoral head was up to 3% with smaller IGA (10 and 20°). CPs were enhanced and MU usage was reduced with larger IGA (30 and 40°). IGA 40° had reduced the MU usage than IGA 30° but the CI and DGI were compromised due to large MLC field segments.

Conclusion: This study recommends that the larger IGA could yield better results when the number of sectors is even, for a cervical cancer patient. However, more data from more patients need to be obtained and analysed to make this an evidence-based hypothesis.

Introduction

External beam radiotherapy (EBRT) followed by intracavitary brachytherapy is the primary treatment protocol for cervical cancer.[1] Conventional EBRT irradiates the whole pelvis region either from anteroposteriorly or/and laterally. Thus, critical organs at risk (OARs) are exposed to radiation and severe radiation-induced toxicities are observed. Over the last decade, interest in the use of intensity-modulated radiotherapy (IMRT) to treat cervical cancer has increased. IMRT technique has the benefit over conventional whole-pelvis irradiation; potentially improves the target dose coverage and reduces the toxicity to OARs).[2,3] IMRT typically involves 5–9 beams placed around the patient at equal angular spacing and the uniform radiation intensities from open fields are modulated by multileaf collimators (MLCs). A novel radiation technique has evolved by replacing 5–9 fixed beam angles in IMRT, with a single gantry arc of up to 360°, known as volumetric-modulated arc therapy (VMAT).[4,5]

VMAT has been introduced to overcome some of the limitations associated with fixed-field IMRT. It allows continuous delivery of radiation by simultaneously varying the dose rate, position of MLCs and gantry rotation speed. VMAT has achieved highly conformal dose distributions, with improved target dose coverage and sparing of normal tissues, as compared to conventional radiotherapy and IMRT techniques.[6–8] VMAT also has the potential to reduce monitor unit (MU) usage and ultimately reduce the treatment delivery time. Each arc is divided into multiple equal sectors in VMAT technique and MLC modulates the open radiation field by to-and-fro movement between successive sectors. Sector angle is defined by the parameter 'Increment of Gantry Angle' (IGA) and the number of sectors is given by arc length divided by IGA. The number of sectors and IGA has the tendency to influence the quality of treatment plan[9,10] along with the number of arcs and arc lengths.[11–13] Influence of smaller and larger IGA was reported as negligible in oesophageal cancer[14] and contrarily, larger IGA yielded significantly better plans in cervical cancer.[15] In this study, we have investigated the influence in VMAT plans by a sequence of IGAs in definitive radiotherapy treatment for cervical cancer. The plans are quantitatively analysed in terms of conformity index (CI), heterogeneity index (HI), dose–gradient index (DGI), target coverage (TC) by prescription dose, MU usage, control points (CPs) and dose to organs.

CAMBRIDGE UNIVERSITY PRESS

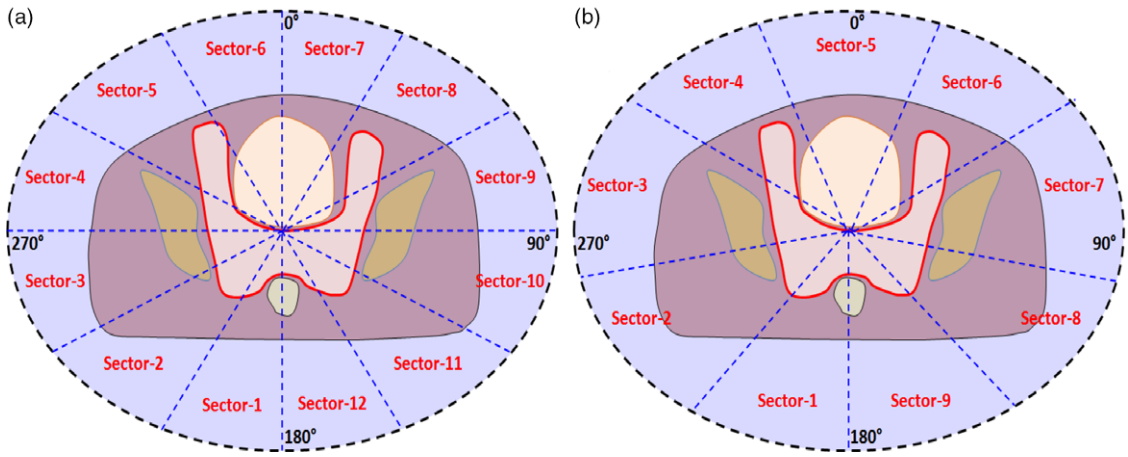

Figure 1. Comparison between the single arc of 360°, VMAT plans with IGA (a) 30° and (b) 40° in cervical cancer.

Materials and Method

Patient selection

In this retrospective study, we selected 27 patients with cervical cancer having aged between 54 and 69. All the patients enrolled in this study were at T3N1M0 stage of cervical cancer.[16] Each of them had evolved lymph nodes and were preparing to undergo definitive radiotherapy treatment. Patients were immobilised on a vacuum bag (vac-loc; Orfit Industries, Wijnegem, Belgium), which hardens as per the shape of overlaying patients when deflated. Computed tomography (CT) images were acquired on Siemens PET-CT (Biopgraph mCT 20, Munich, Germany) at a 3 mm slice thickness. 3D CT images were acquired from the L2 vertebral body to 5 cm below the ischial tuberosity. CT images were transferred to Monaco Sim (CMS Elekta, Sunnyvale, CA, USA) work station for contouring. Planning target volume (PTV) and OAR were delineated on the CT images by an expert radiation oncologist and using the available protocol for definitive treatment of cervical cancer.[17,18] CT images along with delineated structure sets were transferred to Monaco (CMS Elekta, Sunnyvale, CA, USA) treatment planning system (TPS) for planning the VMAT technique. Elekta Versa HD (Elekta AB, Stockholm, Sweden), a linear accelerator was used to deliver the VMAT plans. The linear accelerator is fitted with MLCs having 80 leaf pairs of 5 mm width.

Treatment planning

The prescription dose to PTV was 50 Gy and was administered in 2 Gy per fraction.[17–19] VMAT plan was delivered in a single arc of 360° gantry rotation (clockwise direction from 180 to −180°). Sweep sequencer tool was used for MLC segmentation in VMAT technique. On contrary to static fields in IMRT, the intensity of photon field is modulated in a gantry arc in VMAT plan. The planned arc of VMAT was divided into uniform sectors using the parameter 'IGA' (Figure 1). Intensity modulation was facilitated by MLC; MLC segments move from right to left in a sector and return back from left to right in the following sector during continuous irradiation. Thereby, intensity modulations were done in a to-and-fro movement between successive sectors. 6 MV flattened photon beam was used to deliver the prescribed dose using VMAT plan. VMAT plans were optimised by varying the parameter 'IGA' (as 10, 20, 30 and 40°) and the plans were named as VMAT,[10] VMAT,[20] VMAT,[30] and VMAT,[40] respectively. VMAT plans were optimised to achieve the required dose constraints (Table 1) using the optimisation parameters (Table 2) and calculation parameters (Table 3). The radiation dose from VMAT plan was calculated on 3D CT images and heterogeneous corrections were applied.

Plan quality indices and statistical analysis

CI, HI, DGI and TC by 95% isodose line were derived to compare the dosimetric characteristics of the VMAT plans optimised with different 'IGA'.[15,20] In addition to that, dose to OARs were obtained from dose–volume histogram. The plan quality indices were calculated using the following Equations (1–3):

$$\mathrm{CI} = \frac{(\mathrm{TV_{RI}})^2}{(\mathrm{TV} \times \mathrm{V_{RI}})}, \tag{1}$$

$$\mathrm{HI} = \frac{(\mathrm{D_{2\%}} - \mathrm{D_{98\%}})}{\mathrm{D_{50\%}}}, \tag{2}$$

$$\mathrm{DGI} = \frac{\mathrm{V_{RI}}}{\mathrm{V_{HRI}}}. \tag{3}$$

Volume of PTV receiving prescription dose ($\mathrm{TV_{RI}}$), volume of PTV (TV) and total volume encompassed in prescription dose ($\mathrm{V_{RI}}$) were substituted in Equation (1) to calculate CI. Maximum dose received by 2% of PTV ($\mathrm{D_{2\%}}$), minimum dose received by 98% of PTV ($\mathrm{D_{98\%}}$), dose received by 50% of PTV ($\mathrm{D_{50}}$%) were substituted in Equation (2) to calculate HI. Total volume encompassed in half of the prescription dose ($\mathrm{V_{HRI}}$) and corresponding $\mathrm{V_{RI}}$ were substituted in Equation (3) to calculate DGI.

Physical parameters such as total MU and CPs were recorded. CPs per 10° were calculated to understand the physical constraints in MLC for PTV coverage. The width of PTV required to scale-up by MLC is given at 10° increment for a cervical and oesophageal cancer (Figure 2). IGA 30 had yielded better VMAT plans in earlier studies,[14,15] and so VMAT[30] plan was considered as a reference for statistical comparison. Each of the VMAT plans was renormalised to provide the same mean dose to PTV, as in VMAT[30] to avoid any bias or rescaling effects. The plan quality indices and dose to OARs were compared by paired sample *t*-test; *p*-value <0·05 indicated the difference as significant.[21]

Table 1. Treatment planning objectives

Structure	Parameter	Constraints
PTV	$V_{95\%}$	>47·5 Gy
	$V_{10\%}$	<107% of prescribed dose
Rectum	$V_{60\%}$	<45 Gy
Bladder	$V_{35\%}$	<45 Gy
Bowel	D_{Max}	<50 Gy
Femoral head	$V_{20\%}$	<40 Gy

Table 2. The cost functions for optimization of VMAT plans in cervical cancer

Structure	Cost functions	Parameter	Isoconstraints (Gy)
PTV	Target EUD	0·5	50
	Quadratic overdose	51·5 Gy	0·45
	Target penalty	95%	50
Rectum	Parallel	$k = 3$	35
Bladder	Parallel	$k = 3$	30
Bowel	Parallel	$k = 3$	25
	Maximum dose	Shrink = 3 mm	48
Femoral head	Maximum dose	Shrink = 3 mm	48
Body	Quadratic overdose	Shrink = 0 mm, 50 Gy	0·10
	Quadratic overdose	Shrink = 3 mm, 47 Gy	0·15
	Maximum dose	Shrink = 5 mm	46
	Maximum dose	Shrink = 10 mm	40
	Maximum dose	Shrink = 15 mm	35
	Maximum dose	Shrink = 25 mm	25

Abbreviations: EUD, equivalent uniform dose; k, power-law exponent.

Table 3. Sequencing parameters and calculation properties for VMAT plans

Sequencing parameters	
Maximum number of arcs	1
Maximum control points per arc	200
Minimum segment width	0·5 cm
Fluence smoothing	Medium
Calculation properties	
Grid spacing	0·3 cm
Dose deposition to	Medium
Algorithm	Monte Carlo photon
Statistical uncertainty	1%/calculation

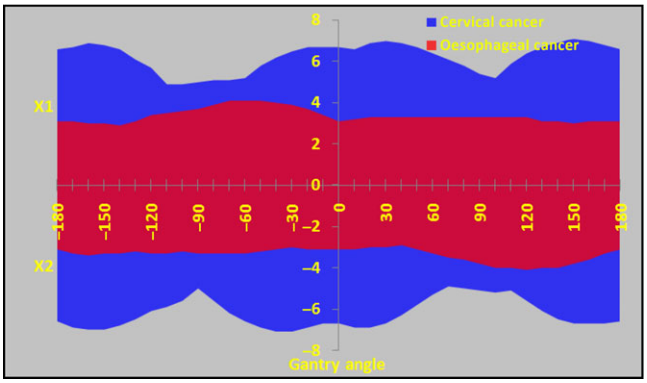

Figure 2. Comparison between the width of PTV in beam's eye view at 10° increment for a cervical and oesophageal cancer.

Results

Plan quality indices

Table 4 compares the plan quality indices of VMAT plans for the range of IGAs. CI indicates the degree of confining prescription dose within PTV and it was worsened with larger IGA (30 and 40°). HI indicates the degree of difference between the minimum and maximum dose within PTV and it was enhanced with larger IGA (30 and 40°). DGI indicates the degree of dose–gradient in fall-off region and it was worsened with larger IGA (30 and 40°). TC was worst in VMAT[10] plan and comparable elsewhere (20, 30 and 40°). Plan quality indices were significantly different ($p < 0{\cdot}05$) with smaller IGA (10 and 20°) and remained unaltered beyond 30°.

Dose to OARs

Dose to OARS and comparison with VMAT plans are given in Table 4. Overall, dose to OARs were reduced with smaller IGA (10 and 20°) and were comparable with 40°; the differences were significant ($p < 0{\cdot}05$). The dose received by 50% of the volume ($D_{50\%}$) in the bladder was worsened up to 6 Gy with larger IGA (30 and 40°). Dose to rectum ($D_{15\%}$, $D_{25\%}$, $D_{35\%}$ and $D_{50\%}$) were comparable among all the plans. The volume receiving 15 Gy (V_{15Gy}) in bowel was worsened up to 10% with larger IGA (30 and 40°). Smaller IGA (10 and 20°), worsened V_{25Gy} up to 3% in the femoral head.

Physical parameters

Table 5 compares the number of sectors, MU and CP of VMAT plans (10, 20, 30 and 40°). MUs required to deliver prescribed doses were reduced with a decrease in the number of sectors. Meanwhile, CPs were increased with a decrease in the number of sectors. The differences were significant ($p < 0{\cdot}05$).

Discussion

In this retrospective study, VMAT plans were analysed by varying the parameter IGA. Initial optimiser in VMAT technique creates an optimal dose–fluence for the required dose constraints. MLC segmentation/CPs are created to achieve the optimal dose–fluence by 'sweep sequencer tool' as per the IGA (10, 20, 30 and 40°). In a similar study, comparing IGA (15, 20, 30 and 40°) in VMAT for oesophageal cancer didn't yield any significant differences in plan quality indices.[14] Larger IGA (30 and 40°) yielded better plan than smaller IGA (10 and 20°) in post-operative cervical cancer; the

Table 4. Plan quality indices of VMAT plans for the range of IGAs

Structure	Parameter	$VMAT^{10}$	$VMAT^{20}$	$VMAT^{30}$	$VMAT^{40}$	*p*-value ($VMAT^{30}$)		
						$VMAT^{10}$	$VMAT^{20}$	$VMAT^{40}$
PTV	CI	0·83 ± 0·03	0·82 ± 0·05	0·80 ± 0·05	0·80 ± 0·05	0·00	0·00	0·75
	HI	0·12 ± 0·02	0·08 ± 0·02	0·07 ± 0·01	0·07 ± 0·01	0·00	0·01	0·66
	DGI	0·28 ± 0·04	0·30 ± 0·04	0·32 ± 0·03	0·33 ± 0·04	0·00	0·00	0·00
	TC	0·95 ± 0·03	0·99 ± 0·01	1·00 ± 0·00	1·00 ± 0·00	0·00	0·04	0·81
Bladder	$D_{15\%}$	42·89 ± 3·96	44·64 ± 4·26	45·54 ± 4·01	45·45 ± 3·77	0·00	0·00	0·62
	$D_{25\%}$	37·38 ± 5·42	40·69 ± 4·79	41·54 ± 4·91	41·63 ± 4·84	0·00	0·00	0·70
	$D_{35\%}$	32·33 ± 6·15	36·66 ± 4·93	37·66 ± 4·95	37·81 ± 5·12	0·00	0·00	0·65
	$D_{50\%}$	26·37 ± 5·91	31·23 ± 5·01	32·69 ± 4·21	32·66 ± 4·71	0·00	0·00	0·93
Rectum	$D_{15\%}$	48·36 ± 1·35	48·44 ± 1·42	49·00 ± 1·45	49·33 ± 1·27	0·00	0·00	0·01
	$D_{25\%}$	46·24 ± 1·83	46·08 ± 1·92	47·08 ± 2·30	47·33 ± 1·99	0·00	0·00	0·18
	$D_{35\%}$	43·25 ± 2·01	43·27 ± 2·17	44·60 ± 2·78	44·75 ± 2·44	0·00	0·00	0·46
	$D_{50\%}$	37·65 ± 1·84	38·46 ± 2·48	39·82 ± 2·99	39·94 ± 2·47	0·00	0·00	0·66
Bowel	V_{15Gy} (%)	71·07 ± 11·44	80·22 ± 7·7	82·84 ± 4·92	82·44 ± 7·43	0·00	0·01	0·58
	V_{30Gy} (%)	22·57 ± 5·65	27·66 ± 5·83	29·36 ± 5·39	29·25 ± 5·13	0·00	0·00	0·74
	V_{45Gy} (%)	3·91 ± 1·46	5·36 ± 1·91	5·88 ± 1·57	6·16 ± 1·78	0·00	0·03	0·09
	Mean dose (Gy)	22·28 ± 2·56	24·53 ± 2·15	25·02 ± 1·72	24·96 ± 2·01	0·00	0·01	0·61
Femoral head	V_{25Gy} (%)	25·58 ± 2·57	24·43 ± 2·98	22·83 ± 4·13	22·18 ± 2·61	0·00	0·00	0·21
	V_{40Gy} (%)	23·85 ± 2·40	22·43 ± 2·79	21·9 ± 2·80	20·75 ± 2·57	0·00	0·00	0·00
	Mean dose (Gy)	22·57 ± 2·49	20·72 ± 2·87	20·98 ± 2·75	20·14 ± 2·90	0·00	0·01	0·00
	Max. dose (Gy)	38·31 ± 4·33	38·81 ± 5·41	39·96 ± 6·10	38·29 ± 7·10	0·06	0·11	0·01

Table 5. Physical parameters of VMAT plans for the range of IGAs

Parameter	IGA 10	IGA 20	IGA 30	IGA 40	*p*-value ($VMAT^{30}$)		
					$VMAT^{10}$	$VMAT^{20}$	$VMAT^{40}$
Sector	36	18	12	9	–	–	–
MU	1124·3 ± 138·2	1055·47 ± 115·35	1057·93 ± 124·9	932·93 ± 79·79	0·00	0·88	0·00
CPs	142·26 ± 10·16	169·33 ± 10·3	178·15 ± 3·43	176·11 ± 3·17	0·00	0·00	0·03
CPs/10°	3·95 ± 0·28	4·7 ± 0·29	4·95 ± 0·1	4·89 ± 0·09	0·00	0·00	0·04

results had a correlation with MLC movements created under reduced freedom of optimisation by 'sweep sequencer tool' for smaller IGA (10 and 20°).[15] The controversial results from previous publications[14,15] could be due to a larger volume of PTV in cervical cancer than oesophageal cancer and are explained in the present study (Figure 2). The dimension of PTV (Figure 2) in lateral directions (−90 and +90°) were smaller than in antero-posterior directions (180 and 0°). For sector 3 (−80 to −120°) and sector 7 (60– 100°) in $VMAT^{40}$ (Figure 1b), the sweep sequencer had to sharply decrease the field size initially, followed by a gradual increase (Figure 2). This fluctuation could be the reason for the superiority of plan quality indices in VMAT.[30] Notably, $VMAT^{30}$ had an even number of sectors and were highly symmetrical (Figure 1a).

IGA 30° yielded better plans as per target dose indices but the dose fall-off region was compromised (more dose to lung) in oesophageal cancer[14] and this trend is even resembled with the present study; dose to bladder, rectum and bowel were higher with larger IGA. Eventually, dose–gradient in fall-off region was worsened with larger IGA (30 and 40°); the reason could be due to larger dimension of PTV (Figure 2) in this study (cervical cancer versus oesophageal cancer). Homogenous dose distribution within PTV was enhanced with larger IGA in this study; more number of CPs was generated by 'sweep sequencer tool' to improve the parameter. Eventually, the number of MUs was reduced by finer resolution of MLC segments for the optimal dose–fluence generated in initial optimisation of VMAT by Monaco TPS. Similar enhancement of homogenous dose distribution was observed within PTV of both oesophageal[14] and cervical[15] cancers with larger IGA (30 and 40°). Increase in the number of CPs enhanced the homogeneity of delivering prescribed dose within PTV but failed to confine the prescribed dose just around the PTV. As a result, confinement of prescribed dose within PTV and dose gradient in dose fall-off regions was compromised to a small extent.

VMAT[40] had reduced the MU usage but the CI and DGI was compromised due to large MLC field segments. Though the difference was significant, the conformal dose to PTV was quite comparable in this study, and also observed both in oesophageal[14] and cervical[15] cancers. Thus, the CI remained unaffected with a change in the size of PTV. TC was affected with smaller IGA (10°) up to 5%, in this study of definitive radiotherapy treatment for cervical cancer, which had a resemblance to a worst of 6% in cervical cancer.[15]

Conclusion

In VMAT technique, defining the IGA remains vital in acquiring better plan quality indices. The current study demonstrates that the strategy of VMAT[30] and VMAT[40] have the potential to enhance plan quality indices/therapeutic gain. This study recommends that the larger IGA (30°) could yield better results when the number of sectors is even, for a cervical cancer patient. However, more data from more patients need to be obtained and analysed to make this an evidence-based hypothesis.

Acknowledgements. The authors are grateful to the Management of Aditya Birla Hospital, Pune for constantly supporting our academic and research pursuits. We are specially thankful to the team of radiotherapists of the hospital where the work was carried out.

Conflict of Interest. The authors declare that they have no conflicts of interest.

Ethical Approval. All procedures in studies involving human participants were performed in accordance with the ethical standards of the Aditya Birla Memorial Hospital Institutional Review Board (IRB) and with the 1964 Declaration of Helsinki and its later amendments or comparable ethical standards.

Informed Consent. Informed consent was obtained from all individual participants included in the study.

References

1. Duan J, Kim RY, Elassal S, Lin HY, Shen S. Conventional high-dose-rate brachytherapy with concomitant complementary IMRT boost: a novel approach for improving cervical tumor dose coverage. Int J Radiat Oncol Biol Phys 2008; 71 (3): 765–771.
2. Georg P, Georg D, Hillbrand M, Kirisits C, Pötter R. Factors influencing bowel sparing in intensity modulated whole pelvic radiotherapy for gynaecological malignancies. Radiother Oncol 2006; 80 (1): 19–26.
3. Portelance L, Chao KS, Grigsby PW, Bennet H, Low D. Intensity-modulated radiation therapy (IMRT) reduces small bowel, rectum, and bladder doses in patients with cervical cancer receiving pelvic and para-aortic irradiation. Int J Radiat Oncol Biol Phys 2001; 51 (1): 261–266.
4. Otto K. Volumetric modulated arc therapy: IMRT in a single gantry arc. Med Phys 2008; 35 (1): 310–317.
5. Teoh M, Clark CH, Wood K, Whitaker S, Nisbet A. Volumetric modulated arc therapy: a review of current literature and clinical use in practice. Br J Radiol 2011; 84 (1007): 967–996.
6. Vanetti E, Clivio A, Nicolini G, et al. Volumetric modulated arc radiotherapy for carcinomas of the oro-pharynx, hypo-pharynx and larynx: a treatment planning comparison with fixed field IMRT. Radiother Oncol 2009; 92 (1): 111–117.
7. Palma D, Vollans E, James K, et al. Volumetric modulated arc therapy for delivery of prostate radiotherapy: comparison with intensity-modulated radiotherapy and three-dimensional conformal radiotherapy. Int J Radiat Oncol Biol Phys 2008; 72 (4): 996–1001.
8. Zhang P, Happersett L, Hunt M, Jackson A, Zelefsky M, Mageras G. Volumetric modulated arc therapy: planning and evaluation for prostate cancer cases. Int J Radiat Oncol Biol Phys 2010; 76 (5): 1456–1462.
9. Yin L, Wu H, Gong J, et al. Volumetric-modulated arc therapy vs. c-IMRT in esophageal cancer: a treatment planning comparison. World J Gastroenterol 2012; 18 (37): 5266–5275.
10. Abbas AS, Moseley D, Kassam Z, Kim SM, Cho C. Volumetric-modulated arc therapy for the treatment of a large planning target volume in thoracic esophageal cancer. J Appl Clin Med Phys 2013; 14 (3): 192–202.
11. Masi L, Doro R, Favuzza V, Cipressi S, Livi L. Impact of plan parameters on the dosimetric accuracy of volumetric modulated arc therapy. Med Phys 2013; 40 (7): 071718.
12. Treutwein M, Hipp M, Koelbl O, Dobler B. Searching standard parameters for volumetric modulated arc therapy (VMAT) of prostate cancer. Radiat Oncol 2012; 7: 108.
13. Wang Y, Chen L, Zhu F, Guo W, Zhang D, Sun W. A study of minimum segment width parameter on VMAT plan quality, delivery accuracy, and efficiency for cervical cancer using Monaco TPS. J Appl Clin Med Phys 2018; 19 (5): 609–615.
14. Nithya L, Raj NA, Rathinamuthu S, Sharma K, Pandey MB. Influence of increment of gantry angle and number of arcs on esophageal volumetric modulated arc therapy planning in Monaco planning system: a planning study. J Med Phys 2014; 39 (4): 231–237.
15. Chen A, Li Z, Chen L, et al. The influence of increment of gantry on VMAT plan quality for cervical cancer. J Radiat Res Appl Sci 2019; 12 (1): 447–454.
16. Edge SB, Compton CC. The American Joint Committee on Cancer: the 7th edition of the AJCC cancer staging manual and the future of TNM. Ann Surg Oncol 2010; 17 (6): 1471–1474.
17. Lim K, Small W Jr, Portelance L, et al. Consensus guidelines for delineation of clinical target volume for intensity-modulated pelvic radiotherapy for the definitive treatment of cervix cancer. Int J Radiat Oncol Biol Phys 2011; 79 (2): 348–355.
18. Forrest J, Presutti J, Davidson M, Hamilton P, Kiss A, Thomas G. A dosimetric planning study comparing intensity-modulated radiotherapy with four-field conformal pelvic radiotherapy for the definitive treatment of cervical carcinoma. Clin Oncol (R Coll Radiol) 2012; 24 (4): e63–e70.
19. Vrdoljak E, Omrcen T, Novaković ZS, et al. Concomitant chemobrachyradiotherapy with ifosfamide and cisplatin followed by consolidation chemotherapy for women with locally advanced carcinoma of the uterine cervix–final results of a prospective phase II-study. Gynecol Oncol 2006; 103 (2): 494–499.
20. Paddick I. A simple scoring ratio to index the conformity of radiosurgical treatment plans. Technical note. J Neurosurg 2000; 93 (Suppl. 3): 219–222.
21. R Development Core Team (2016). R: A Language and Environment for Statistical Computing. R Foundation for Statistical Computing, Vienna, Austria. http://www.R-project.org. Accessed on 10th August 2020.

MUNIRATHINAM, N
Ph.D student in D.Y.Patil University,
Kolhapur-416006

LIST OF PAPER PUBLISHED IN JOURNAL:

S.No	Name of the Journal	Tittle of the Paper	Date Submission	Date of Accepted
1.	Journal of Radiotherapy in Practice-Cambridge University Press	Dosimetric comparison of flattened and flattening filter-free beams for liver stereotactic body irradiation in deep inspiration breath hold, and free breathing conditions	18 -04-2018	16-10-2018
2.	Journal of Radiotherapy in Practice-Cambridge University Press	Dosimetric characteristics of VMAT plans with respect to a different increment of gantry angle size for Ca cervix	10 -08- 2020	2-10- 2020

LIST OF POSTER PRESENTATION IN CONFERENCE:

S.No	Name of the Conference	Location	Tittle of the Paper	Date of
1.	AMAR-2015	D.Y.Patil university-Kolhapur	To Determine Spectral differences for flattening-filter-free (FFF) versus standard flattened beam .	17-03-2015
2.	ETNA-2017	D.Y.Patil university-Kolhapur	Characteristics study of flattening filter free beams on VMAT advanced Radiotherapy planning using ca cervix	02-06- 2017
3.	AOCMP AMPICON 2017	Jaipur	On the Dosimetric Behavior of VMAT Plans With Respect to Various Photons Beam (FF& FFF) Energy Using Monte Carlo Dose Calculation For Carcinoma Cervix	04-11-2017

MUNIRATHINAM, N
Ph.D student in D.Y.Patil University,
Kolhapur-416006

LIST OF CONFERENCE ATTEND:

1. **37th Annual Conference of the Association of Medical Physicists of India; AMPICON-2016 is scheduled during 18-20 November, 2016 at Hotel Marriott & Convention Centre, Hyderabad.**

2. **39 Annual National Conference Association of Medical Physicists of India (AMPICON-2018) November 2 - 4, November 2018, Chennai, Tamil Nadu, India**

3. **40 Annual National Conference Association of Medical Physicists of India (AMPICON-2018) November 7 - 9, November 2019, Kolkata**